

eman ta zabal zazu



Universidad  
del País Vasco

Euskal Herriko  
Unibertsitatea

DOCTORAL THESIS

# LIPIDOMICS IN MELANOMA: IDENTIFICATION OF NEW LIPID PROGNOSTIC BIOMARKERS

Arantza Perez Valle

Cell Biology and Histology department

Faculty of Medicine and Nursing

Leioa, 2020



This doctoral thesis has been conducted thanks to the funding by:

1. Desarrollo del Sistema ONCOFINDER para la detección y pronosis de tumores mediante biomarcadores lipídicos utilizando microarrays de membranas. Ministry of Economy, Industry and Competitiveness of Spain. 2015-2018 (RTC-2015-3693-1).
2. Movilidad y difusión de los resultados de la investigación en la UPV/EHU. Scholarship provided by UPV/EHU. 2018.
3. ONKOiker. Investigación multidisciplinar en nuevas estrategias para el diagnóstico temprano y tratamiento personalizado del cáncer. Department of Economic Development and Infrastructures of the Basque Government. 2018. (KK-2018/00090).
4. Proyectos grupos consolidados IT1275-19. Grupo A. Basque Government. 2017-2018.
5. Melamics. Investigación Multidisciplinar del Melanoma Maligno. Identificación de nuevos biomarcadores de utilidad en el pronóstico y tratamiento del melanoma. Department of Economic Development and Infrastructures of the Basque Government. 2016-2017. (KK2016-00036; KK2017-00041).

Some of the results obtained in this work have been object of patenting:

- Oncofinder: A novel platform for screening benign nevi from melanomas based on lipid phenotype using mass spectrometry and machine learning.

The results of this thesis have been published in the following works:

1. Influence of lipid fragmentation in the data analysis of imaging mass spectrometry experiments. J. Garate, S. Lage, L. Martín-Saiz; A. Perez-Valle, B. Ochoa, M.D. Boyano, R. Fernández, J.A. Fernández. *Journal of the American Society for Mass Spectrometry Experiments*. 2020.
2. Lipidomics Biomarkers for Melanoma. A. Perez-Valle, J. Garate, R. Fernandez, S. Lage, E. Astigarraga, G. Barreda-Gomez, J. Fernandez, A. Asumendi, B. Ochoa, M.D. Boyano. *Journal of investigative Dermatology*.137(10).289.2017
3. Fosfolipasa D2 entzimaren garrantzia melanomaren sorreran eta garapenean. A. Perez-Valle, M.D. Boyano, A. Asumendi. *Osagaiz*. 2. Bolumena. 2. Ale berezia. 13(52). 2018

The results of this thesis have been presented in the following congresses:

1. Lipidic biomarkers in melanoma. 47th annual ESDR meeting. Salzburg, Austria. 2017. Winner of the best poster presentation.
2. Comparative lipidomic study of normal skin melanocytes, nevus melanocytes and melanoma cells. SEBC Joint Congress. Gijon, Spain. 2017.
3. Fosfolipasa D2 entzimaren garrantzia melanomaren sorreran eta garapenean. Osasun-zientzietako ikertzaileen III. Topaketak. Eibar, Spain. 2018.
4. Identificación de nuevos biomarcadores en melanoma. III Reunión de Investigación translacional en melanoma. Iruña-Pamplona, Spain. 2018.
5. Melanomaren biomarkatzaile lipidikoak. II. Ikerketa. Nazioarteko ikerketa euskaraz. Iruña-Pamplona, Spain. 2017.
6. These results have been presented in five other international congresses by other authors of the research group.



## ESKER ONAK

Ezin da esan erraza izan denik, baina, dudarik gabe, 5 urte hauetan nire bizi osoan gogoratuko ditudan uneak bizi izan ditut. Eskerrak eman nahi dizkizuet bizitzako etapa garrantzitsu honetan nirekin egon zareten guztiei, zuek gabe ezingo nukeen hau idatzi!

Lehenik eta behin eskerrak eman nahi dizkiet nire tesi zuzendariei, Lola Boyano eta Aintzane Asumendi. Ikertzaile eta irakasle ezin hobek zaretela argi dago, baina ziur asko esan dezaket pertsona bikainak zaretela ere! Eskerrak asko zuen laborategiko ateak zabaltzeagatik eta tesi hau burutzeko behar izan dudan guztia emateagatik, eskerrak asko nigan sinesteagatik! Mila esker Aintzane beti entzuteko prest agertzeagatik, zure laguntza ezinbestekoa izan da gaur tesi hau amaitu ahal izateko!! Gracias Lola por tener siempre unas palabras amables que ayudan a seguir adelante y por demostrar día tras día que trabajar con humildad también te permite abrirte paso en este mundo de la investigación. Eskerrak asko ere ikerketa taldea osatzen duten irakasle eta kide guztiei! Zuen laguntza ezinbestekoa izan da tesi hau burutzeko.

También quiero agradecer la excepcional ayuda de la Doctora Begoña Ochoa. Gracias por todo el apoyo y dedicación, además enseñarme todo sobre el mundo de los lípidos. No hay duda de que sin tu ayuda esta tesis no hubiera sido posible.

Esta tesis es fruto del trabajo en equipo, y quiero agradecer el gran trabajo y ayuda a Jose Andrés, Rober y Jone del departamento de Química Física de la UPV/EHU, y a todos los miembros de la empresa IMG Pharma.

Gracias a mi equipo de Biocruces, Isabel y Cristina. Gracias por todas las facilidades para que pudiera acabar esta tesis, por todos los consejos y ayuda!

Thanks to Krushangi, and all my colleagues in Professor Julian Gomez-Cambronero's lab in Wright State University. And specially to Dr. Cambronero and his lovely family. Thank you for welcoming me during such a hard time. Of course, thanks to my American family. It had a blast living you, and I will never forget it. Thank you for opening me the door of your house and giving me everything I needed to make the most of my experience in Ohio.

Eskerrak asko laborategiko eta departamentuko kide guztiei. Ez gara soilik lankideak, asko lagunak zaretela ziurtatu dezaket. Aldara, Maddalen, Miguel, Igor, Patri Garrido, Irene, Alba, Maider, Patri Garcia Gallastegi, Xan, Lutxu, Aitor, Maria, Vero, eta beste denak, milesker irribarre eta momentu ezin hobe guztiengatik, ez ditut inoiz ahaztuko!! Eskerrak ere spanx gazteei, Itziar, Iraia, Aitor! Plazerra izan da zuekin batera lan egitea, beti irribarre batekin eta laguntzeko prest!

Tesi honek oparitu dizkidan nire bi lagun minei. Maddalen, zalantzarik gabe, zure laguntza gabe ez nukeen tesia amaituko!! Ez dakit zenbat kafe amaigabe, afari, farra, teki-fresa, bidai, kontzertu, barre partekatu ditugun, baina ziur oraindik askoz gehiago egongo direla. Lagun aparta zarela erakutsi didazu, eta ezin dizut hitzekin eskertu niregatik egin duzun guztia!! Aldarari, la gallega más vasca! Gracias por todo o apoio no laboratorio, pero especialmente por todas as conversas, risas, cafés, kalimotxos, festas, viaxes... a pesar da distancia e do tempo aínda eres un gran amiga.

Nire lagunei. Lideri, beti irribarre bat ateratzeagatik, entzuteko prest agertzeagatik, momentu bakoitzean behar ditudan animo-hitzak aurkitzeagatik, zure laguntasuna eta babesagatik! Roselis, gracias por tu cariño, por escucharme e intentar entenderme. Por confiar en mí, apoyarme y estar siempre ahí a pesar de la distancia. Palomares, Amaia, Monika. Benetan

eskertzen dizuet bidai honetan zehar nire ondoan egon izana eta ikerketaren mundu zoro hau ulertzen saiatzea!! Laura, gracias por todos estos años de amistad, por todos los festivales, escapadas, ruedas pinchadas, viajes a Canarias a visitar Esther, y buenos momentos!!

Eta azkenik nire familiari, nire euskarria. Eskerrik asko zuen hurbiltasunagatik, tesiaren egoeragatik interesa agertu izanagatik. Momentu zailenetan ere, gure bazkari/ afari batek dena konpontzen duelako! Arkaitzi, zure kafe askok tesi honen idazkeraren bidean lagundu didate! Ainhoari, tesia nola doan galdetzeagatik, ahal izan duzun guztian laguntzeagatik eta niretzako eredu bat izateagatik. Ama, gracias por introducirme en el mundo de la ciencia, seguramente si no fuera por ti hoy no estaría escribiendo esta tesis. Gracias por enseñarme a trabajar duro, con constancia y a darle importancia a cada detalle.

Elizmendiri. Lehengusina baino gehiago izateagatik, nire ahizpa, nire bidai-laguna.

Amamari. Nire ispilua izateagatik. Konturatu gabe irakatsi didazun guztiagatik. Kemena eta indarraren eredu. Aurrera!!

Nire bi izartxoei. Annetxu eta Laia. Maitasuna zer den erakusteagatik. Egun zailenetan ere milaka irribarre ateratzeagatik. Ezerk ez dezala zuen irribarrea gelditu!!

Eta azkenik, nire Aitari. Gugatik dena emateagatik. Beti gu zure aurretik jartzeagatik ezeren truke. Beti irribarre batekin, laguntzeko prest eta ondo pasatzeko prest. Eskerrik asko ni honaino heltzeko egin dituzun sakrifizio guztiengatik. Ezin da hitzekin eskertu niregatik egiten duzun guztia.

Eskerrik asko benetan nire ondoan egon zareten guztiei! Beti aurrera!!







Nire gurasoei

Annetxu eta Laiari,  
gogor borrokatu zuen ametsak lortu arte



# **SUMMARY**



Melanoma is the cancer that arises upon the malignant transition of melanocytes and, even though it can occur in different locations of the body, it preferentially appears on the skin. In this way, it is representative of 4% of all skin tumors; however, 80% of deaths from skin cancer are due to melanoma. Moreover, the incidence rates of melanoma have steadily increased in recent decades, and it is the seventh most diagnosed cancer in Europe.

Melanoma tumors are very heterogeneous, which has complicated the finding of an efficient biomarker or therapy for this cancer. As a matter of fact, in the present, there is no specific biomarker or effective therapy for melanoma. It is considered a very aggressive tumor and metastasizes easily; thus, if it is not diagnosed early, survival rates drop dramatically. It stands to reason that there is a great need to identify new biomarkers to improve the early detection, diagnosis and prognosis of melanoma, in addition to finding new therapeutic targets.

In this regard, cellular metabolism has gained attention in cancer research recently. Indeed, the disruption of cancer metabolism has been established as a hallmark of cancer. A large body of work demonstrates that cancer cells undergo metabolic rewiring that supports the augmentation in cellular activities that guarantees their malignant phenotype. It is known that the variations in metabolic pathways within cells alter the amount and composition of some lipid species. In particular, alterations in lipid metabolism of cancer cells have been linked to increased proliferation and metastasis, reduction of cell death and resistance to therapy, among other issues. Most lipidomic studies in cancer have mainly focused in breast, colon, lung and prostate cancers, but unfortunately, little is known about melanoma's lipidome. Therefore, we hypothesize that, like in other types of cancer, the malignant transformation of healthy melanocytes into tumor cells might be favored by the adaptation of their metabolism and, thereby, the amount and composition their lipid content. Hence, the principal objective of this thesis was to identify new lipid biomarkers by comparing the lipidome of non-pathological melanocytes and malignant melanomas to detect the particular lipid species that drive the differentiation between these tumor and non-pathological cells. In addition, a secondary objective was to determine the biological effects that these alterations in the lipid content could have on cells.

For biomarker research, the lipidome of skin and nevus melanocyte cell lines, and primary and metastatic melanoma cell lines were studied using different lipidomic approaches. Lipidomic analyses enable the classification of tumor and healthy tissues by comparing the lipid fingerprint of the samples and the interactions of those lipids with other lipids, proteins, metabolites and genetic material. Most lipidomic analyses are based on mass spectrometry. In this work, two different lipidomic strategies have been carried out. First, lipid extracts of several skin and nevus melanocytes, and primary and metastatic melanoma cell lines were obtained using Bligh & Dyer methodology. The extraction method used hampered the extraction of all lipid classes, and the most polar molecular species were not extracted. The obtained lipid extracts were studied using an UHPLC-ESI-MS/MS mass spectrometry approach. This allowed a global lipidomic study, which confirmed that malignant and non-malignant cells might have a different lipid profile. Besides the global lipidome of the cells, a deeper insight into the results revealed that we could detect differences in the intensities of the lipid species that make up the various lipid families. Specifically, we found that a panel of 45 lipid species presents significantly altered levels that allows classifying healthy and malignant cells. The detected alterations in lipid content are proposed to support the malignant phenotype of cancer cells.

The results obtained with the first lipidomic approach confirmed that there are particular lipid species that have a differential presence in healthy and malignant cells, and these lipids

pertained to the lipid subclasses that are mainly located in the cell membranes. For this reason, the following lipidomic strategy was performed on functional cell membrane microarrays, a promising biotechnological tool with translational potential. Here, functional cell membranes of the studied cell lines were immobilized, and then a MALDI-MS lipidomic approach was applied. This is a useful tool, as a small amount of each sample is needed, the preparation of the samples is fast and reproducible, no lipid extraction is needed, and MALDI-MS is the gold standard method for biomarker discovery. After performing different statistical analyzes, we could detect 116 species of lipids that show a significantly altered intensity in healthy melanocytes and malignant melanoma cell lines. In particular, there are 48 and 54 lipid species with a differential levels between skin or nevus melanocytes and primary melanomas, respectively. The difference between the lipid content of skin/nevus melanocytes and metastatic melanoma is also evident, since there are 82 molecules that are potential biomarkers to differentiate between skin melanocytes and metastatic melanomas, and 81 lipid species in the comparison of nevus melanocytes and metastatic melanomas cell lines. Moreover, with this analytical approach we were able to detect 11 lipid species that exhibited differential intensities between skin and nevus melanocytes. Interestingly, three lipid species show differential levels in primary and metastatic melanoma, and, although further research is needed, they could be useful prognostic markers.

Lipidomic analyses demonstrated that phospholipids have an altered presence in melanoma cells compared to non-transformed melanocytes. These lipids are metabolized by phospholipase enzymes, which have been previously described to exhibit altered expression and activity in different cancers. Hence, we studied the expression levels of this family of enzymes in melanomas and found that PLD2 has upregulated protein expression and activity in melanoma cells compared to skin melanocytes. PLD2 metabolizes phosphatidylcholines (PC), which is consisted with the results obtained in the lipidomic analyses, since PCs have also been detected with greater intensity in melanoma cells compared to normal melanocytes. Therefore, we hypothesize that PLD2 plays a role in some of the processes involved in melanoma development and metastatic dissemination *in vitro*. To study the particular implication of PLD2 in the carcinogenic process, this enzyme was overexpressed and silenced in various primary and metastatic melanoma cell lines. The results showed that the augmented activity and expression of this enzyme significantly increases the proliferation, migration and invasion of these cells, while the downregulation of PLD2 reduces these processes. Thus, PLD2 seems to be involved in melanoma development and progression, and its blockade could be a promising therapeutic strategy.

**LABURPENA**







Melanoma melanozitoen gaiztotzearen ondorioz sortzen den minbizia da eta, gorputzaren hainbat tokitan gerta daitekeen arren, nagusiki larruazalean agertu ohi da. Izan ere, larruazalean ematen diren tumore guztien %4 melanoma dira; aldiz, horien ondorioz ematen diren heriotzen %80aren erantzule da. Gainera, melanomaren intzidentzia tasak etengabe gora egin du azken hamarkadetan, eta Europako zazpigarren minbizi diagnostikatuena da.

Melanoma tumoreak oso heterogeneoak dira, eta horrek asko zaildu du biomarkatzaile edo terapia eraginkor bat aurkitzea. Hortaz, gaur egun ez dago biomarkatzaile edo terapia zehatzik melanomarako, batez ere, melanoma metastatikorako. Oso tumore oldarkorra da eta erraz sortzen ditu metastasiak; beraz, ez bada garaiz diagnostikatzen, biziraupen-tasak behera egiten du nabarmenki. Horregatik, melanomaren antzemate goiztiarra, diagnostikoa eta pronostikoa hobetuko luketen biomarkatzaile berriak identifikatzea ezinbestekoa suertatzen da.

Metabolismo zelularrak garrantzia irabazi du azken urteotan minbiziaren ikerketan. Izan ere, minbizi zeluletan ematen den bidezidor metabolikoen eraldaketa minbiziaren bereizgarri gisa ezarri da. Aldaketa metaboliko horiek, minbizi zelulen fenotipo gaiztoa bermatzen dituzten zelula-jarduerak sustatzen dituzte. Jakina da zelulen bidezidor metabolikoen aldaketek lipido-espezie batzuen kantitatea eta konposaketa aldatzen dituztela. Zehazki, minbizi-zeluletako lipidoen metabolismoan ematen diren alterazioek zelulen hazkuntzan eta metastasian eragiten dute, eta aldi berean, zelulen heriotza murriztu eta terapiarekiko erresistentzia sortzen dute, besteak beste. Minbiziaren ikerketan burutu diren analisi lipidomiko gehienak bularreko, koloneko, biriketako eta prostatako minbizietan izan dira, baina, zoritxarrez, ezer gutxi dakigu melanomaren lipidomari buruz. Beraz, gure **hipotesia** ondokoa da: beste minbizi mota batzuetan bezala, metabolismoaren egokitzapenak, eta beraz, lipido edukia aldatzeko, melanozito osasuntsuen eraldaketa gaiztoa bultzatzen dutela. Hori dela eta, tesiaren **helburu nagusia** lipido biomarkatzaile berriak identifikatzea izan zen, larruazaleko melanozitoen eta melanoma gaiztoen lipido edukia aldatuz, tumore horien eta zelula ez patologikoen arteko desberdintasuna gidatzen duten espezie lipidiko partikularrak hautemateko. Bigarren helburua, lipidoen edukian sortutako alterazio horiek zeluletan izan ditzaketen eragin biologikoa zehaztea izan zen.

Biomarkatzaileak ikertzeko, larruazaleko melanozitoen, nevuseko melanozitoen, melanoma primarioen eta melanoma metastatikoaren lipidomak aztertu ziren. Horretarako tumore eta ehun osasuntsuak sailkatzea ahalbidetzen duten hainbat teknika lipidomiko erabili ziren. Analisi lipidomikoek laginen lipido edukia eta lipido horiek beste lipido, proteina, metabolito eta material genetikoarekin duten elkarrekin aztertzen dituzte eta gehienak masa espektrometria oinarritzen dira. Lan honetan, bi estrategia lipidomiko desberdin erabili dira. Lehenik, larruazaleko eta nevuseko melanozitoetatik, melanoma primario eta metastatikoetatik lipido erauzketa egin zen Bligh & Dyer metodologia erabiliz. Metodo horrekin ezin izan ziren lipido mota guztiak lortu, lipido polarrenak deuseztatu baitziren. Lipido erauzkin horiek UHPLC-ESI-MS/MS masa espektrometria estrategia erabiliz aztertu ziren. Horrek, azterketa lipidomiko orokor bat ahalbidetu zuen, zeinak zelula gaizto eta osasuntsuen lipido profila ezberdina dela baieztatu zuen. Zelulen lipidoma orokorrak gain, emaitzen ikuspegi sakonago batek agerian utzi zuen lipido familia ezberdinak osatzen dituzten lipido espezie konkretuen artean intentsitate desberdintasunak antzeman genitzakeela. Zehazki, zelula osasuntsu eta gaiztoetan intentsitate mailak esanguratsuki ezberdinak dituzten 45 lipido espeziez osatutako multzo bat aurkitu genuen. Lipidoen edukian antzemandako alterazioek minbizi-zelulen fenotipo gaiztoasostengatzen dutela proposatzen da.

Aipaturiko estrategia lipidomikoarekin baieztatu genuen zelula osasuntsu eta gaiztoetan presentzia diferentziala duten espezie lipidiko partikularrak daudela, eta aurkitutako lipido horiek batez ere zelula mintzetan kokatzen diren lipido familien osagaiak direla. Horregatik, hurrengo teknika lipidomikoa mintz zelular funtzionalez osatutako mikroarraiak erabiliz burutu zen. Hemen, aztertutako lerro zelularren mintz-esekidurak jarri ziren eta MALDI-MS teknika lipidomikoa erabili. Hori, translazio-potentziala duen tresna erabilgarria da; izan ere, lagin bakoitzaren kantitate txiki bat nahiko da, laginen prestaketa azkarra eta erreproduziblea da, ez da lipido erauzketarik behar, eta MALDI-MS teknika biomarkatzaileak aurkitzeko metodo estandarra da. Analisi estatistiko ezberdinak burutu ondoren, melanozito osasuntsuetan eta melanoma gaiztoaren lerro zelularretan intentsitate nabarmen ezberdina erakusten duten 116 lipido espezie daudela aurkitu zen. Konkretuki, adierazpen diferentzial duten 48 eta 54 lipido espezie daude larruazaleko edo nevuseko melanozitoen eta melanoma primarioen artean, hurrenez hurren. Larruazaleko edo nevuseko melanozitoen eta melanoma metastatikoaren lipido edukiaren arteko aldea agerikoa da ere. Izan ere, 82 lipido-espezie aurkitu dira larruazaleko melanozitoak eta melanoma metastatikoak bereizteko biomarkatzaile potentzialak izan daitezkeenak, eta 81 lipido espezie nevuseko melanozitoak eta melanoma metastatikoaren arteko konparaketan. Gainera, ikuspegi analitiko horrek, larruazaleko eta nevuseko melanozitoen artean intentsitate diferentzialak dituzten 11 lipido-espezieak hautematea ahalbidetu zuen. Bestalde, hiru lipido espezie detektatu dira pronostiko markatzaile bezala erabilgarriak izan daitezkeenak, melanoma primarioan eta metastatikoan maila diferentzial nabarmenak dituztenak alegia.

Analisi lipidomikoek fosfolipidoak melanoma zeluletan bestelako presentzia dutela frogatu zuten. Lipido horiek fosfolipasa entzima-familiako kideen bitartez metabolizatzen dira. Aurretik, entzima horiek hainbat minbizietan euren proteina adierazpena eta jarduera aldatzen dutela deskribatu da. Beraz, entzima-familia horren proteina adierazpen mailak aztertu genituen melanozito eta melanoma lerro zelularretan. Emaitzak erakutsi zuten, PLD2-ren adierazpena eta jarduera handitua dago ere melanoma zeluletan. PLD2-k fosfatidilkolinak (PC) metabolizatzen ditu, eta hori bat dator analisi lipidomikoetan lortutako emaitzekin, PC-ak melanoma zeluletan intentsitate handiagoz detektatu baitira melanozitoekin alderatuta. Beraz, PLD2-k melanomaren garapenean eta metastasian parte hartzen duten hainbat prozesutan eragina duela proposatu da. PLD2-k prozesu kantzerigenoan duen inplikazio partikularra aztertzeke, entzima hori hainbat melanoma primario eta metastatiko lerro zelularretan gain-adierazi eta isildu zen. Emaitzek erakutsi zuten entzima horren jarduera eta adierazpena handitzeak nabarmenki areagotzen dutela zelula horien hazkuntza, migrazioa eta inbasioa; PLD2-ren isilerak, berriz, prozesu horiek murrizten ditu. Beraz, PLD2-a melanomaren garapenean eta progresioan parte hartzen duela antzematen da, eta hortaz, bere blokeoa etorkizun handiko estrategia terapeutikoa izan liteke.



---

## LIPIDOMICS IN MELANOMA: IDENTIFICATION OF NEW LIPID PROGNOSTIC BIOMARKERS

### Introduction

1. Melanoma	1
1.1. Epidemiology.....	1
1.1.1. Incidence.....	1
1.1.2. Mortality.....	3
1.2. Etiology.....	4
1.2.1. Intrinsic factors.....	4
1.2.2. Extrinsic factor.....	5
1.3. Histopathology.....	6
1.3.1. Skin.....	6
1.3.2. Melanoma development.....	8
1.3.3. Melanoma diagnosis and staging.....	9
1.3.4. Clinical classification of melanoma.....	15
1.4. Melanoma treatment.....	16
1.4.1. Metastatic melanoma.....	16
1.4.2. New challenges.....	17
1.5. Melanoma biomarkers.....	18
1.5.1. Biomarker discovery.....	19
1.6. Melanoma hallmarks.....	19
2. Lipids, cell metabolism and cancer	21
2.1. Lipids.....	21
2.1.1. Lipid classification.....	21
2.1.2. Lipid nomenclature.....	35
2.2. Lipidomic analyses.....	37
2.2.1. UHPLC-ESI-MS/MS methodology.....	37
2.2.2. MALDI-MS methodology.....	40
2.3. Cancer metabolism.....	41
2.3.1. Lipid metabolism and cancer.....	42
3. Phospholipase D and cancer	46

### Hypothesis & Objectives

1. Hypothesis	53
2. Objectives	54

---

## Materials & Methods

1. Materials	57
1.1. Reactants.....	57
1.2. Commercial cell lines.....	58
2. Methods	59
2.1. Cell culture .....	59
2.1.1. Defrosting cells.....	60
2.1.2. Cell subculture.....	60
2.1.3. Freezing cells .....	61
2.1.4. Mycoplasma detection.....	61
2.1.5. Cell pellet collection .....	61
2.1.6. Cell transfection .....	61
2.1.7. Cell proliferation assay.....	63
2.1.8. Cell invasion assay.....	63
2.1.9. Cell migration assay.....	64
2.2. Melanocyte isolation from human nevus .....	65
2.3. Cellular lipids analysis.....	66
2.3.1. Sample homogenization.....	66
2.3.2. Protein quantification .....	66
2.3.3. Lipid extraction.....	66
2.3.4. Lipidomic analysis.....	67
2.4. Cell membrane analysis.....	71
2.4.1. Cell membrane isolation .....	71
2.4.2. Protein quantification .....	71
2.4.3. Microarray development .....	71
2.4.4. Lipidomic analysis.....	72
2.5. Protein analysis .....	73
2.5.1. Western blot .....	73
2.5.2. Immunofluorescence .....	77
2.6. PLD enzymatic activity assay <i>in vitro</i> .....	78

---

**Results**

1. Lipidomic analysis of lipid extracts of melanocyte and melanoma cell lines	83
1.1. Differential global lipotype between melanocytes and melanoma cells.....	84
1.2. Different lipid classes exhibit altered levels in melanoma cells.....	89
1.2.1. Glycerophospholipids.....	89
1.2.2. Glycerolipids.....	95
1.2.3. Free fatty acids.....	96
1.2.4. Sphingolipids.....	97
1.2.5. Cholesterol esters.....	98
1.3. Lipid biomarker discovery for malignancy.....	99
2. Lipidomic analysis of functional membrane microarrays	117
3. Phospholipase D2 enhances melanoma progression and metastatic behavior	131
3.1. PLD2 enzyme is upregulated in melanoma cells.....	131
3.2. PLD2 involvement in the carcinogenic process.....	135

**Discussion**

1. Global lipid profiling of human melanocytes and melanoma cell lines	141
2. Finding new lipid biomarkers for melanoma	149
3. Phospholipase D2 promotes tumorigenic and metastatic activities in melanoma cells	155

**Conclusions** 161**Appendix** 165**References** 262





---

## LIPIDOMIKA MELANOMAN: PRONOSTIKORAKO LIPIDO BIOMARKATZAILE BERRIEN IDENTIFIKAZIOA

### Sarrera

1. Melanoma	184
1.1. Epidemiologia.....	184
1.1.1. Intzidentzia.....	184
1.1.2. Heriotza-tasa.....	186
1.2. Etiologia.....	187
1.2.1. Faktore intrintsekoak.....	187
1.2.2. Faktore estrintsekoak.....	188
1.3. Histopatologia.....	189
1.3.1. Larruazala.....	189
1.3.2. Melanoma garapena.....	191
1.3.3. Melanomaren diagnostikoa eta estadifikazioa.....	192
1.3.4. Melanomaren sailkapen klinikoa.....	198
1.4. Melanoma tratamenduak.....	199
1.4.1. Melanoma metastatikoa.....	199
1.4.2. Aukera terapeutiko berriak.....	200
1.5. Melanomaren biomarkatzaileak.....	201
1.5.1. Biomarkatzaile berrien aurkikuntza.....	202
1.6. Melanomaren ezaugarri bereizgarriak.....	203
2. Lipidoak, zelula-metabolismoa eta minbizia	205
2.1. Lipidoak.....	205
2.1.1. Lipidoen sailkapena.....	205
2.1.2. Lipidoen izendapena.....	219
2.2. Analisi lipidomikoak.....	220
2.2.1. UHPLC-ESI-MS/MS metodologia.....	221
2.2.2. MALDI-MS metodologia.....	224
2.3. Minbizi zelulen metabolismoa.....	225
2.3.1. Lipidoen metabolismoa eta minbizia.....	226
3. D Fosfolipasa eta minbizia	230

### Hipotesia eta helburuak

1. Hipotesia	236
2. Helburuak	237

**Eztabaida**

1. Giza melanozito eta melanoma lerro zelular ezberdinen profil lipidiko globala 240
2. Melanomarako biomarkatzaile lipidiko berrien aurkikuntza 248
3. D2 fosfolipasak melanomaren ezaugarri protumoral eta prometastatikoak sustatzen ditu 253

**Ondorioak** 258

**References / Erreferentziak** 262

## FIGURE INDEX

Figure 1. Estimated incidence rates of the diagnosed top 10 cancer types in Europe in 2018. Both sexes and all ages are considered. ....	1
Figure 2. Incidence of melanoma in the U.S. according to the different ethnic groups, between the years 1975-2011. ....	2
Figure 3. Melanoma incidence by age and sex, during 2007-2011 in the United States.....	2
Figure 4. Estimated worldwide skin melanoma incidence distribution for 2018 .....	3
Figure 5. Fitzpatrick scale. ....	4
Figure 6. The principal cell types present in the epidermis .....	7
Figure 7. Representation of the Clark model for melanoma developmen .....	8
Figure 8. Examples of the ABCDE criteria for the early detection of melanoma. ....	10
Figure 9. Clinical description of each stage of melanoma development. ....	14
Figure 10. Timeline of melanoma treatment options since 2011.....	17
Figure 11. General structure of the different lipid classes.....	21
Figure 12. De novo synthesis pathways of PC, PE and PS. Adapted from.....	24
Figure 13. PI cyce.....	27
Figure 14. Glycerophospholipid biosynthesis. ....	30
Figure 15. Schematic representation of the general structure of sphingolipids .....	31
Figure 16. Representation of the metabolic pathways of sphingolipid metabolism .....	33
Figure 17. Schematic representation of the different components of a mass spectrometer ....	39
Figure 18. Workflow of tandem MS/MS strateging .....	40
Figure 19. Schematic representation of the signaling pathways that regulate metabolic rewiring in cancer cell.....	42
Figure 20. Schematic representation of the lipid metabolism rewiring in cancer cells.....	43
Figure 21. Cleavage sites of the different phospholipases .....	46
Figure 22. Workflow schema of PLD2 overexpression and silencing.....	63
Figure 23. Scheme of the transwell in vitro invasion assay, and eventual visualization of the cells that invaded .....	64
Figure 24. Nevus melanocyte isolation process at different steps .....	66
Figure 25. Injection order of the samples analyzed .....	68
Figure 26. Schematic representation of the PLD enzymatic assay reaction .....	79
Figure 27. Categorization of the lipid species identified in the UHPLC-ESI-MS/MS method.....	83
Figure 28. PCA of the study samples and QC samples in both ESI + and ESI- .....	84
Figure 29. Principal components analysis of the samples in ESI+ and ESI- .....	85
Figure 30. PLS-DA analysis of the samples detected in ESI+ classified into groups. ....	87
Figure 31. PLS-DA analysis of the samples detected in ESI- classified into groups.).....	88
Figure 32. Comparison of the sum of the intensities of all the ethanolamine lipid species (A) and choline bearing lipid species in the four study groups. Ratio of the intensities of choline/ethanolamine lipid species in the four study groups. All the sums are related to skin melanocyte values (M = 1). ....	93
Figure 33. Comparison of the sum of the intensities detected for all the phosphatidylinositol species (PI), phosphatidylglycerol species (PG) and phosphatidylserine species (PS) in the four study groups, related to skin melanocyte values (M=1).....	94
Figure 34. Comparison of the sum of the intensities obtained for diglycerides (DG) and triglycerides (TG) in the four study groups, related to skin melanocyte values (M=1). ....	95

---

Figure 35. Comparison of the intensities obtained for all the free fatty acid (FFA) species detected in the four study groups, related to skin melanocyte values (M=1) .....	96
Figure 36. A) Comparison of the sum of the intensities obtained for all the detected ceramides (Cer) in the four study groups, related to skin melanocytes (M=1). B) Comparison of intensities of short and long-ceramides, related to skin melanocytes (M=1).....	97
Figure 37. Comparison of the sum of intensities obtained for all the sphingomyelin (SM) species and hexosylceramide (HexCer) species detected in the four study groups, related to skin melanocytes (M=1). .....	98
Figure 38. Comparison of the sum of intensities detected for all the cholesterol esters (CE) species in the four study groups, related to skin melanocytes (M=1).....	98
Figure 39. Identification of the possible lipid biomarkers for healthy and malignant cells in ESI+.	100
Figure 40. Identification of the possible lipid biomarkers for healthy and malignant cells in ESI-.....	100
Figure 41. Identification of the potential lipid biomarkers for nevus melanocytes and primary melanoma cells in ESI+.....	102
Figure 42. Identification of the potential lipid biomarkers for nevus melanocytes and primary melanoma cells in ESI-.....	102
Figure 43. Identification of the potential lipid biomarkers for nevus melanocytes and metastatic melanoma cells in ESI+.....	104
Figure 44. Identification of the potential lipid biomarkers for nevus melanocytes and metastatic melanoma cells in ESI-.....	104
Figure 45. Identification of the potential lipid biomarkers for primary and metastatic melanoma cells in ESI-.....	106
Figure 46. Box-Whisker graphs for the SMs identified as potential biomarkers for melanoma .....	110
Figure 47. Box-Whisker graphs for the TGs identified as potential biomarkers for melanoma. ....	111
Figure 48. Box-Whisker graphs for the FAs identified as potential biomarkers for melanoma. ....	112
Figure 49. Box-Whisker graphs for the PIs identified as potential biomarkers for melanoma. ....	113
Figure 50. Box-Whisker graphs for the ethanolamine lipids identified as potential biomarkers for melanoma .....	114
Figure 51. Box-Whisker graphs for the choline lipids identified as potential biomarkers for melanoma. ....	115
Figure 52. Box-Whisker graphs for the PGs identified as potential biomarkers for melanoma. ....	116
Figure 53. A) Schema of the sample distribution in the cell membrane microarrays. B) Clustering aggrupation of the samples in 5 clusters (Cl) and 15 clusters (Cl), representing the similarity based on the color scale.....	118
Figure 54. Overview of the lipid species detected in MALDI-MS and representation of their significance to differentiate melanocytes from melanoma cells.....	119
Figure 55. Protein expression pattern of different phospholipases (PLA <sub>2</sub> , PLC, PLD1, PLD2) in 3 skin melanocytes, 5 primary melanomas and 9 metastatic melanoma cell lines assessed by Western blot. ....	132
Figure 56. Identification of PLD2 expression pattern in skin melanocytes, primary melanoma and metastatic melanoma cell lines by immunofluorescence.....	133

---

Figure 57. PLD enzymatic activity for melanocytes, primary melanomas and metastatic melanomas.....	134
Figure 58. PLD2 protein expression (A) and PLD enzymatic activity (B) studies in PLD2 overexpressed and silenced cell lines.....	135
Figure 59. (A) Summary of the results obtained for PLD2 overexpressed and silenced melanoma cell lines in PLD activity, cell proliferation, migration and invasion. Graphical visualization of cell proliferation (B), migration (C) and invasion (D). studies in PLD2 overexpressed and silenced cell lines.....	137
Figure 60. Permutation tests for the validation of PLS-DA analysis of the samples detected in ESI+ ionization mode classified in groups.....	176
Figure 61. Permutation tests for the validation of PLS-DA analysis of the samples detected in ESI- ionization mode classified in groups.....	177



---

## **IRUDIEN ZERRENDA**

Irudia 1. European 2018an diagnostikatutako 10 minbizi mota nagusien intzidentzia-tasa zenbatetsia.....	184
Irudia 2. Melanoma intzidentzia AEB-etan, talde etniko ezberdinen arabera, 1975-2011 urteen artean.....	185
Irudia 3. Melanoma intzidentzia adina eta sexuaren arabera, AEB-tan 2007-2011 urteen artean.....	185
Irudia 4. 2018-ko larruzaleko melanomaren intzidentziaren banaketa zenbatetsia mundu osoan.....	186
Irudia 5. Fitzpatrick eskala.....	187
Irudia 6. Epidermisan dauden zelula mota nagusiak.....	190
Irudia 7. Clark eredu melanomaren garapena irudikatzen.....	191
Irudia 8. Melanoma goiz detektatzeko ABCDE irizpideen adibideak.....	193
Irudia 9. Melanomaren garapen-etapa bakoitzaren deskribapen klinikoa.....	197
Irudia 10. Melanoma tratatzeko aukeren kronologia 2011tik.....	200
Irudia 11. Lipido mota ezberdinen egitura orokorra.....	205
Irudia 12. De novo sintesi-bideak PC, PE eta PS molekulak sortzeko. Epanand et al.-etik hartuta.....	209
Irudia 13. PI zikloa.....	211
Irudia 14. Glizerofosfolipidoen biosintesia.....	214
Irudia 15. Esfingolipidoen egitura orokorraren irudikapen eskematikoa.....	215
Irudia 16. Esfingolipido-metabolismoaren bideen irudikapen eskematikoa.....	217
Irudia 17. Masa-espektrometro baten osagaien irudikapen eskematikoa.....	223
Irudia 18. Tandem MS/MS estrategiaren lan-fluxua eskematikoki adierazita.....	224
Irudia 19. Minbizi-zeluletako bidezidor metabolikoa erregulatzen duten seinaleztapen bideen irudikapen eskematikoa.....	226
Irudia 20. Minbizi zelulen lipido metabolismoan ematen diren aldaketen irudikapen eskematikoa.....	227
Irudia 21. Fosfolipasa ezberdinen hidrolizazio lekuak.....	230





## TABLE INDEX

Table 1. Description of the criteria used to classify the staging of melanoma.....	12
Table 2. Staging of melanoma based on TNM system.....	13
Table 3. Short description of the three most common fatty acid molecules.....	22
Table 4. Abbreviations of the lipid classes detected in this work.....	36
Table 5. Recovery rates (%) of the different standards performing the lipid extraction of a sample using Bligh & Dyer method and precipitation with isopropanol.....	38
Table 6. List of the reactants used for the experiments and the supplier.....	57
Table 7. Detailed description of the commercial cell lines used in this study.....	59
Table 8. Complete cell culture media composition for each cell line.....	60
Table 9. UHPLC-ESI-Q-TOF analysis condition.....	68
Table 10. Percentage of acrylamide needed to resolve the proteins according to their molecular weight.....	74
Table 11. Composition of the running and stacking gels relying on the acrylamide percentage.....	75
Table 12. Reagents used for casting the gels and their functions.....	75
Table 13. Loading buffer composition.....	75
Table 14. Primary antibodies used for western blot.....	77
Table 15. Secondary antibodies used for western blot.....	77
Table 16. Pathological classification of the cell lines studied by UHPLC-ESI-MS/MS methodology.....	83
Table 17. Validation of the PLS-DA models.....	89
Table 18. Sum of the intensities obtained for all lipid species that make up each lipid subclass and comparison of the intensity variation of each subclass in the different study groups, related to control group (Melanocytes [M]=1).....	90
Table 19. Sum of the intensities obtained for all the PC, PC(P/O), PE and PE(P/O) lipid species detected, and the ratios PC/PC(P/O), PE/PE(P/O), choline lipids/ethanolamine lipids, PC/PE, PC(P/O)/PE(P/O), LPC/LPE. The results of each study group are compared to the values obtained for skin melanocytes, that is considered the control group (Melanocytes [M]=1).....	92
Table 20. Sum of the intensities obtained for all glycerolipid species (TG & DG) and comparison of the intensity variation of each class in the different study groups, related to control group (Melanocytes [M]=1).....	95
Table 21. Sum of the intensities obtained for all lipid free fatty acid (FFA) species detected and comparison of the intensity variation of this class in the different study groups, related to control group (Melanocytes [M]=1).....	96
Table 22. Sum of the intensities obtained for all lipid the species that make up each lipid subclass within the sphingolipids and comparison of the intensity variation of each subclass in the different study groups, related to control group (Melanocytes [M]=1).....	97
Table 23. List of lipid potential biomarkers to discriminate between non-malignant and malignant cells.....	101
Table 24. List of lipid potential biomarkers to differentiate between nevus and primary melanoma cells.....	103
Table 25. List of lipid species that discriminate nevus melanocytes from metastatic melanoma cells.....	105
Table 26. List of lipid potential biomarkers of metastatic melanoma compared to primary melanoma cells.....	106
Table 27. Summary of the potential biomarkers.....	107

---

Table 28. List of lipids with significantly higher intensity in melanocytes (skin and nevus) or in melanoma cells (primary and metastatic) .....	120
Table 29. List of significant lipids with differential higher intensity in skin melanocytes or nevus melanocytes .....	124
Table 30. List of significant lipids with differential higher intensity in skin melanocytes or primary melanomas .....	124
Table 31. List of significant lipids with differential higher intensity in nevus melanocytes or primary melanomas. ....	126
Table 32. List of significant lipids with differential higher intensity in skin melanocytes or metastatic melanomas .....	127
Table 33. List of significant lipids with differential higher intensity in nevus melanocytes or metastatic melanoma .....	129
Table 34. List of significant lipids with differential higher intensity in primary or metastatic melanoma .....	130
Table 35. PC/PE ratio of the intensities obtained for the different PC and PE species that have the same acyl-chains, related to control group (skin melanocytes =1). ....	144
Table 36. PC/PS ratio of the intensities obtained for the different PC and PS molecules that share the same acyl-chains, related to control group (skin melanocytes=1) .....	145
Table 37. PE/PS ratio of the intensities obtained for the different PE and PS molecules that share the same acyl-chains, related to control group (skin melanocytes=1). ....	146
Table 38. SM/Cer ratio of the intensities obtained for the different SM and Cer molecules that share the same acyl-chains, related to control group (skin melanocytes=1). ....	147
Table 39. List of lipid molecules with significantly altered levels in the different statistical comparisons .....	151
Table 40. List of the detected lipid species by UHPLC-ESI-MS/MS approach, the media and standard deviation of their intensity, and the % of presence of each specie within its subclass .....	165

---

**TAULEN ZERRENDA**

Taula 1. Melanomaren estadifikazioa sailkatzeko erabiltzen diren irizpideen deskribapena ..	195
Taula 2. TNM sisteman oinarritutako melanomaren estadifikazioa.....	196
Taula 1. Gantz-azido molekula arruntenen deskribapena.....	206
Taula 4. Azilo albo-kate berdinak dituzten PC eta PE espezieen intentsitatearen PC/PE proportzioa, kontroleko taldeak lortutako emaitzekin erlazionatuta.....	243
Taula 5. Azilo albo-kate berdinak dituzten PC eta PS espezieen intentsitatearen PC/PS proportzioa, kontroleko taldeak lortutako emaitzekin erlazionatuta.....	244
Taula 6. Azilo albo-kate berdinak dituzten PE eta PS espezieen intentsitatearen PE/PS proportzioa, kontroleko taldeak lortutako emaitzekin erlazionatuta.....	245
Taula 7. Azilo albo-kate berdina duten SM eta Cer espezieen intentsitatearen SM/Cer proportzioa, kontroleko taldeak lortutako emaitzekin erlazionatuta.....	246
Taula 8. Konparazio estatistikoetan euren mailak esanguratsuki aldatuta dituzten lipido espezieen zerrenda.....	250



**ABBREVIATIONS / LABURDURAK**

	<b>ENGLISH</b>	<b>EUSKARA</b>
<b>AA</b>	Arachidonic acid	Azido arakidoniko
<b>ACAT</b>	Acyl-CoA:cholesterol acyltransferase	Azil-CoA:kolesterol aziltransferasa
<b>ACC</b>	Acetyl-CoA carboxylase	Azetil-CoA karboxilasa
<b>ACDase</b>	Acid ceramidase	Zeramidasazido
<b>ACLY</b>	ATP citrate lyase	ATP zitrato liasa
<b>ACS</b>	Acyl-CoA synthetase	Azil-CoA sintetasa
<b>ADAPS</b>	Alkyl-DHAP synthase	Alkil-DHAP sintasa
<b>ADP</b>	Adenosine diphosphate	Adenosina difosfato
<b>AGPS</b>	Alkylglycerone phosphate synthase	Alkilglizerona fosfato sintasa
<b>AIDS</b>	Acquired immune deficiency syndrome	HIES-Hartutako immunoeskasiaren sindromea
<b>AJCC</b>	American Joint Committee on Cancer	Minbiziari buruzko Amerikako Komite Bateratua
<b>ALM</b>	Acral lentiginous melanoma	Melanoma akral lentiginosoa
<b>ALT</b>	Alanine aminotransferase	Alanina aminotransferasa
<b>APAF-1</b>	Apoptosis protease-activating factor-1	Apoptosiaren proteasa aktibatzen duen faktore-1
<b>ATP</b>	Adenosine triphosphate	Adenosina trifosfato
<b>BCA</b>	Bicinchoninic Acid Solution	Azido bizinkoniniko soluzioa
<b>BCL-2</b>	B-Cell lymphoma 2	B-zelulen linfoma 2
<b>CCT</b>	CTP:phosphocholine cytidyltransferase	CTP:fosfokolina zitidiltransferasa
<b>CDASE</b>	Ceramidase	Zeramidasazido
<b>CDKN2A</b>	Cyclin-dependent kinase inhibitor 2A	Ziklina-menpeko kinasa inibitzailea 2A
<b>CDP</b>	Cytidine diphosphate	Zitidina difosfato
<b>CDP-DG</b>	Cytidine diphosphate diglyceride	Zitidina difosfato diglizerido
<b>CE</b>	Cholesterol ester	Kolesterol ester
<b>CER</b>	Ceramide	Zeramida
<b>CERK</b>	Ceramide kinase	Zeramida kinasa
<b>CERS</b>	Ceramide synthase	Zeramida sintasa
<b>CERT</b>	Ceramide transporter	Zeramida garraiatzaile
<b>CK</b>	Choline kinase	Kolina kinasa
<b>CL</b>	Cardiolipin	Kardiolipina
<b>CMP</b>	Cytidine monophosphate	Zitidina monofosfato
<b>CDP</b>	Cytidine diphosphate	Zitidina difosfato
<b>CPT1</b>	Carnitine palmitoyltransferase 1	Karnitina palmitoiltransferasa 1
<b>CTLA-4</b>	Cytotoxic T lymphocyte-associated protein 4	T linfozito zitotoxikoen proteina 4
<b>CTP</b>	Cytidine triphosphate	Zitidina trifosfato
<b>DAG OR DG</b>	Diglyceride or diacylglycerol	Diglizerido edo diazilglizerido
<b>DAN</b>	2,5-diaminonaphtalene	2,5-diaminonaftaleno
<b>DCRIT</b>	Maximum tolerable distance	Gehienezko distantzia onargarria

<b>DGAT</b>	Diacylglycerol acyltransferase	Diazilglizerol aziltransferasa
<b>DHA</b>	Docosahexaenoic acid	Azido dokosaheaxenoiko
<b>DHAP</b>	Dihydroxyacetone phosphate	Dihidroxiacetona fosfato
<b>DHAPAT</b>	Dihydroxyacetonephosphate acyltransferase	Dihidroxiacetonafosfato aziltransferasa
<b>DMODX</b>	Distance to the model in X-space	X-planoan egindako eredurako distantzia
<b>DMSO</b>	Dimethyl Sulfoxide	Dimetil sulfoxido
<b>DNA</b>	Deoxyribonucleic acid	Azido desoxirribonukleiko
<b>DTT</b>	Dithiothreitol	Ditiotreitol
<b>ECL</b>	Enhanced ChemiLuminescence	Areagotutako kimioluminiszentzia
<b>ECT</b>	CTP:phosphoethanolamine cytidyltransferase	CTP:fosfoetanolamina zitidiltransferasa
<b>EGF</b>	Epidermal growth factor	Hazkuntza faktore epidermiko
<b>EGFR</b>	Epidermal growth factor receptor	Hazkuntza faktore epidermikoaren hartzaile
<b>EK</b>	Ethanolamine kinase	Etanolamina kinasa
<b>ELOVL5</b>	Elongases of very long fatty acids protein	Kate oso luzeko gantz azidoen elongasak
<b>EMA</b>	European Medicines Agency	Europako Medikamentuen Agentzia
<b>EPA</b>	Eicosapentaenoic acid	Azido eikosapentaenoiko
<b>EPT</b>	Ethanolamine phosphotransferase	Etanolamina fosfotransferasa
<b>ER</b>	Endoplasmic reticulum	Erretikulu endoplasmiko
<b>ERK</b>	Extracellular signal-regulated kinase	Zelula-kanpoko seinalez erregulaturiko kinasa
<b>ESI</b>	Electrospray ionization	Elektroesprai bidezko ionizazioa
<b>H<sub>2</sub>O</b>	Water	Ur
<b>FA</b>	Fatty acid	Gantz azido
<b>FABP7</b>	Fatty acid-binding protein 7	Gantz azidoetara lotzen den proteina 7
<b>FADS</b>	Fatty acid desaturase	Gantz azido desaturasa
<b>FAMMM</b>	Familial Atypical Multiple Moles and Melanoma	Orezta atipiko aniztun melanoma familiarra
<b>FAO</b>	Fatty acid oxidation	Gantz azidoen oxidazio
<b>FAS</b>	Fatty acid synthase	Gantz azido sintasa
<b>FBS</b>	Fetal Bovine Serum	Behi serum fetala
<b>FDA</b>	Food and Drug Administration	Elikagai eta Farmakoen Administrazioa
<b>FFA</b>	Free Fatty Acid	Gantz azido askea
<b>G3P</b>	Glycerol-3-phosphate	Glizerol-3-fosfato
<b>GALCER</b>	Galactosylceramide	Galaktosilzeramida
<b>GCS</b>	Glucosylceramide synthase	Glukosilzeramida sintasa
<b>GEF</b>	Guanine nucleotide exchange factor	Guanina nukleotidoa trukatzeko faktore
<b>GL</b>	Glycerolipids	Glizerolipido
<b>GLCCER</b>	Glucosylceramide	Glukosilzeramida
<b>GPL</b>	Glycerophospholipid	Glizerofosfolipido
<b>GM-CSF</b>	Granulocyte-macrophage colony-stimulating factor	Granulozito-makrofagoen koloniak estimulatzeko faktore
<b>GP-100</b>	Glycoprotein 100	Glikoproteina 100

<b>GPAT</b>	Glycerol-3-phosphate acyltransferase	Glizerol-3-fosfato aziltransferasa
<b>HBSS</b>	Hank's Balanced Salt Solution	Hank soluzio gazi orekatua
<b>HEXCER</b>	Hexosylceramide	Hexosilzeramida
<b>HIF-1</b>	Hypoxia Inducible Factor-1	Hipoxia-eragile faktorea 1
<b>HMB45</b>	Human Melanoma Black-45	Giza melanoma beltza 45
<b>HMGB1</b>	High mobility group box 1	Mugikortasun handiko box 1 talde
<b>HMG-COA</b>	Hydroxymethylglutaryl CoenzymeA	Hidroximetilglutaril KoentzimaA
<b>HMGR</b>	HMG-CoA reductase	HMG-CoA erreduktasa
<b>HMGS</b>	Human Melanocyte Growth Supplement	Giza melanozitoen hazkuntzarako osagarria
<b>HRP</b>	Horseradish peroxidase	Errefau peroxidasa
<b>HSV1</b>	Herpes simplex virus	Herpes simplex birusa
<b>IFN-A</b>	Interferon-alpha	alpha-interferona
<b>IL-2</b>	Interleukin-2	2 Interleukina
<b>IL-8</b>	Interleukin-8	8 Interleukina
<b>INK4A</b>	Cell-cycle inhibitor of kinase 4A	Zelula-zikloaren inhibitzailea den kinasa 4A
<b>JAK3</b>	Janus kinase 3	Janus kinasa 3
<b>LCL</b>	Lysocardiolipin	Lisokardiolipina
<b>LD</b>	Lipid droplets	Gantz tantak
<b>LDH</b>	Lactate dehydrogenase	Laktato deshidrogenasa
<b>LMM</b>	Lentigo maligna melanoma	Lentigo maligna melanoma
<b>LPA</b>	Lysophosphatidic acid	Azido lisofosfatidiko
<b>LPAAT</b>	LysoPA acyltransferase	LisoPA aziltransferasa
<b>LPC</b>	Lysophosphatidylcholine	Lisofosfatidilkolina
<b>LPCAT</b>	LPC acyltransferase	LPC aziltransferasa
<b>LPCLAT</b>	LCL acyltransferase	LCL aziltransferasa
<b>LPE</b>	Lysophosphatidylethanolamine	Lisofosfatidiletanolamina
<b>LPEAT</b>	LPE acyltransferase	LPE aziltransferasa
<b>LPG</b>	Lysophosphatidylglycerol	Lisofosfatidilglizerol
<b>LPGAT</b>	LPG acyltransferase	LPG aziltransferasa
<b>LPI</b>	Lysophosphatidylinositol	Lisofosfatidilinositol
<b>LPIAT</b>	LPI acyltransferase	LPI aziltransferasa
<b>LPLAT</b>	Acyl-CoA:lysophospholipid acyltransferases	Azil-CoA:lisofosfolipidoen aziltransferasa
<b>LPS</b>	Lysophosphatidylserine	Lisofosfatidilserina
<b>M</b>	Skin melanocytes	Larruazaleko melanozitoak
<b>M/Z</b>	mass-to-charge ratio	masa-karga ratioa
<b>MAGL</b>	Monoacylglycerol lipase	Monoazilglizerol lipasa
<b>MALDI</b>	Matrix-assisted laser desorption and ionization	Laser bidezko desortzioa eta ionizazioa matrize bidez lagunduta
<b>MAPK</b>	Mitogen-activated protein kinase	Mitogenoz aktibatutako proteina kinasa
<b>MBT</b>	2-mercaptobenzothiazole	2-merkaptobezotiazol
<b>MCT</b>	Monocarboxylate transporter	Monokarboxilato garraiatzaile
<b>MG</b>	Monoglyceride	Monoglizerido
<b>MM</b>	Metastatic melanoma	Melanoma metastatiko

<b>MMGL</b>	Lymph-node metastatic melanoma	Gongoil linfatikoetako melanoma metastatiko
<b>MMNS</b>	Subcutaneous metastatic melanoma	Larruazalpeko melanoma metastatiko
<b>MP</b>	Primary melanoma	Melanoma primario
<b>MRNA</b>	Messenger RNA	RNA mezulari
<b>MS</b>	Mass spectrometry	Masa espektrometria
<b>MS/MS</b>	Tandem mass spectrometry	Tandem masa-espektrometria
<b>MTOR</b>	Mammalian target of rapamycin	Rapamizinareen itua ugaztunetan
<b>MUFA</b>	Monounsaturated fatty acids	Gantz azido monoinsaturatua
<b>N</b>	Nevus melanocytes	Nevus melanozitoak
<b>NADPH</b>	Nicotinamide adenine dinucleotide phosphate	Nikotinamida adenina dinukleotido fosfato
<b>NER</b>	Nucleotide excision repair	Nukleotidoen erauzketa bidezko konponketa
<b>NM</b>	Nodular melanoma	Melanoma nodular
<b>NMR</b>	Nuclear magnetic resonance	Erresonantzia magnetiko nuklear
<b>OPLS-DA</b>	Orthogonal partial least squares discriminant analysis	Minimo karratu partzial ortogonalak bereizteko analisisa
<b>OXPHOS</b>	Oxidative phosphorylation	Fosforilazio oxidatibo
<b>PA</b>	Phosphatidic acid	Azido fosforiko
<b>PAF</b>	Paraformaldehyde	Paraformaldehido
<b>PAGE</b>	Polyacrilamide gel electrophoresis	Poliakrilamidazko gelen bitarteko elektroforesia
<b>PAP</b>	Phosphatidic acid phosphatase	Azido fosfatidikoaren fosfatasa
<b>PBS</b>	Phosphate saline buffer	Fosfato gatz soluzio indargetzailea
<b>PC</b>	Phosphatidylcholine	Fosfatidilkolina
<b>PC(P/O)</b>	Phosphatidylcholine ether	Fosfatidilkolina eter
<b>PC8</b>	Short side-chain phosphatidylcholine [PC(8:0/8:0)]	Kate-laburreko fosfatidilkolina [PC(8:0/8:0)]
<b>PCA</b>	Principal Components Analysis	Osagai nagusien analisisa
<b>PD-1</b>	Programmed cell death protein 1	Programatutako zelula heriotzaren proteina 1
<b>PDAT</b>	Phospholipid:diacylglycerol acyltransferase	Fosfolipido:diailgizerol aziltransferasa
<b>PDGF</b>	Platelet-derived growth factor	Plaketetik eratorritako hazkuntza faktorea
<b>PDGFR</b>	Platelet-derived growth factor receptor	Plaketetik eratorritako hazkuntza faktorearen hartzailea
<b>PD-L1</b>	Programmed cell death ligand 1	Programatutako zelula heriotzaren proteina 1-aren hartzailea
<b>PE</b>	Phosphatidylethanolamine	Fosfatidiletanolamina
<b>PE(P/O)</b>	Phosphatidylethanolamine ether	Fosfatidiletanolamina eter
<b>PEMT</b>	Phosphatidylethanolamine methyltransferase	Fosfatidiletanolamina metiltransferasa
<b>PG</b>	Phosphatidylglycerol	Fosfatidilgizerol
<b>PH</b>	Pleckstrin homology domain	Pleckstrina homologia duen domeinua
<b>PI</b>	Phosphatidylinositol	Fosfatidilinositol
<b>PI3K</b>	Phosphatidylinositol 3-kinase	Fosfatidilinositol 3-kinasa



<b>PIP</b>	Phosphatidylinositol phosphate	Fosfatidilinositol fosfato
<b>PIP<sub>2</sub></b>	Phosphatidylinositol 4,5-biphosphate	Fosfatidilinositol 4,5-bifosfato
<b>PIP<sub>3</sub></b>	Phosphatidylinositol triphosphate	Fosfatidilinositol trifosfatao
<b>PKC</b>	Protein kinase C	Proteina kinasa C
<b>PLA<sub>2</sub></b>	Phospholipase A <sub>2</sub>	A <sub>2</sub> Fosfolipasa
<b>PLB</b>	Phospholipase B	B Fosfolipasa
<b>PLC</b>	Phospholipase C	C Fosfolipasa
<b>PLD1</b>	Phospholipase D1	D1 Fosfolipasa
<b>PLD2</b>	Phospholipase D2	D2 fosfolipasa
<b>PLS-DA</b>	Partial least squares discriminant analysis	Minimo karratu partzialak bereizteko analisia
<b>PMEL</b>	Premelanosome protein	Premelanosoma proteina
<b>PPI</b>	Pyrophosphate	Pirofosfato
<b>PPIN</b>	Phosphoinositides	Fosfoinositidoak
<b>PPP</b>	Pentose phosphate pathway	Pentosa fosfatoen bidea
<b>PRB</b>	Retinoblastoma protein	Erretinoblastoma proteina
<b>PS</b>	Phosphatidylserine	Fosfatidilserina
<b>PSD</b>	Phosphatidylserine decarboxylase	Fosfatidilserina descarboxilasa
<b>PSS</b>	Phosphatidylserine synthase	Fosfatidilserina sintasa
<b>PSS1</b>	Phosphatidylserine synthase 1	Fosfatidilserina sintasa 1
<b>PSS2</b>	Phosphatidylserine synthase 2	Fosfatidilserina sintasa 2
<b>PTEN</b>	Phosphatase and tensin homologue	Fosfatasa eta tensinaren homologoa
<b>PUFA</b>	Polyunsaturated fatty acid	Gantz azido poliinsaturatua
<b>PX</b>	Phox homology domain	Phox homologia duen domeinua
<b>QC</b>	Quality Control	Kalitate-Kontrola
<b>Q-TOF</b>	Quadrupole-time-of-flight	Kuadrupolo-hegaldi-denbora
<b>RGP</b>	Radial growth phase	Hazkuntza erradialeko fasea
<b>RNA</b>	Ribonucleic acid	Azido erribonukleiko
<b>RTK</b>	Receptor tyrosine kinase	Tirosina kinasa hartzaile
<b>S1P</b>	Sphingosine 1-phosphate	Esfingosina 1-fosfato
<b>SCD</b>	Stearoyl-CoA desaturases	Estearoil-CoA desaturasa
<b>SDS</b>	Sodium Dodecyl Sulfate	Sodio dodezil fosfato
<b>SDS-PAGE</b>	SDS-polyacrylamide gel electrophoresis	SDS-poliakrilamida gelen bidezko elektroforesia
<b>siRNA</b>	Small interfering RNA	Interferentziako RNA laburra
<b>SK</b>	Sphingosine kinase	Esfingosina kinasa
<b>SM</b>	Sphingomyelin	Esfingomielina
<b>SMASES</b>	Sphingomyelinases	Esfingomielinasa
<b>SMS</b>	Sphingomyelin synthase	Esfingomielina sintasa
<b>SMS1</b>	Sphingomyelin synthase 1	Esfingomielina sintasa 1
<b>SPL</b>	Sphingolipids	Esfingolipidoak
<b>SPT</b>	Serine palmitoyltransferase	Serina palmitoiltransferasa
<b>SREBP</b>	Sterol regulatory element-binding proteins	Esterola erregulatzen duen elementuarekin lotzeko proteinak

<b>SSM</b>	Superficial spreading melanoma	Azalerako hedadura duen melanoma
<b>TBS-T</b>	TBS-Tween 20	TBS-Tween 20
<b>TCA</b>	Tricarboxylic acid cycle	Azido trikarboxilikoaren zikloa
<b>TCR</b>	T-cell receptor	T zelulen hartzaile
<b>TG</b>	Triglyceride	Triglizerido
<b>TIC</b>	Total ion current	Gutzizko ioien korronea
<b>TILS</b>	Tumor infiltrating lymphocytes	Tumorean infiltraturiko linfuzitoak
<b>TLC</b>	Thin layer chromatography	Geruza finean egindako kromatografia
<b>TVEC</b>	Talimogene laherparepvec	Talimogene laherparepvec
<b>UHPLC</b>	Ultra-high pressure liquid chromatography	Presio ultra handiko kromatografia likidoa
<b>UICC</b>	Union for International Cancer Control	Minbiziaren kontrolerako nazioarteko batasuna
<b>UV</b>	UltraViolet light	Erradiazio ultramore
<b>VEGF</b>	Vascular Endothelial Growth Factor	Endotelio baskularraren hazkuntza faktore
<b>VGP</b>	Vertical growth phase	Hazkuntza bertikaleko fasea
<b>VIP</b>	Variable Importance in Projection	Aldagaien inportantzia proiektzioan





# **INTRODUCTION**



## 1. Melanoma

Melanoma is the cancer that arises upon the malignant transformation of the melanocytes that acquire the ability to grow and proliferate uncontrollably. Melanocytes generate melanin, which spreads to neighboring cells and protects them from UV radiation. Although the main majority of melanomas occur in the skin, there are also non-skin melanomas, such as, uveal and mucosal melanomas, among others. Despite representing only 4% of all skin tumors diagnosed, skin melanoma is the most lethal form, since it is responsible for 80% of the deaths caused by these cancers. Moreover, every hour a person dies in the U.S.A. due to melanoma<sup>1</sup>.

### 1.1. Epidemiology

#### 1.1.1. Incidence

The incidence of melanoma has steadily increased during the last decades throughout the world. For instance, in the United States in 1930, the probability of suffering from melanoma was 1 in 1,500; however, in 2011 that risk was 1 in 52<sup>2</sup>. Concretely in Spain, it is predicted that there will be 150,000 new cases in 2019<sup>3</sup>. Furthermore, it is estimated that it was the seventh type of cancer with the highest incidence in Europe in 2018, affecting 11.2 people per 100,000 (**Fig. 1**).

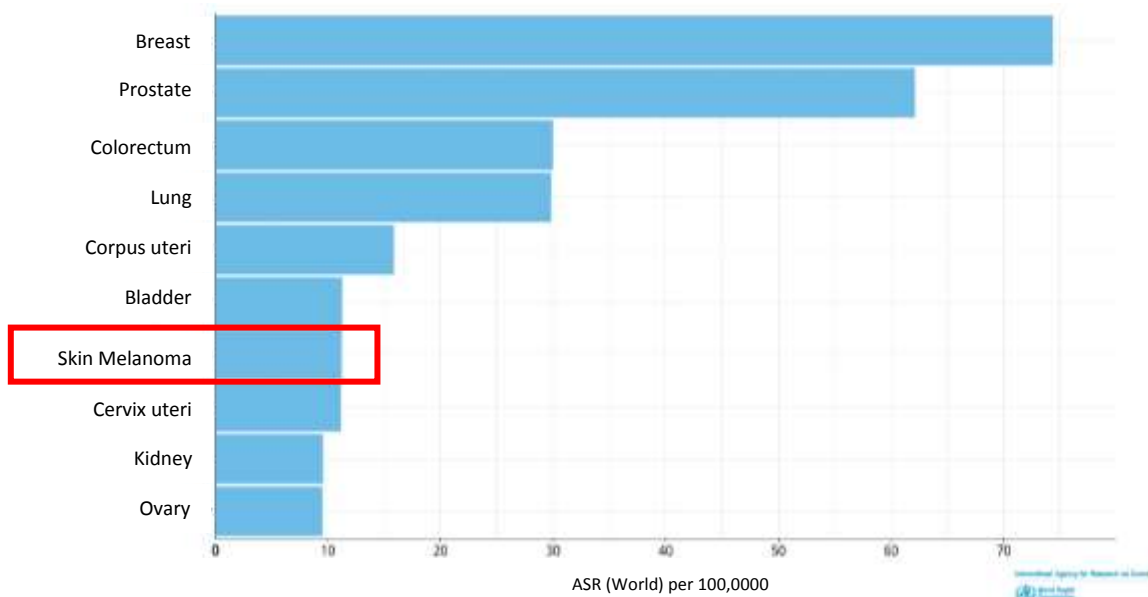


**Figure 1.** Estimated incidence rates of the diagnosed top 10 cancer types in Europe in 2018. Both sexes and all ages are considered<sup>3</sup>.

The incidence varies according to ethnicity, sex, age and the geographical region studied. Concretely, the incidence of melanoma is reasonably higher among fairly-skinned Caucasians. As it is known, UV radiation is the main risk factor for melanoma, so the melanin of the darker-pigmented individuals forms a barrier that protects cells from the carcinogenic effects of sunlight. Although melanoma is disproportionately related to Caucasians, the overall five-year survival rate is lower for African Americans, since the diagnosis is usually made earlier in the individuals with milder pigmentation. Furthermore, the tumors arise in different areas depending on the ethnicity; in Caucasians, it tends to appear in sun-exposed areas, while in dark-

skinned people it usually develops in non-sun-exposed areas such as mucous membranes, nail beds, and the palms of hands and soles of the feet. Thus, making it more difficult to detect the tumors<sup>4</sup>.

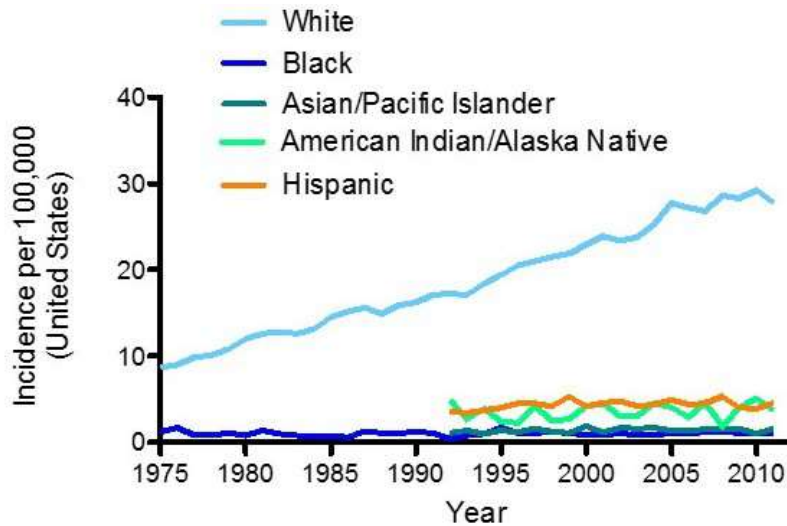


Figure 2. Incidence of melanoma in the U.S. according to the different ethnic groups, between the years 1975-2011<sup>4</sup>.

Melanoma affects each sex differently. Besides, the incidence rates also depend on the age of the patient. Melanoma is more common among adolescent and young women, than in men. However, at the age of 40, the trends are reversed and men are more likely to suffer from melanoma. Altogether, the incidence rates are higher in men. Regardless of the increase in the incidence in both sexes, the rates have spread massively among women under 40 years, probably due to the popularization of the use of tanning beds and having a tanned complexion among women<sup>5</sup>.

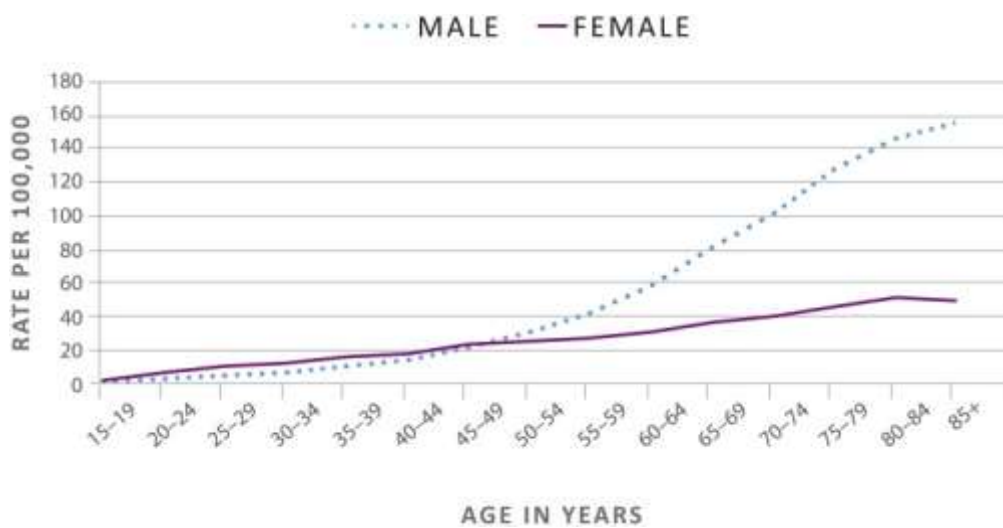
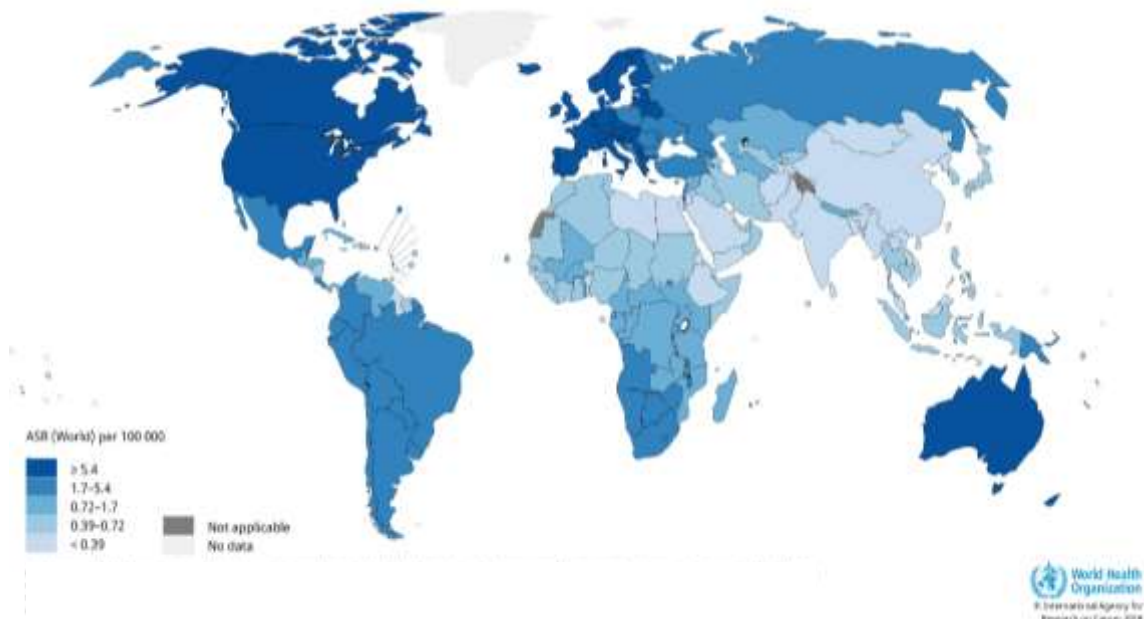


Figure 3. Melanoma incidence by age and sex, during 2007-2011 in the United States<sup>5</sup>.



Even among individuals of the same ethnic group, the incidence of melanoma varies according to geographical location. Taking into account lightly-pigmented individuals, countries located close to the equator have higher rates of melanoma, since they are exposed to higher UV intensities. Notably, the countries with the highest rates of melanoma are New Zealand and Australia (Fig. 4), as they have high rates of lightly-pigmented individuals and are found in lower latitudes. However, within Europe, an inverse latitude gradient has been perceived. In fact, central and northern countries such as Switzerland, the Netherlands, Denmark, Norway and Sweden present a three-to-six times higher risk of melanoma than in southern countries. This could be partly due to the lighter skin phototype of the population these countries and the sun exposure pattern.

While people in northern countries have occasional sun exposure and sunburn easily, individuals in southern countries have a cumulative sun exposure. Significantly, a north-south incidence gradient has been observed within the population of Australia and the Scandinavian countries, where the people living in closer to the equator present a greater risk of melanoma<sup>6</sup>.



**Figure 4. Estimated worldwide skin melanoma incidence distribution for 2018<sup>3</sup>.** Dark blue represents 5.4 melanoma cases per 100,000 inhabitants, while light blue represents less than 0.39 melanoma cases per 100,000 inhabitants.

### 1.1.2. Mortality

Similarly to incidence, melanoma mortality rates are also related to sex, age, ethnicity and geographical location. However, mortality rates have not followed the same trends as incidence. In fact, in the last 20 years they have stabilized, probably due to the advances in awareness, early diagnosis and medical and surgical care<sup>4</sup>. Equally to incidence, melanoma mortality is higher in the low latitude regions near the equator. According to sex and age, men have higher mortality rates than women worldwide, and the peak of mortality is beyond the seventh decade of life. Within the ethnic groups in the United States, mortality is greater among Caucasians than among African-Americans. However, even if Caucasians are more prone to suffer melanoma,

this is usually detected at an earlier stage than in dark pigmented ethnic groups. Thus, 5-year survival is lower for African-Americans than for Caucasians. In fact, the 5-year survival rate has risen among Caucasians over the past decade, while it has declined for African-Americans. However, the socioeconomic status has been blamed for this trend<sup>5</sup>.

### 1.2. Etiology

Although the etiology of melanoma is still unknown, some risk factors have been identified to favor the appearance and development of this cancer. These factors can be divided in intrinsic factors that are inherent to the patient and extrinsic or environmental factors.

#### 1.2.1. Intrinsic factors

As mentioned above, the **age** and **sex** of the patient are important factors in determining the probability of developing melanoma. In this regard, there is a greater overall risk of melanoma with advanced age for both women and men, with the average age of diagnosis being 60 years. In general, there is a higher risk in males, with a ratio of 2 men: 1 women at age 80; conversely, as seen in **Figure 3**, the rate is greater for women under 40 years of age in the U.S.<sup>2</sup>.

The amount of melanin in the skin of an individual defines its **skin phototype**, which determines the patient's susceptibility to developing melanoma. In 1975, Thomas B. Fitzpatrick established the Fitzpatrick scale that numerically categorizes an individual's vulnerability to UV, and its risk to consequently develop melanoma based on its tendency to tan and burn, and its basal levels of pigment. Individuals with pale skin, blond or red hair, freckles, high tendency to burn and inability to tan have been associated with a low Fitzpatrick score and are more likely to develop melanoma (**Fig. 5**). In contrast, people with a higher Fitzpatrick score have darker skin, do not burn, tan easily, and this is associated with a relative lower risk of developing melanoma<sup>2,4</sup>.

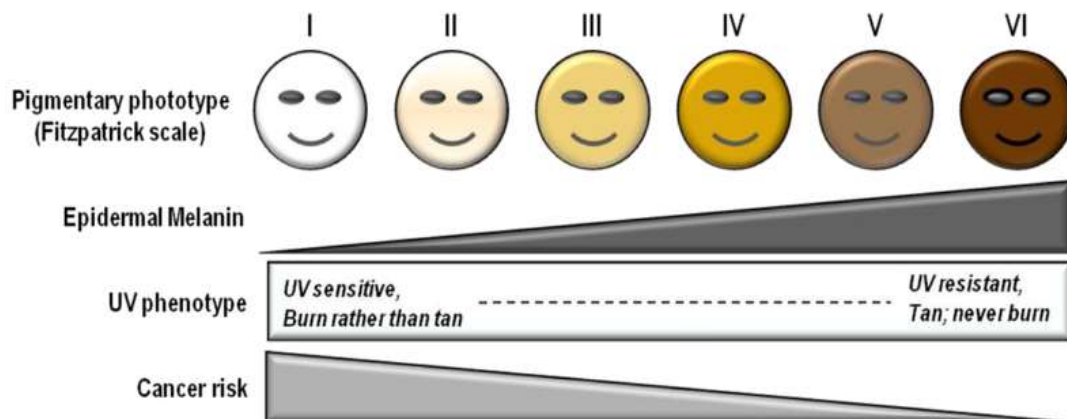


**Figure 5. Fitzpatrick scale.** Numerical classification to determine the susceptibility of an individual to UV radiation and melanoma development. Taken from<sup>7</sup>.

Only 5-10% of melanoma cases have a **genetic component**, but the **family history** of melanoma has been related to an increased risk of developing this disease. Notably, if a primary relative has suffered melanoma, the risk is 1.7 higher, and if one parent has multiple melanoma, the risk is 61.78 greater<sup>2,5</sup>. Although it is still unknown if this increased risk is due to an inherited genetic predisposition or shared environmental factors, some genetic disorders have been linked to an

increased risk of developing melanoma. The most studied disorder is Xeroderma pigmentosum<sup>2,4,7</sup>. This is an autosomal recessive condition that increases the risk in a 1000-fold. Patients with this syndrome have a defective nucleotide excision repair (NER) that is the responsible for correcting DNA lesions. Thus, the cells are unable to repair the DNA damage generated by UV radiation, and individuals develop UV hypersensitivity and 65% of the tumors originate in sun-exposed anatomical areas. Another alteration is Familial Atypical Multiple Moles and Melanoma (FAMMM) syndrome. This is described as having two or more direct relatives with a history of both melanoma and dysplastic nevi. In particular, at age 50, an individual diagnosed with this syndrome has a 49% greater risk of suffering from melanoma, and 82% at 72 years. This disorder is caused by mutations in the CDKN2A gene, which encodes p16 and p14 tumor suppressor proteins<sup>2,4,5,7</sup>. Furthermore, in 90% of melanoma cases there is an enhanced expression of Bcl-2 protein, which is an apoptosis inhibitor. The mTOR pathway, a pivotal regulator of the cell cycle, is activated in 67-77% of cases. The gain-of-function mutation of MAPK/ERK pathway generates the constant activation of BRAF kinase in 60-80% of the melanomas, favoring the proliferation of the melanocytes<sup>8</sup>.

In addition, previous **personal history** of any type of skin cancer increases the chance of having melanoma. Unsurprisingly, people with melanoma have a 8% risk of having a second one<sup>4,7</sup>. Besides, it has been reported that other personal medical conditions are also related to an increased likelihood of developing melanoma. As it is known, the immune system plays a key role in protecting the body against cancer. Therefore, people with AIDS have an elevated chance of developing melanoma. Similarly, people who have received an organ transplant are 6% more likely to have melanoma if the transplant was during adulthood, and a 14% chance in children's transplants. In addition, a link with breast cancer has been detected. People who have had breast cancer and are carriers of the BRCA2 mutation have a relative risk of 2.58 to develop melanoma. Among patients with a history of lymphocytic leukemia or non-Hodgkin's lymphoma, there is a greater chance of having melanoma, since this is one of the most probable secondary cancer in both conditions<sup>2</sup>.

The presence of a large number of **nevi** has been connected to a higher chance of having melanoma. Most nevi and melanoma share the BRAF mutation, which is able to create nevus, but additional mutations are needed for melanoma development. The malignant transformation of typical moles is rare, whereas the presence of dysplastic nevi increases the risk. In fact, a dysplastic nevus increases the risk by two, while 16 to 40 typical moles increase the risk by 1.47. Significantly, no association has been detected between congenital nevi and melanoma development<sup>2,4,7</sup>.

#### 1.2.2. Extrinsic factor

**UV radiation** has been clearly related to the appearance of melanoma. In fact, it is considered the most important carcinogen for this condition, since it is responsible for 80% of the cases<sup>4</sup>. UV radiation generates DNA damage and cell injury by inducing mutations. Defective DNA repair machinery cannot replace the damaged DNA sequences and melanoma arises. The exposure pattern also plays a role. Recreational or intermittent exposure, especially in light-skinned vacationers, results in a 65% higher risk of melanoma and nevi. However, it has been shown that the use of sunscreens reduces melanoma incidence rate, especially that of invasive melanomas<sup>2</sup>. During the last decades, the use of tanning beds has become very popular, however, this social activity is strongly linked to melanoma. Notably, several meta-analyzes suggest that the frequent use of tanning beds triples or quadruples the risk of developing melanoma, and increases this risk to 75% if the first artificial UV exposure was performed before the age of 35<sup>7</sup>.

Since countries located closer to equator are exposed to higher UV intensity, this results in higher melanoma rates, highlighting the importance of **geographic location**. As mentioned before, Australia and New Zealand, which are close to equator and have a fair-skinned population, have the greatest rates of melanoma. Despite being an important feature, geographical location is not determinant. For instance, in spite of being close to equator, Central America has low melanoma rates, since most people are dark-skinned.

A link has been established between **exposure to heavy metals, various chemicals**, and the development of melanoma, since these compounds generate mutations in the DNA of the melanocytes. Occupational exposure to ionizing radiation, heavy metals, polycyclic hydrocarbons (petroleum, printing chemicals, and electronic products), pesticides and polyvinyl chloride increases the risk of melanoma. However, the mechanism for this is still under study<sup>9</sup>.

### 1.3. Histopathology

Due to the neural crest-origin of melanocytes, melanoma can occur in the uveal tract and on the mucosal surface, for example, but in 95% of cases, it arises in its cutaneous form.

#### 1.3.1. Skin

Skin is the largest organ of the body, covering an area of 2 m<sup>2</sup>. It acts as a protective shield against heat, light, pathogens and injuries. In addition, it also helps to regulate body temperature, vitamin D synthesis, cutaneous sensitivity (touch, heat and cold) and it prevents water loss.

According to its structure, it is divided into two different portions: epidermis and dermis<sup>10</sup>. Besides, underneath the dermis, but without belonging to the skin, is the hypodermis, which can also be called subcutaneous tissue. It is composed mainly of loose connective tissue and fat accumulations. The cellular content of the hypodermis is made up mainly of adipocytes, fibroblast and macrophages. Its principal function is to store fat and help maintain body temperature.

The **epidermis** is the outermost layer of the skin, and acts as a barrier to the internal structures of the body, regulates the hydration of the skin and provides color to the skin. It is composed of a thin stratified squamous epithelium that lies on a basement layer that separates it from the dermis. Among all the cells found in this structure, the main ones are keratinocytes, melanocytes, Langerhans cells and Merkel cells (**Fig. 7**). A 90% of these cells are keratinocytes, which produce keratin, a resistant and fibrous protein that protects the skin. In addition, the cells responsible for producing melanin and determining skin color are melanocytes, which represent 8% of the cells of the epidermis. Also, there are Langerhans cells, which participate in the reinforcement of the immune response against the microorganisms present in the skin, and Merkel cells, which make synaptic contact with sensitive neurons and act as mechanoreceptors for tactile sensation.

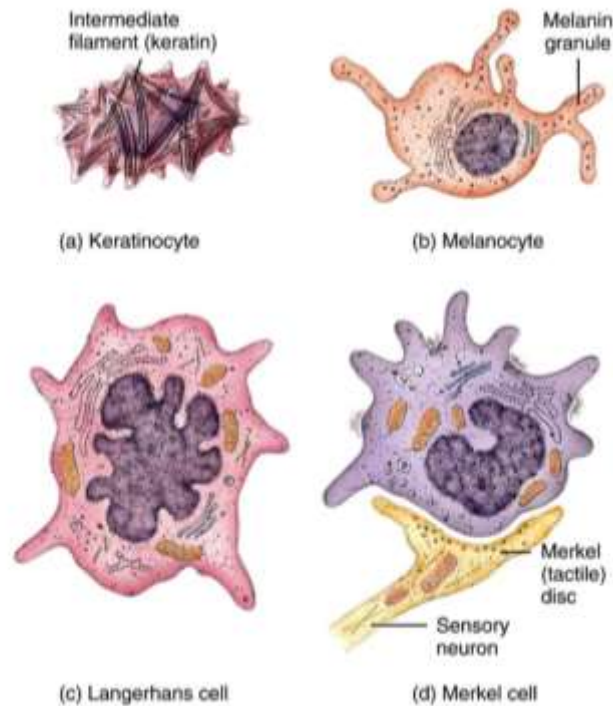


**Figure 6.** The principal cell types present in the epidermis: (a) keratinocytes, (b) melanocytes, (c) Langerhans cells and (d) Merkel cells<sup>10</sup>.

Beneath the epidermis is the **dermis**. This is a thick layer of connective tissue that contains blood vessels, nerves, glands and hair follicles, and is tightly connected to the epidermis by the basement layer. Therefore, it acts as support, nourishment and waste removal for the cells of the epidermis and dermis.

Since **melanocytes** are responsible for the development of melanoma, we have focused our attention on this type of cells. They are derived from the embryonic ectoderm. Hence, after the closure of the neural tube, the melanoblasts, precursors of the melanocytes, migrate from the neural crest to different parts of the body, such as skin, uveal tract, mucosal surfaces, meninges, inner ear and heart. This is the reason why melanoma could arise in any of these locations, although it develops mainly on the skin.

The density of the melanocytes varies depending on the anatomic region of the body (higher in the breast area and the genital region). However, it remains fairly constant between individuals of different ethnicities. Therefore, the color of the skin is determined by the quantity of melanin produced instead of the number of melanocytes.

Under physiological conditions, melanocytes are found mainly on the basal layer of the epidermis, attached to up to 36 keratinocytes through their dendritic projections, forming the epidermal melanin unit. Melanocytes have a low replication capacity, light cytoplasm and do not present desmosomes. Besides, their main role is to fabricate melanin, the photoprotective pigment that acts as a barrier for the skin, since it blocks the harmful effects that UV radiation could cause on cells, such as oxidative stress and DNA mutagenesis. Inside the melanocytes there are the melanosomes organelles, where melanin is manufactured and stored. Then, these vesicles are distributed to the surrounding keratinocytes of the epidermal melanin unit via the dendritic projections of the melanocytes.

## 1.3.2. Melanoma development

As mentioned above, skin melanoma arises after the malignant transformation of the melanocytes present in the epidermis of the skin. These cells undergo different molecular alterations, among which there are mutations in genes that control cell cycle regulation, cell differentiation, cell adhesion, cell signaling and apoptosis<sup>11</sup>.

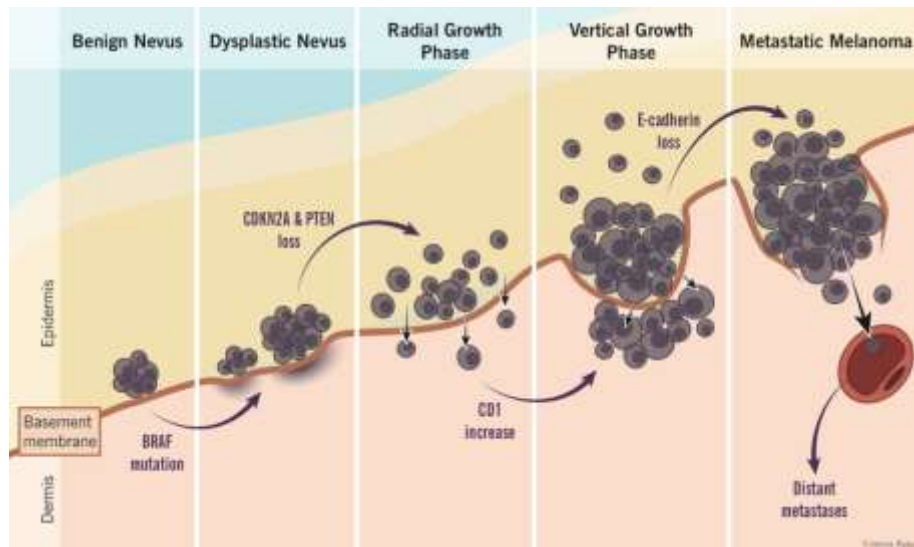


Figure 7. Representation of the Clark model for melanoma development <sup>12</sup>.

Different models have been proposed to explain melanoma development. One of the most popular is the Clark model, which, as represented in the **Figure 7**, explains the melanoma development in different steps: benign nevi, dysplastic nevi, primary melanoma in the radial growth phase (RGP), primary melanoma in the vertical growth phase (VGP) and metastatic melanoma. Although this model of progression is explained as a linear stepwise transformation, many melanoma tumors may not follow it in an orderly fashion. For example, RGP or VGP melanomas can arise from pre-existing nevi lesions or *de novo* from normal melanocytes. Also, either RGP or VGP tumors can progress directly to metastatic tumors<sup>12</sup>.

The first event in Clark's progression model is the formation of benign nevi, since the epidermal melanocytes undergo some molecular changes that alter their growth control. However, the proliferation of nevus melanocytes is limited; the cells enter into senescence induced by oncogenes and advance scarcely towards melanoma. Clinically, they can be described as brown moles with regular surface and borders. Some of the identified molecular changes are the aberrant activation of the MAPK signaling pathway, which results in an increased proliferation of melanocytes. This constitutive activation of the ERK-MAPK pathway occurs due to mutations in N-RAS, observed in 15% of melanomas, or BRAF, associated with 50% of melanoma cases. The frequency of BRAF mutations is similar to that observed in melanomas. Therefore, additional alterations must occur so that the melanocytes become malignant. Some authors suggest that the BRAF mutation induces cellular senescence because it increases the expression of the cell-cycle inhibitor of kinase 4A (INK4A). This protein causes cell-cycle arrest and the stimulation of growth produced by BRAF mutation is limited<sup>12</sup>.

This benign tumor can progress to dysplastic nevus, which are considered precancerous lesions between benign nevus and melanoma. They can arise from pre-existing benign nevus or as new lesions. Despite being considered risk factors and having the ability to be precursors of melanoma, the majority of the dysplastic nevus remain stable over time and do not progress to melanoma. In fact, only 20% of melanoma cases develop from these precancerous lesions. Several studies have concluded that the risk of a nevus becoming melanoma is 1 in 200,000 for patients under 40 and 1 in 33,000 for men over 60<sup>13</sup>. Clinically, these moles are larger than 5 mm, with irregular borders and variegated color, and histologically, the cells show cytological atypia. At the molecular level, they undergo alterations that modify cell growth, DNA repair machinery and susceptibility to cell death<sup>12</sup>.

Eventually, the cells can acquire the ability to grow limitlessly and form the malignant tumor. Moreover, melanomas have two distinct growth phases that will determine their clinical outcome. The first phase RGP, is where the tumor grows laterally along the epidermis and do not generate metastasis. This could last for years and the tumor can be surgically removed with a recovery rate close to 100%. The second phase is VGP, in which the tumor acquires the ability to grow deeply and invades the dermis and hypodermis, resulting in metastasis.

Melanoma is one of the most aggressive tumor types, and survival rates drop dramatically when diagnosed in the metastatic phase. To form a metastasis, the cells lose cell-cell adhesions, separate from the primary tumor, and invade the surrounding stroma. Melanoma cells use different migration mechanisms to spread: intravascular dissemination through lymphatic or blood vessels, or extravascular migration called angiotropism. The latter is defined as the dissemination of the tumor without entering the vasculature, since the cells mimic the pericytes of the vessels and migrate along the abluminal vascular surfaces without intravasation. Melanoma cells share this migratory mechanism with neural crest cells<sup>14,15</sup>. The tumor can metastatize loco-regionally or to distant sites. Commonly, it metastatizes regionally to nearby skin (satellite or in-transit metastasis), lymph nodes and subcutaneous tissue. Besides, the most common distant metastases are to skin, lung, brain, liver, bone and intestine<sup>16</sup>.

### 1.3.3. Melanoma diagnosis and staging

Survival rates are significantly higher with early detection of the tumor. However, if the lesion is not surgically removed in time and continues to grow, it becomes in one of the deadliest cancers. Therefore, it is strikingly important to have resources to help with early detection. Melanoma tumor can be identified if it meets the ABCDE criteria<sup>17</sup>:

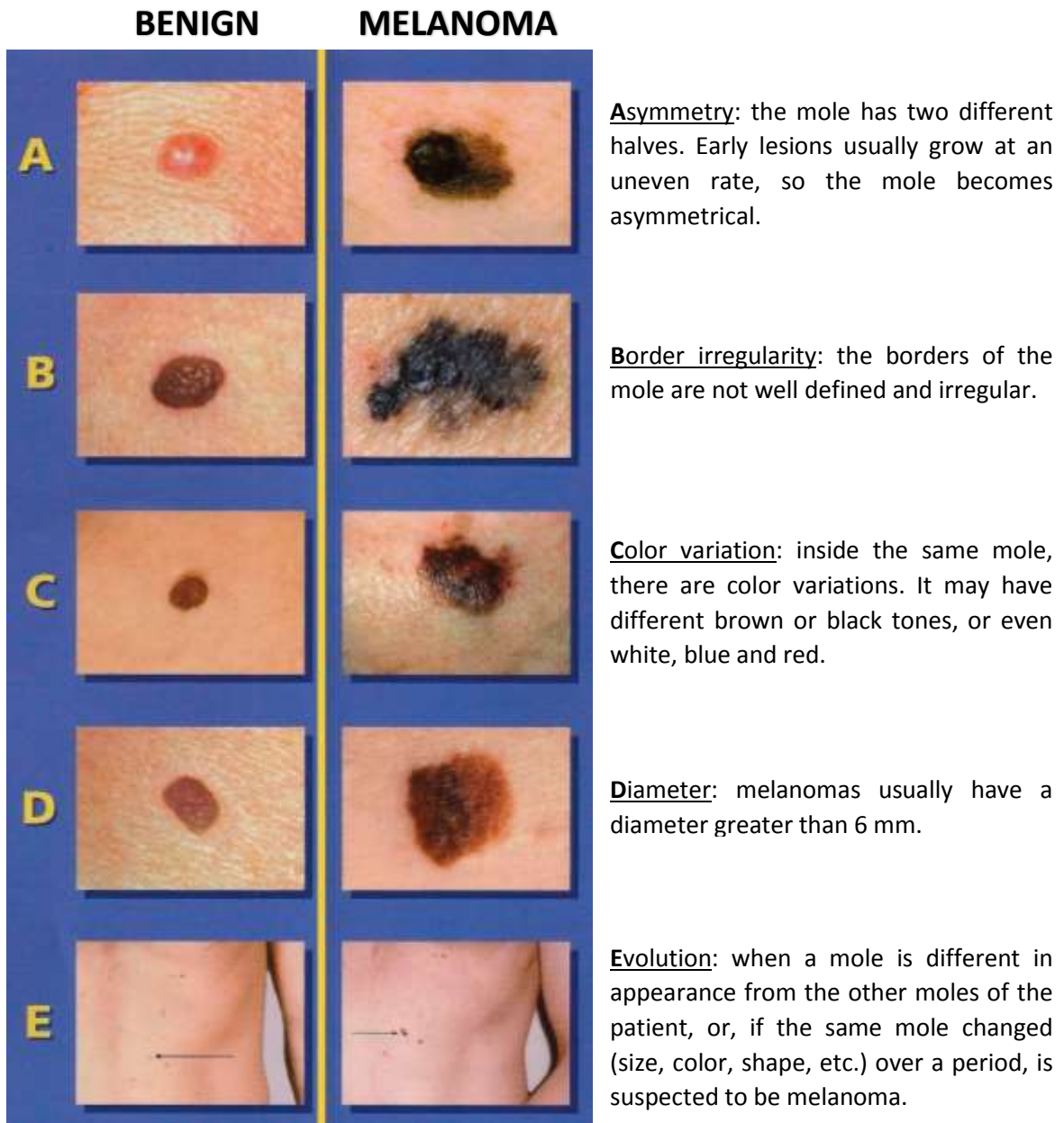


Figure 8. Examples of the ABCDE criteria for the early detection of melanoma<sup>20</sup>.

Unfortunately, the ABCDE criteria allows for the correct diagnosis of only 60-65% of cases, so additional criteria are needed to aid in the diagnosis and prognosis of melanoma. For this, the Clark scale and the Breslow scale are employed together.



---

The Clark scale determines invasion level of the tumor and the skin layers affected. Wallace H. Clark developed this staging system in 1966 and 5 different levels are recognized:

- I: melanoma cells are only confined to the epidermis. It is also called melanoma *in situ*.
- II: the cells invade the papillary dermis, right under the epidermis.
- III: melanoma cells invade the junction of the papillary and reticular dermis.
- IV: the melanoma invades the reticular or deep dermis.
- V: the tumor grows to the subcutaneous fat beneath the dermis.

However, the Clark scale is rarely used nowadays because it has been shown to have a lower predictive value, be more subjective and less reproducible than the Breslow scale. Furthermore, it is often difficult to differentiate between Clark's level II and III, and cannot be used for melanomas on the soles and palms. Thus, the Clark scale has been relegated to cases where the Breslow depth is less than 1 mm<sup>18</sup>.

The Breslow scale was reported by Alexander Breslow in 1970 and determines how deeply the tumor has grown. The thickness of the excised tumor is measured and 5-year survival rates are estimated based on the depth of the tumor. Commonly, the higher the Breslow thickness, the worse the outcome<sup>18</sup>.

- <1 mm: 5-year survival is 92-97%.
- 1 to 2 mm: 5-year survival is 80-92%.
- 2 to 4 mm: 5-year survival is 60-75%.
- >4 mm: 5-year survival is 50%.

This is a very accurate method for predicting the prognosis of melanoma, so it has been introduced into the standard TNM staging system for melanoma. The TNM staging is a globally recognized system that alphanumerically describes the stage of a cancer. It was developed by the Union for International Cancer Control (UICC) and the American Joint Committee on Cancer (AJCC), and has been updated several times since then due to advances in melanoma research<sup>17</sup>. This system is used for many solid tumors and is based on the evaluation of three mandatory parameters:

- **T**: describes the size and extension of the primary tumor. It is based on the Breslow scale to determine tumor thickness and analyzes for the presence of ulceration.
- **N**: describes the spread of the tumor to nearby lymph nodes and if the metastasis present in the node is microscopic or macroscopic. Besides, it also identifies in-transit metastasis that are more than 3 cm away from the primary tumor but have not yet reached a lymph node, and satellite lesions, which are tumors larger than 0.5 mm that are located within the same histologic section as the primary tumor.
- **M**: describes the presence of distant metastasis.

Table 1. Description of the criteria used to classify the staging of melanoma<sup>17</sup>.

Stage	Description
<b>Tumor (T)</b>	
<b>Tx</b>	Primary tumor cannot be assessed
<b>T0</b>	No evidence of primary tumor
<b>Tis</b>	Melanoma <i>in situ</i> . Precancerous lesion. Melanoma cells are found between the epidermis and dermis of the skin, and have not invaded yet these layers.
<b>T1</b>	Tumor ≤1 mm thick
<b>T1a</b>	Tumor ≤1 mm thick, no ulceration and mitotic rate < 1/mm <sup>2</sup>
<b>T1b</b>	Tumor ≤1 mm thick, either with ulceration or mitotic rate > 1/mm <sup>2</sup>
<b>T2</b>	Tumor 1-2 mm thick
<b>T2a</b>	Tumor 1-2 mm thick, no ulceration
<b>T2b</b>	Tumor 1-2 mm thick, with ulceration
<b>T3</b>	Tumor 2-4 mm thick
<b>T3a</b>	Tumor 2-4 mm thick, no ulceration
<b>T3b</b>	Tumor 2-4 mm thick, with ulceration
<b>T4</b>	Tumor >4 mm thick
<b>T4a</b>	Tumor >4 mm thick, no ulceration
<b>T4b</b>	Tumor >4 mm thick, with ulceration
<b>Node (N)</b>	
<b>Nx</b>	Regional lymph nodes cannot be assessed
<b>N0</b>	No melanoma found in regional lymph nodes
<b>N1</b>	Melanoma found in 1 lymph node
<b>N1a</b>	Melanoma found in 1 lymph node, microscopic metastasis
<b>N1b</b>	Melanoma found in 1 lymph node, macroscopic metastasis
<b>N2</b>	Melanoma found in 2-3 lymph nodes
<b>N2a</b>	Melanoma found in 2-3 lymph nodes, microscopic metastasis
<b>N2b</b>	Melanoma found in 2-3 lymph nodes, macroscopic metastasis
<b>N2c</b>	In-transit melanoma or satellite lesions are found, without metastasis to lymph nodes.
<b>N3</b>	Melanoma is found in ≥4 lymph nodes, or in ≥2 lymph nodes that appear to be joined together. In-transit melanoma or satellite lesions are found, with metastasis to lymph nodes.
<b>Metastasis (M)</b>	
<b>Mx</b>	Metastasis cannot be assessed
<b>M0</b>	No metastasis
<b>M1a</b>	Metastasis to skin, subcutaneous tissues or distant lymph nodes
<b>M1b</b>	Metastasis to lung
<b>M1c</b>	Metastasis to any other distant organs

After classification of melanoma according to the TNM system, an overall stage of the disease is assigned (**Table 2**), where stage 0 is melanoma *in situ* and is recognized as precancerous. Stages I and II are considered localized lesions. Stage III corresponds to regional disease and Stage IV is considered as advanced disease<sup>17,19</sup>.

Table 2. Staging of melanoma based on TNM system<sup>17</sup>.

Stage	T	N	M
<b>0</b>	Tis	N0	M0
<b>IA</b>	T1a	N0	M0
<b>IB</b>	T1b T2a	N0	M0
<b>IIA</b>	T2b T3a	N0	M0
<b>IIB</b>	T3b T4a	N0	M0
<b>IIC</b>	T4b	N0	M0
<b>IIIA</b>	T1-T4a	N1a N2a	M0
<b>IIIB</b>	T1-T4b  T1-T4a	N1a N2a N1b N2b N2c	M0
<b>IIIC</b>	T1-T4b  Any T	N1b N2b N2c N3	M0
<b>IV</b>	Any T	Any N	M1

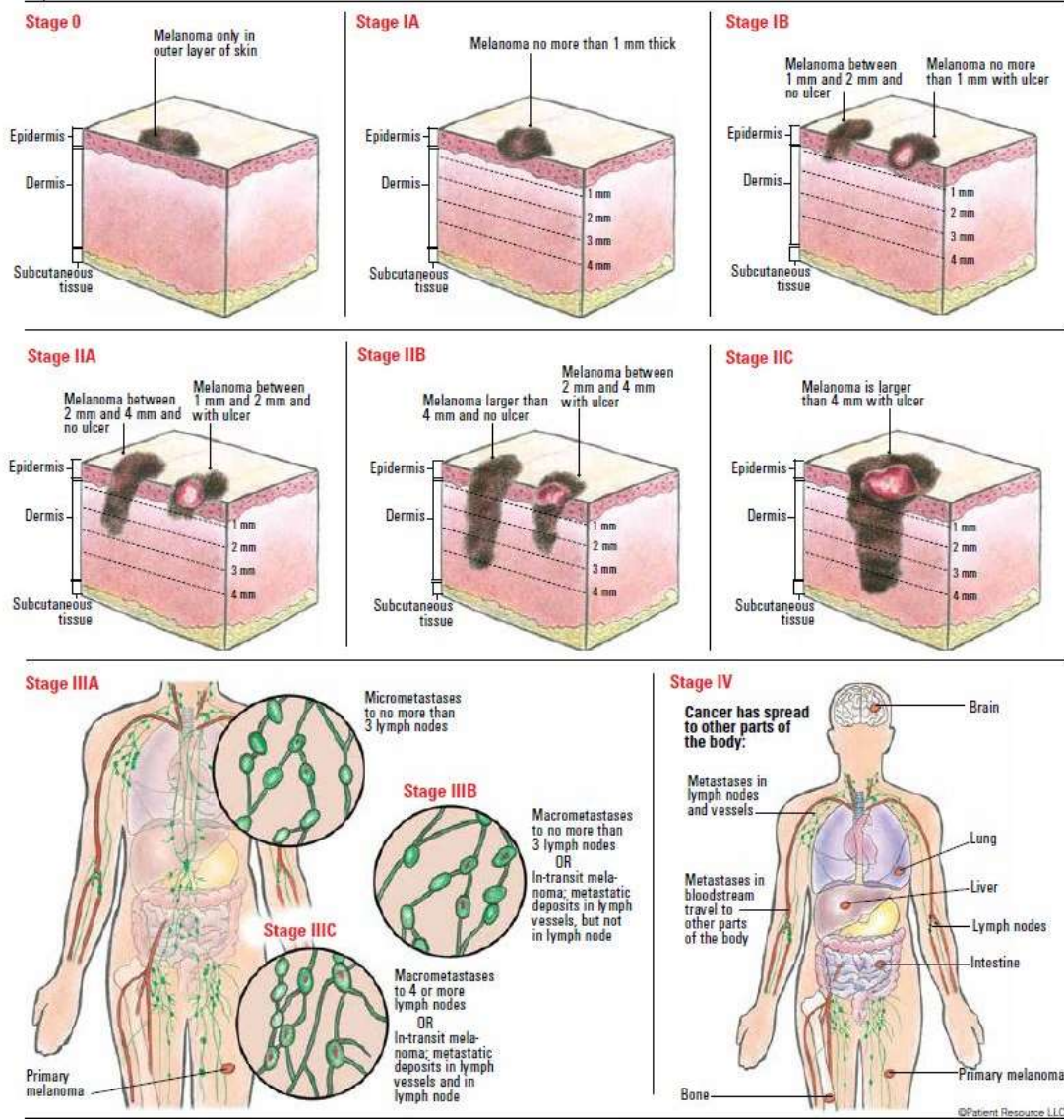


Figure 9. Clinical description of each stage of melanoma development<sup>17</sup>.

#### 1.3.4. Clinical classification of melanoma

Classically, four different clinical types of melanoma have been distinguished based on their anatomical localization and evolution.

- **Superficial spreading melanoma (SSM):**

It is the most common form of melanoma among Caucasians, representing 70-80% of all the melanoma cases in this ethnic group. It usually arises on sun-exposed skin, such as the trunk and back in males and the back and lower limbs in females. Besides, about 40% of SSM evolve from a pre-existing lesion such as a common or a dysplastic nevus. The clinical features of this lesion meet the ABCDE criteria, as it typically has irregular and asymmetrical edges, with color variation and is larger than 6 mm. This type of melanoma presents a prolonged radial growth phase, where the lesion remains thin as the melanocytes grow along the epidermis. However, if the tumor is not excised, it may eventually begin the vertical growth phase and invade the dermis and reach the hypodermis, compromising the patient's survival<sup>19-21</sup>.

- **Nodular melanoma (NM):**

Despite being the second most common type of melanoma with an incidence of 15-25%, it is identified as the most aggressive form since it presents a quick growth that begins directly with the vertical growth phase. In addition, it develops *de novo*, not needing a pre-existing lesion, so its identification is more difficult and is usually diagnosed when it already has metastatic capacity. It regularly appears on the head, neck or trunk of middle-aged patients, and it is more common in men than in women. Macroscopically, it can be described as a fast-growing, dome-shaped, blue-black lesion, with high tendency to ulceration<sup>20</sup>.

- **Lentigo maligna melanoma (LMM):**

It accounts for less than 10% of all melanoma cases. It originates from a pre-existing *in situ* melanoma called lentigo maligna that is found in the epidermis and grows peripherally; in fact, it can reach a diameter of 5-7 cm at this stage. Over a period of years, the tumor acquires the invasive phenotype and grows vertically; henceforth, it is called lentigo maligna melanoma. It arises in sun-exposed areas of sun-damaged skins, principally on the face and neck of Caucasian elders. It is a large lesion (>3 cm), multicolored (different shades of brown, black), and with elevated areas<sup>20</sup>.

- **Acral lentiginous melanoma (ALM):**

Unlike the other variants, ALM is more frequent in black (60-70%) and Asian (35-45%) populations than in fair-skinned individuals (<5%). It occurs on non-hairy body surfaces such as palms, soles, and beneath nail beds, although most ALM develop on the soles of the feet of elderly individuals. Their appearance is similar to that of lentigo maligna melanoma, since they are also black, irregular and large.

In addition, there are other less common variants such as spitzoid melanoma, small cell melanoma, malignant blue nevus, desmoplastic melanoma, ocular melanoma (conjunctival or uveal) and mucosal melanoma, among others.

#### 1.4. Melanoma treatment

The recovery and therapy election of melanoma patients is directly correlated to the stage at which it is diagnosed. While the recovery rate is almost 100% when diagnosed early, there is no utterly effective therapy for metastatic melanoma. The treatment of choice for localized melanomas in stage 0 to II is surgical excision with a wide margin to prevent local recurrence<sup>22,23</sup>. Moreover, if Breslow's thickness is high and there is metastatic suspicion, sentinel lymph node biopsy is carried out. This is defined as the first draining node of the primary tumor, so it would be the first to receive metastatic cells. This clinical approach allows the identification and subsequent excision of this lymph node, which is then histologically examined, and if metastatic cells are found, an immediate lymphadenectomy is carried out.

Melanoma has long been considered a radioresistant tumor and the use of radiotherapy has been reserved for palliative treatment. However, recent findings suggest that radiotherapy can be applied as adjuvant therapy post-surgery or when the suggested excision margins cannot be applied in surgery, especially in elderly patients with lentigo maligna melanoma<sup>24</sup>.

##### 1.4.1. Metastatic melanoma

The treatment of metastatic patients remains the main obstacle to overcome in the management of melanoma. These patients have a very poor prognosis, and surgery and radiotherapy are not effective for advanced disease. Dacarbazine chemotherapy has been the first-line treatment from 1975 to 2011. Until recently, the only FDA-approved treatment for metastatic melanoma was dacarbazine, but temozolomide is also used as chemotherapy today. However, they exhibit low response rate and the effect lasts only 5 to 6 months<sup>25-27</sup>.

A further treatment option for metastatic melanoma is immunotherapy, which uses the patient's own immune system to attack the tumor. The first immunomodulatory agent approved for melanoma was cytokine IL-2 in 1998. It is usually administered as an adjuvant therapy together with chemotherapy or radiotherapy. However, it is associated with significant toxicities, so its use is limited to patients in a good performance status<sup>25</sup>. Interferon- $\alpha$  (IFN- $\alpha$ ) and peginterferon  $\alpha$ -2b are also used although they have low antitumor response and are associated with severe side effects, so their use have been reserved to stage IV patients<sup>25,28</sup>.

The revolution in the treatment of advanced melanoma began in 2011 when ipilimumab was approved for metastatic melanoma or as adjuvant therapy in patients with resected stage III melanoma. This humanized monoclonal antibody acts against cytotoxic T lymphocyte-associated protein 4 (CTLA-4), resulting in the secretion of IL-2 and activation and proliferation of cytotoxic T cells<sup>25,28-30</sup>.

Other checkpoint inhibitors are the PD-1 pathway inhibitors. In 2015, the FDA approved nivolumab and pembrolizumab for their use in advanced melanoma or as adjuvant therapy after surgery. These monoclonal antibodies block the interaction between PD-1 receptor of T cells with PD-L1 antigen of melanoma cells, boosting the antitumor response of T cells. Interestingly, the combination of ipilimumab and nivolumab has been studied, but important adverse effects have been described<sup>25,28-32</sup>.

Targeting therapy has become another treatment option for melanoma. In approximately 50% of cases, there is BRAF-V600E mutation. Therefore, the FDA and EMA (European Medicines Agency) have approved two different BRAF-V600E inhibitors to use in metastatic melanoma, namely vemurafenib, approved in 2011, and dabrafenib, in 2013. Although they have shown significant improvement in patients, they tend to generate resistance to the treatment and the

effect does not last long<sup>29,33</sup>. Additionally, the MEK inhibitors approved for monotherapy are trametinib and cobimetinib, which can be used with patients that have the frequent BRAF or NRAS mutations. Significantly, MEK and BRAF inhibitors can be combined generating a highly efficient synergistic outcome<sup>25,29,33</sup>. The combination therapies that are approved at this time are vemurafenib and cobimetinib; dabrafenib and trametinib<sup>32,34</sup>.

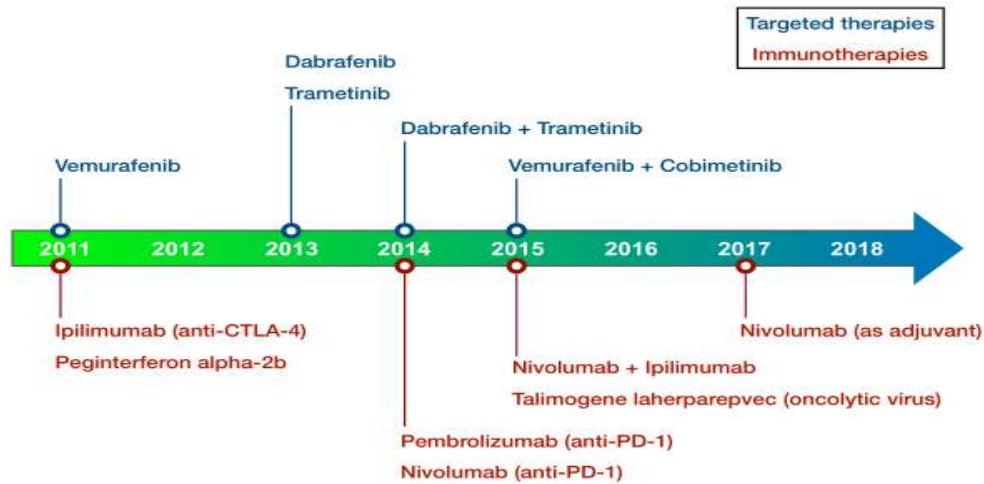


Figure 10. Timeline of melanoma treatment options since 2011<sup>34</sup>.

#### 1.4.2. New challenges

Lately, several clinical trials have been conducted to study the efficacy of new agents for the treatment of melanoma. Some of these new therapeutic approaches include the use of oncolytic viruses, being Talimogene laherparepvec (TVEC) the only approved option to date. Viruses replicate within cancer cells, generating GM-CSF and producing the lysis of neoplastic cells<sup>29</sup>.

An interesting strategy under study are cancer vaccines, which stimulate the host's immune system to act against the tumor. The vaccines studied so far have been designed against antigens such as gp-100, Melan-A and tyrosinase. However, the response rates achieved have been low<sup>35</sup>.

Another treatment option under research is adoptive cell therapy, which uses isolated tumor infiltrating lymphocytes (TILs) that have potent anti-tumor properties. TILs are expanded ex vivo and reinserted into the host to treat different metastases<sup>35</sup>. In another study, autologous lymphocytes were genetically engineered to detect and attack melanoma cells. Despite promising results, this treatment option needs further research to achieve more specific binding to tumor cells<sup>36</sup>.

### 1.5. Melanoma biomarkers

In spite of the relevant advances recently achieved in the diagnosis and treatment of melanoma, there are no fully effective therapy or biomarkers for this disease.

A biomarker is an objectively measurable biological substance, structure, or process found in the body or in its waste products that indicates the risk to suffer a particular disease, the presence of a disease, the state of a disease and possible outcome, and determines the susceptibility to therapy. These biomarkers can be, for instance, genetic pathways or particular genes, metabolism routes, proteins or lipids that are modified after genetic, cellular, biochemical or molecular alterations generated by the carcinogenesis process<sup>37</sup>.

An ideal cancer biomarker should be involved in the process by which the tumor develops, so it could also be a therapeutic target. Therefore, changes in its levels should be correlated with variations in the stage of the disease or with successful treatment. Moreover, it should not appear in healthy tissues or individuals, and should be specific for a concrete type of cancer. Ideally, this biomarker would be used to assess predisposition to a particular type of cancer, early diagnosis, prognosis, and drug response. Besides, it must be detected easily and non-invasively.

Particularly in melanoma, the diagnosis is based on clinical screening and identification, followed by histopathological confirmation after studying the subsequent histological biomarkers:

**HMB45** antibody recognizes premelanosome protein (**Pmel**) that is present in melanoma and junctional nevus. However, it has shown little sensitivity for desmoplastic malignant melanoma.

**Melan-A** protein is present in the cytoplasm of both melanocytes and melanoma. It shows a high specificity to differentiate between melanoma and non-melanocytic tumors, although it is less sensitive when detecting metastatic melanoma and desmoplastic melanoma, compared with primary tumors.

**Tyrosinase** enzyme is implicated in the production of melanin and is very good at differentiating melanoma and non-melanocytic tumors. However, it also demonstrates a lower sensitivity to detect desmoplastic melanoma.

**S100B** protein is routinely used as an immunohistochemical biomarker for melanoma. Although it is not specific for melanoma, since it is also elevated in patients with kidney and liver damage, liver metastases from other types of tumors, and diverse infectious and inflammatory disorders. It presents high sensitivity for desmoplastic melanoma, so it is of great utility for pathologist.

Although these markers help in the confirmation of the histopathological diagnosis of melanoma, none of them is able to distinguish between malignant and non-malignant melanocytic lesions.

Additionally, there are other biomarkers that help determine which patients are likely to progress to more advanced stages or would benefit from a concrete treatment.

Although they can not be considered biomarkers, the **Breslow thickness** and the **mitotic rate** are the most precise factors to determine melanoma prognosis and survival of patients, and are part of the TNM staging system. In fact, tumors with high Breslow thickness and mitotic rate, together with absence of infiltrated lymphocytes are more likely to be positive for sentinel lymph node.



Moreover, the assessment of the presence of the **BRAF V600E** mutation helps to determine the suitable treatment for patients, since vemurafenib has been shown to significantly increase the survival of individuals who have this mutation.

In addition to histopathological markers, there are also serum biomarkers, which are detected less invasively. Among them, **lactate dehydrogenase** (LDH) enzyme is found. High levels of serum LDH are associated with metastatic melanoma, especially with liver metastases. In fact, it has been introduced in the TNM staging system as an adverse prognostic marker and a negative predictor of response to therapy. However, it is not exclusive for melanoma.

**S100B** protein can not only be considered a histological biomarker for diagnosis as explained above, but also a serum biomarker for advanced melanoma, since it is associated with metastatic melanoma, reduced survival, relapse and poor response to treatment<sup>38</sup>.

Besides, there are other biomarkers that, although not exclusive of melanoma, are also used in the evaluation of prognosis, since they have increased levels in various inflammatory processes, such as tumor inflammation, angiogenesis and metastasis. These include VEGF, metalloproteinases and cyclooxygenase-2 enzyme, among others<sup>39</sup>.

#### 1.5.1. Biomarker discovery

The research process to discover new biomarkers can be divided into three different phases. The first one is based on basic studies and is called discovery phase. Here, the hypothesis and the analytical approach are defined, and the proposed assays are carried out. This is the phase where potential biomarkers are identified. In order to discover robust candidates, the analytical processes employed must be precise and reproducible, to ensure the reproducibility of the results across different laboratories.

In the second phase, the analytical validity and clinical validation of the biomarkers is studied. For this, the biomarkers are implemented in the platform that would be used in clinic. Then, new samples are studied and the biomarker must faithfully classify the samples in the appropriate validation groups.

A biomarker that has successfully fulfilled analytical and clinical validation is ready to determine its clinical utility. In this phase, clinical effectiveness is assessed together with the benefit-to-harm ratio. A biomarker that would be used in patient care must present high levels of clinical evidence. Besides, for clinical implementation, the biomarker must achieve regulatory approval, commercialization and incorporation into clinical practice guidelines<sup>37,40</sup>.

### 1.6. Melanoma hallmarks

In order to identify new cancer biomarkers, the complex nature of tumors must be well understood. For this purpose, the hallmarks of cancer were defined, which comprise 10 different and complementary capacities acquired by different cancer cells to guarantee their survival, proliferation and dissemination, regardless of the cancer type<sup>41</sup>. This simplified conceptualization defines a framework for understanding the sophisticated biology of different types of cancers. They affect both tumor and stroma cells, and are established as follows:

- **Genomic instability:** In melanoma cells, UV radiation produces genomic instability, inducing the appearance of mutations, which allows the development of other cancer hallmarks and, therefore, tumor progression<sup>42</sup>.

- **Tumor promoting inflammation:** Tumor tissues present chronic inflammation enabling the release of many signaling molecules from the immune cells. These factors promote proliferation and resistance to death, contribute to genomic instability and stimulate angiogenesis and metastasis<sup>41</sup>. In melanoma, concretely, UV radiation damages melanocytes and keratinocytes, which release HMGB1 cytokine that recruits neutrophils to the tumor microenvironment<sup>42</sup>. These immune cells release pro-inflammatory proteins that promote genome instability, angiogenesis and metastasis.
- **Sustaining proliferative signaling:** Cancer cells produce and release growth factors, and also increase the expression of the receptors for these ligands. In addition, they send signals to stromal cells in order to make them produce more growth supporting molecules. Besides, this can also be achieved independently from growth factors, by constitutively activating downstream proliferative signaling pathways. In melanoma, very often, this is achieved due to BRAF activating mutation, which keeps the RAS/RAF/MERK/ERK pathway continuously activated resulting in excessive proliferation<sup>42</sup>.
- **Evading tumor growth suppressors:** Two major tumor suppressor proteins, p53 and pRb, arrest the cell cycle and induce senescence or apoptosis. In melanoma, deactivating mutations in tumor suppressor gene CDKN2A are common. It encodes p16 protein that can dephosphorylate pRb, and therefore, deactivate it and arrest cell cycle. If CDKN2A is mutated, p16 does not deactivate pRb, and the cell cycle is continuously on<sup>42</sup>.
- **Resisting cell death:** Apoptosis is essential for the proper homeostasis of the tissues. If there is any defect in the apoptotic pathways the cells can acquire resistance to cell death. In cutaneous melanoma, defects in the apoptotic pathways have been reported. For instance, in metastatic melanoma Apaf-1 protein, which plays a key role in activating apoptosis, when cytochrome c is released from the mitochondria following DNA damage, is absent<sup>42</sup>.
- **Enabling replicative immortality:** Cancer cells have the ability to replicate limitlessly. This is achieved by the upregulation of telomerase, which constantly adds telomeric DNA to the ends of the telomeres, so they are not shortened, and therefore senescence or apoptosis is not triggered<sup>41</sup>.
- **Inducing angiogenesis:** angiogenesis is essential for tumor progression and dissemination. Melanoma cells release glycoproteins that aid in angiogenesis processes<sup>42</sup>.
- **Activating invasion and metastasis:** Melanoma cells produce different proteins, such as metalloproteinases, that help in the degradation of the basal layer of the tissues and the extracellular matrix favoring the metastatic process<sup>42</sup>.
- **Avoiding immune destruction:** Both innate and adaptive immune systems play a role in eradicating tumor cells. Some cancer cells, for instance melanoma cells, are able to escape immune detection and avoid immune destruction<sup>42</sup>.
- **Deregulating cellular energetics:** In order to meet all the needs that cancer cells have, metabolism adapts to provide them with building blocks and energy to sustain the high proliferation and division. Melanoma cells switch their metabolism from oxidative phosphorylation to glycolysis, and the glucose uptake is significantly upregulated<sup>42</sup>. Besides, other anabolic and catabolic pathways are also altered in the cancer cells. Among these, lipid metabolism has gained striking importance over the last years, as it will be explained in the next section.

## 2. Lipids, cell metabolism and cancer

### 2.1. Lipids

Lipids are ubiquitous molecules that participate in a wide variety of vital physiological processes in the cells. In short, they are involved in cellular signaling, energy storage, structural support in biological membranes, and synthesis of physiologically important molecules, such as bile acids, some hormones and vitamins. They therefore control cellular processes such as proliferation, migration, survival and death, all of which are closely related to the carcinogenic process.

#### 2.1.1. Lipid classification

In spite of existing beyond thousands of different lipid molecules, they all share some common features such as poor or no solubility in water, but good solubility in polar solvents. Generally, they are described as either hydrophobic or amphipathic molecules. Based on their molecular structure, they can be categorized into eight classes: fatty acids, glycerolipids, glycerophospholipids, sphingolipids, sterol lipids, prenol lipids, saccharolipids and polyketides.

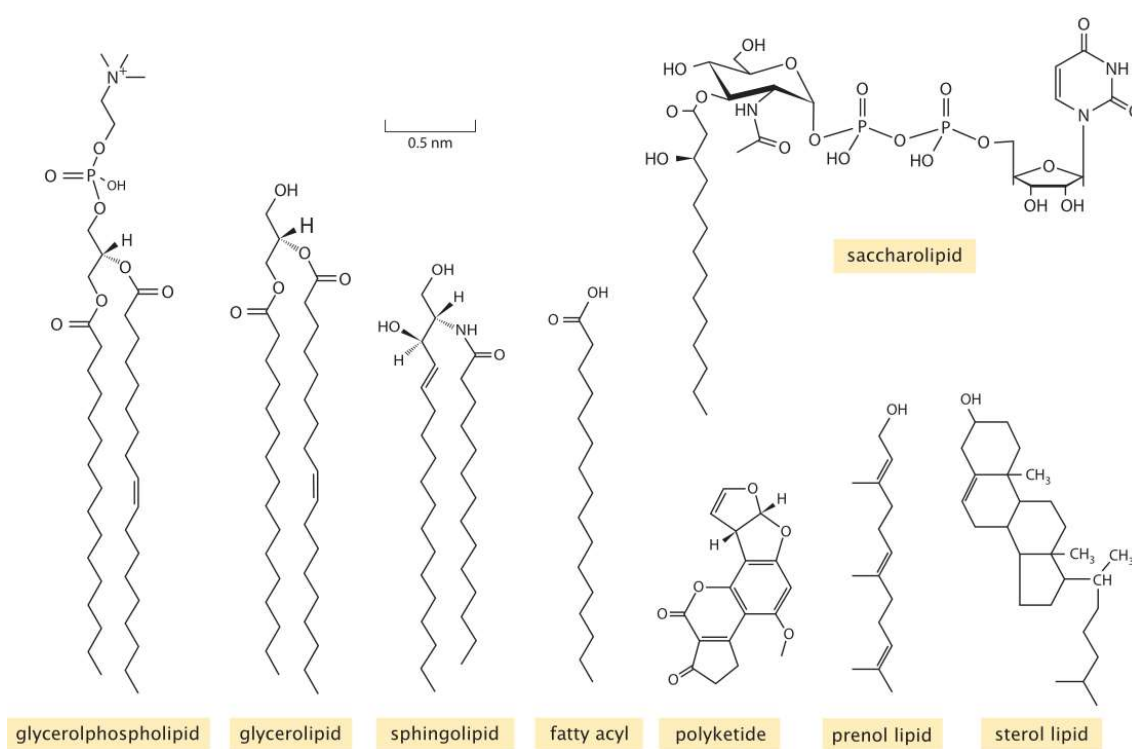


Figure 11. General structure of the different lipid classes<sup>46</sup>.

**Fatty acids (FA)** are considered the simplest lipid molecules and one of the most fundamental classes of biological lipids, as they serve as building blocks for more complex lipids. Their structure can be divided in two parts; a non-polar hydrocarbon chain of different lengths, mostly with an even number of carbon atoms, and a polar carboxylic acid group at the end. In addition, there can be double and triple bonds within the hydrocarbon chain, forming monounsaturated FAs (one double or triple bond; MUFA) or polyunsaturated FAs (more than one insaturation; PUFA). If there is no insaturations, these FAs are named saturated FAs. The presence of insaturations in the acyl-chains creates a bend in the structure of the molecule. There have been identified over 1000 FA structural variants, by the combination of different chain lengths,

number and position of insaturations, and the presence of additional substituents along the hydrocarbon chain, such as sugar molecules. Nonetheless, the more common FAs in nature are around 20, with palmitic acid (16:0), oleic acid (18:1) and linoleic acid (18:2) making up around the 80% of the most ordinary FAs<sup>43</sup>.

Table 3. Short description of the three most common fatty acid molecules.

Fatty acid	N. of carbons	N. of insaturations
<b>Palmitic acid</b>	16	0
<b>Oleic acid</b>	18	1
<b>Linoleic acid</b>	18	2

FAs can be synthesized *de novo* inside the cell or taken up from the extracellular space<sup>44</sup>. The absorption of FA by the cells can be divided in two different mechanisms: transporter mediated up-take, by CD36 fatty acid translocase among others, and passive permeation<sup>45</sup>. There are essential fatty acids that can not be synthesized and are fundamental for some biological functions, so they need to be taken up from the diet. These are polyunsaturated FAs with the double bonds close to the methyl end, and are divided in two series: omega-3 series based on linolenic acid with the double bond between the position C3 and C4, and omega-6 series based on linoleic acid with the double bond between the C6 and C7 position. After the acquisition of these lipids, there are different metabolic modifications catalyzed by elongases and desaturases and these lipids are transformed to other FAs, such as eicosapentaenoic acid (20:5) (EPA; omega-3) and arachidonic acid (20:4) (AA; omega-6)<sup>46</sup>.

On the other hand, FAs can be newly synthesized by condensation of two-carbon units provided by malonyl-CoA and acetyl-CoA molecule, by the action of acetyl-CoA carboxylase (ACC) and fatty acid synthase (FAS) enzymes, yielding palmitic acid (16:0). For the synthesis of other FAs, starting from the newly formed palmitic acid or externally absorbed FAs, the acyl chain of these lipids can be further elongated and desaturated. The elongation of the carbon chain implies the action of different elongases (ELOVLs) that cyclically add two-carbon units. Moreover, the FAs may have a straight saturated chain, or can contain one or more double bonds or insaturations. Mammalian cells contain specific desaturases that introduce double bonds in a defined position of the long-chain FAs. There are two different families of desaturases: stearoyl-CoA desaturases (SCD) introduce a double bond in C9 of the carbon chain, whereas FA desaturases (FADS) introduce the double bond in C5 and C6<sup>47</sup>.

Once the FA is synthesized, it needs to be covalently bound to a CoA by the action of fatty acyl-CoA synthetases (ACS), in order to enter the bioactive lipid pool of the cells. FAs have two main functions. On the one hand, they can be incorporated to other molecules forming more complex lipids. The fabricated lipids can be used for several purposes within the cells: precursor of lipid signaling molecules, store energy by generating triglycerides, fabricate phospholipids for structural purposes in the cell membranes and modify proteins through palmitoylation, among others<sup>48,49</sup>. The combination of different FAs in the structure of more complex lipids generates the structural variants of these complex lipids, changing their biological function. Some biologically important FAs act also as signaling molecules. Among them, the oxidation of arachidonic acid (20:4) or other polyunsaturated FAs (PUFAs), gives rise to eicosanoids, including

prostaglandins, leukotrienes and thromboxanes, with dramatically important biological functions<sup>44</sup>.

On the other hand, they can also be used as fuel after their oxidation in the mitochondria.

**Glycerolipids (GL)** are formed by the esterification of one, two or three FAs to a glycerol backbone, forming mono- (MG), di- (DG) or tri-glycerides (TG), respectively. They function mainly as energy stores since the excess of energy in the body is kept in TGs containing 3 FAs for further oxidation when required. Moreover, DGs are signaling molecules. They are second messengers as they participate in the transmission of signals across the cellular membranes and participate in the biosynthesis of TGs and glycerophospholipids<sup>50</sup>.

**Glycerophospholipids (GPLs)** are the main components of cell membranes, as well as important actors in cell metabolism and signaling. These lipids contain a glycerol backbone, with two FAs bond in sn-1 and sn-2. Frequently, GPLs contain a saturated FA at sn-1 and an unsaturated FA at sn-2. In the third carbon of the glycerol there is a phosphate followed by different polar heads, and based on the nature of which GPLs are divided into different subclasses. Therefore, they are amphipathic molecules, since they have a polar head group and two hydrophobic hydrocarbon tails. Depending on the polar head, and the length of the carbon chains and the number of insaturations of the fatty acids, there are variations on the biological function of the lipid and the physicochemical properties of the membranes where these lipids are located.

- Phosphatidic acid (PA) or phosphatidate is the intermediary for the synthesis of other glycerophospholipids and triacylglycerols, so it is present in low amounts in the tissues. It is formed by a glycerol molecule with two FAs esterified in sn-1 and sn-2, and in the third carbon, it has phosphoric acid. Thus, the polar group of PA is a hydrogen. At least four distinct pathways can generate PA. The main one takes place in the endoplasmic reticulum or mitochondria, GPAT (glycerol-3-phosphate acyltransferase) performs two sequential acylations in the sn-3-glycerol-3-phosphate that is generated in the catabolism of glucose. Another biosynthetic route of PA is the hydrolysis of other GPLs, yielding PA and the free polar head. For instance, Phospholipase D1 and D2 enzymes control the conversion of phosphatidylcholine lipids into PA and free choline<sup>51,52</sup>.

In addition to being a precursor of other lipids, overwhelming evidences reveal its role as a signaling molecule. Indeed, its presence affects cell growth, proliferation, motility and survival<sup>51,52</sup>.

- Phosphatidylcholine (PC) has choline as the head group. Frequently, PCs contain palmitic acid (16:0) or stearic acid (18:0) molecules in sn-1, and unsaturated oleic acid (18:1), linoleic acid (18:2) or linolenic acid (18:3) in sn-2<sup>52,53</sup>.

Choline is an essential nutrient for humans, with very high requirements for pregnant and lactating women, as it cannot be synthesized and is taken from the diet. The human body requires choline to synthesize phosphatidylcholine, choline ether lipids, and sphingomyelins; all these lipid subclasses are fundamental structural components of cell membranes. Indeed, the uptake of choline is mediated by choline transporters and it is mainly converted to PCs, which are very abundant in the lipid bilayers, particularly in the outer side, representing around 50% of all the GPLs in the membranes<sup>54</sup>. The presence of unsaturated FAs in the structure of PCs confers fluidity to the cell membranes. Interestingly, in order to fabricate the strikingly important acetylcholine neurotransmitter choline is also needed.

Although there are additional routes, the predominant PC synthesis pathway is the Kennedy pathway (Fig. 12). Here, a choline that is transported inside the cell is phosphorylated by choline kinase (CK) in the cytoplasm, and activated by the addition of cytidine triphosphate (CTP) via CTP:phosphocholine cytidyltransferase (CCT). The formed CDP-choline is transported to the endoplasmic reticulum, where, eventually, CDP-choline reacts with a lipid anchor, a diglyceride molecule, yielding a PC. Another synthesis route to produce PCs takes place in the liver mainly, where PE methyltransferase (PEMT) catalyzes three sequential methylations of the ethanolamine moiety of phosphatidylethanolamine (PE), yielding a PC<sup>55</sup> (Fig. 12). After their synthesis there is a remodeling process called Lands' cycle (Fig. 14). This is a strikingly important metabolic process common to all GPLs, where after their synthesis their FA chains are released by fosfolipase A<sub>2</sub> (PLA<sub>2</sub>) enzyme and a different FA is incorporated by reacylation.,

On the other hand, there are several catabolic routes for PCs. Phospholipase enzymes catalyze the hydrolysis of the different GPLs, as it will be further explained in section 3 (page 46). Phospholipase D family enzymes hydrolyze PCs releasing PA and choline. This choline is frequently used for the production of new PCs. In addition, via phospholipase C, DG and phosphocholine are generated, and via phospholipase A family of enzymes (PLA<sub>1</sub> and PLA<sub>2</sub>) a free fatty acid and lyso-phosphatidylcholine are produced. All the byproducts of these catalytic routes have extremely important roles as signaling molecules.

Interestingly, PCs are precursors for the synthesis of other lipids, including sphingomyelins, platelet-activating factor and PEs, all of them playing important structural and signaling roles<sup>53,55</sup>.

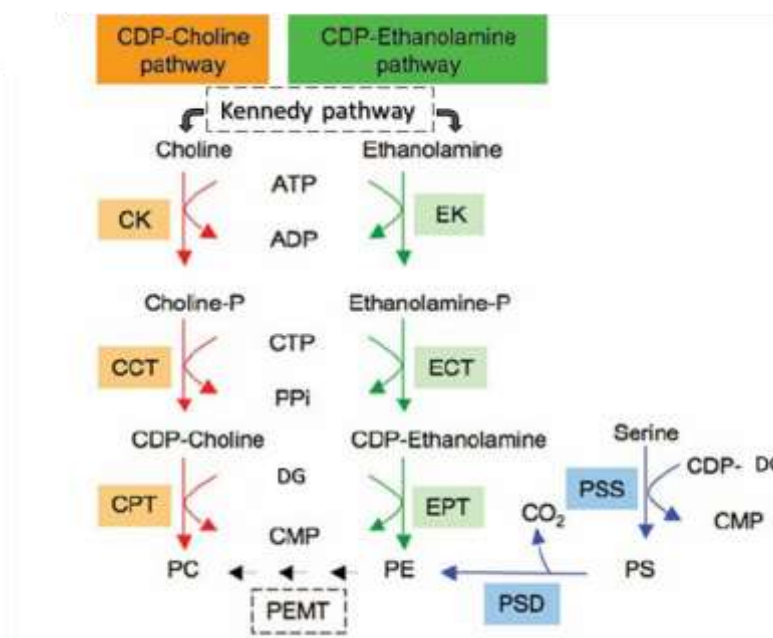


**Figure 12. De novo synthesis pathways of PC, PE and PS. Adapted from <sup>61</sup>.** Abbreviations: CK –choline kinase, CCT –CTP:phosphocholine cytidyltransferase; CPT –choline phosphotransferase; EK –ethanolamine kinase; ECT –CTP:phosphoethanolamine cytidyltransferase; EPT –ethanolamine phosphotransferase; PEMT –PE methyltransferase; PSS –phosphatidylserine synthase; PSD –phosphatidylserine decarboxylase; ATP –adenosine triphosphate; ADP –adenosine diphosphate; CTP – cytidine triphosphate; PPI –pyrophosphate; DG –diglyceride; CMP –cytidine monophosphate; CDP-DG – cytidine diphosphate diglyceride.

- Phosphatidylethanolamine (PE) contains ethanolamine as the polar group, and is the second most common GPL in mammals. PEs are present in every cell of the human body, representing about 25% of all the GPLs, while in nervous tissue they can make up to 45% of all GPLs. Moreover, its abundance varies from one organelle to another, accumulating greater amounts in mitochondria. Like PCs, they commonly contain palmitic acid (16:0) or stearic acid (18:0) in sn-1, but a longer unsaturated FA (20-22 C) in sn-2. They are also major components of the cell membranes, and can be found mainly in the cytoplasmic side of the lipid bilayers. However, they are present in both the inner and outer leaflet of mitochondria membrane, where they exert fundamental functions. In particular, they facilitate the protein movement across the membranes and membrane fusion. In addition, they are precursors of 35% of PCs synthesized in the liver. In the brain, they are precursor for the synthesis of anandamide, a cannabinoid ligand. Moreover, they are important for mitosis as they control the fusion of mitotic Golgi membranes. They are also significant in autophagy. Thus, they are important not only for their structural function but also for some fundamental cellular processes. Furthermore, they act as growth factor in cell cultures and have been proven to overcome the apoptosis produced by low serum culture conditions<sup>26,56,57</sup>.

PEs can be synthesized through different pathways. Like for PCs, Kennedy pathway is the principal route (**Fig. 12**), albeit ethanolamine is the substrate and its phosphorylation is performed by ethanolamine kinase (EK). In the second step, CTP is condensed with the phosphoethanolamine by the action of ECT enzyme (CTP:phosphoethanolamine cytidyltransferase), yielding CDP-ethanolamine. In the final step, EPT (ethanolamine phosphotransferase) catalyzes the reaction between CDP-ethanolamine and a lipid anchor, normally DG, giving rise to PE. The *de novo* synthesized PEs are mainly mono- or di-unsaturated acyl chains at the sn-2 position, such as 18:2<sup>26,55</sup>. The second source of PE is the mitochondria, where phosphatidylserine decarboxylase (PSD) decarboxylates a PS molecule yielding a PE (**Fig. 12**). Another minor synthesis route for PE takes place in the ER, and is a calcium-dependent base-exchange reaction where the serine of a PS is substituted by an ethanolamine<sup>56,57</sup>. As well as PCs, after the synthesis of PEs, they are remodeled in Lands' cycle (**Fig. 14**).

However, mammals cannot synthesize ethanolamine, so it is acquired from the diet as free ethanolamine, or from existing PEs, which are hydrolyzed by phosphodiesterases to produce free ethanolamine and glycerol. Another source of ethanolamine is the degradation of sphingosine phosphate by sphingosine phosphate lyase and the lysis of the endocannabinoid anandamide by the fatty acid amine hydrolase<sup>56</sup>.

- Phosphatidylserine (PS) has a serine head group and accounts for the 3-15% of all the GPLs. However, the brain and retina are enriched with PS. There is also different concentrations of PSs within organelles, being abundant in plasma membranes, specially the inner leaflet, and scarce in mitochondria inner membrane<sup>58</sup>. In mammals, the synthesis of these lipids is carried out by the calcium-dependent substitution of a polar group (choline or ethanolamine) for a serine, in preexisting PCs or PEs. Conversely, PSs can be decarboxylated in the mitochondria producing PEs. The main functions of PSs are being the precursors of PE in mitochondria, targeting some proteins to the phagosomes, and modifying the catalytic activity of some enzymes, such as Annexin V and protein kinase C. To gain insight into the fundamental role of PSs in mammalian cells, a study unraveled that mutant mice with impaired PSs synthesis did

not outlast during development. Indeed, PS play a role in blood clotting and apoptosis<sup>57-59</sup>.

- Phosphatidylinositol (PI) carries an inositol molecule as polar head group, which is a cyclic hexalcohol. Essentially, they contain stearic acid (18:0) at sn-1 and arachidonic acid (20:4) at sn-2. They are structural components of the outer leaflet of cell membranes, making up around 10% of all GPLs, and aid in anchoring proteins to the outer surface of the cells, playing a strikingly important role in cell signaling<sup>60</sup>.

The *de novo* biosynthesis of PIs is carried out in the PI cycle (**Fig. 13**), similar to the Kennedy pathway of PCs and PEs. First, CDP-DG is conjugated with inositol, catalyzed by phosphatidylinositol synthase, in the endoplasmic reticulum. Then, the formed PI can be remodeled by Lands' cycle, where there is a PI specific acetyltransferase, LPIAT (lyso-PI acyltransferase). PIs are the primary source of arachidonic acid (AA) that is needed for eicosanoid biosynthesis.<sup>52,60,61</sup>

As part of the PI cycle, the inositol ring can be reversibly phosphorylated in the positions 3, 4 and/or 5 yielding 7 different phosphoinositides (PPI<sub>n</sub>). These can be phosphatidylinositol phosphate (PIP), phosphatidylinositol biphosphate (PIP<sub>2</sub>) or phosphatidylinositol triphosphate (PIP<sub>3</sub>), that are very important signaling molecules. Although they represent only around 1% of all the GPLs in cell membranes, they can be second messengers or modulate the anchorage and activity of different membrane proteins, actively participating in several basic cellular processes, such as signal transduction, membrane dynamics, cytoskeleton reorganization, membrane and vesicular trafficking<sup>52,62</sup>.

Moreover, they have been largely investigated, since the phosphorylation of these molecules is driven by PI3K (phosphatidylinositol 3-kinase), which is mutated in several cancers leading to an aberrant activation of these enzymes. Moreover, PTEN lipid phosphatase that is responsible for the dephosphorylating of PI3Ks, thus inactivation of the enzymes, is also frequently mutated in several cancers. These results in increased PIP<sub>3</sub> levels, trait that has been strongly related to elevated metastatic capacity. Therefore, both PI3Ks and PTEN are among the most promising drug targets in cancer<sup>52,62,63</sup>.



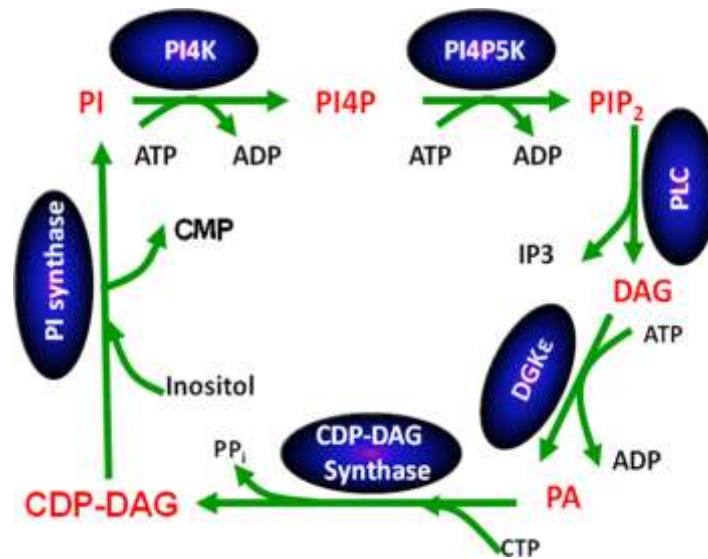


Figure 13. PI cycle. In blue ovals are the enzymes that catalyze each reaction of the route. In red are the lipid intermediaries<sup>61</sup>.

- Phosphatidylglycerol (PG) is formed by a glycerol-3-phosphate backbone that has two FAs esterified in sn-1 and sn-2, and another glycerol molecule as the head group. It is commonly found in the inner mitochondria membrane. Although it appears at a low abundance in the membranes (1% of all PLs), its main function is being the precursor of mitochondrial cardiolipins.

The *de novo* biosynthesis of this subclass is carried out by the condensation of CDP-DAG and glycerol-3-phosphate catalyzed by phosphatidylglycerolphosphate synthase, yielding phosphatidylglycerol-phosphate. Then, the intermediary is dephosphorylated with phosphatidylglycerolphosphate phosphatase producing PG phospholipid. Like in the rest of GPLs, the FAs of PGs can be remodeled in Lands' cycle. Concretely, a PG specific acyl-transferase has been found, LPGAT1, which shows a preference for 16:0, 18:0 and 18:1 FAs. As opposed to other GPLs, they often have more unsaturated FAs in sn-1 position<sup>64,65</sup>.

Due to the low abundance of these GPLs in mammal cells, little is known about their physiological and pathological functions.

- Cardiolipins have a unique dimeric structure as they are formed by a central glycerol molecule with two phosphatidic acids attached. Therefore, they content four FAs, which are commonly mono- or di-unsaturated chains with 16-18 carbons. Moreover, the distribution of the carbons and the double bonds is homogeneous within the four-acyl chains, since almost half of the cardiolipin structures studied are symmetrical. They are mainly found in the inner mitochondria membrane, making up to 20% of all the GPLs of this structure<sup>66</sup>. Here, they are important for membrane fusion and maintaining the enzymatic function of some enzymes of the electron transport chain, thereby influencing the energy production of the cells and acting as a proton trap during OXPHOS<sup>67</sup>. Besides, they trigger the apoptosis machinery when they are translocated to the outer side of the mitochondrial membrane<sup>68,69</sup>.

- Ether phospholipids present an alkyl or alkenyl/vinyl bond between the glycerol and a fatty alcohol in sn-1, instead of an ester bond with a fatty acid. There can be ether lipids of all the glycerophospholipid subclasses, although choline and ethanolamine are the most abundant. In particular, plasmalogens are the most abundant ether lipids, and carry a double bond next to the ether bond, therefore forming a vinyl ether bond. Commonly, the fatty alcohols in sn-1 position are 16:0, 18:0 and 18:1, whereas polyunsaturated FAs concentrate in sn-2 position, generally docosahexaenoic (22:6) or arachidonic acid (20:4). Alkyl ether bonds are commonly found in ether phospholipids containing choline, and vinyl ether bonds are more prominent in ethanolamine plasmalogens<sup>70,71</sup>.

Their presence is very variable and depends on the tissue or organ, representing around 20% of all the glycerophospholipids, increasing their abundance in heart, nervous tissue and inflammatory cells. According to the subcellular localization, they are enriched in plasma, nucleus, endoplasmic reticulum and mitochondria membranes. The main functions of these lipids are structural support in the nucleus and mitochondria, and cell vesicle formation, membrane fusion and ion transport. The presence of plasmalogens in biological membranes generates a tighter packing of the lipids forming the bilayer, thereby increasing rigidity and decreasing fluidity. Moreover, they have been found enriched in the lipid rafts of the bilayers, and the accumulation of these lipids together with sphingolipids and cholesterol was associated with increased stability of the membrane rafts. Indeed, several studies unraveled that the blockage of plasmalogen presence in the membranes is translated into oxidative stress and cell apoptosis, highlighting the importance of these lipids in the membrane homeostasis. In addition, they also have important signaling roles and antioxidant scavenging properties. Indeed, the vinyl-ether bond is able to capture reactive oxygen species and avoid the oxidation of the so sensitive PUFAs. Besides, they generate less persistent oxidative byproducts compared to other phospholipids<sup>70,72-74</sup>.

Ether lipids are synthesized by unusual and complex biosynthetic pathways that start in peroxisomes and finish in the endoplasmic reticulum. The peroxisomes are significant metabolic organelles as they participate in strikingly important metabolic processes including oxidation of branched and very-long-chain FAs, ether phospholipids synthesis, bile acid synthesis, amino acid catabolism, polyamine oxidation, and the oxidative arm of pentose phosphate pathway (PPP)<sup>72,74,75</sup>.

For the synthesis of ether phospholipids, first, inside the peroxisome, dihydroxyacetone phosphate (DHAP) is esterified at sn-1 with a long-chain acyl-CoA, what is carried out by dihydroxyacetonephosphate acyltransferase (DHAPAT). Then, the ether bond is introduced via alkyl-DHAP synthase (ADAPS), by the substitution of the acyl of acyl-DHAP with a long-chain fatty alcohol. The remaining catalytic reactions take place in the endoplasmic reticulum, so 1-alkyl-DHAP is transported to that organelle. The first reaction in the ER is the reduction of the ketone group to form a glycerol, and an acyl group is introduced at sn-2, yielding a 1-alkyl-2-acyl-glycero-3-phosphate. Afterwards, the phosphate group is removed by a phosphohydrolase, and upon the activity of different enzymes the intermediary is transformed to either ethanolamine or choline ether lipids, in a process similar to the Kennedy pathway. As well as PCs, ether-PCs can also be synthesized by the methylation of ether-PEs through PEMT enzyme in the ER and mitochondria. At this point, the produced ether lipids are transported from the endoplasmic reticulum to the other organelles and plasma membrane, distributing

ethanolamine plasmalogens within the inner leaflets of the membranes and choline ether lipids within the outer side<sup>65,66,71</sup>.

Ether lipids are also remodeled by phospholipases, as there is an ether lipid-specific PLA<sub>2</sub> isoform. In this way, ether lipids are considered important signaling lipids, since they usually contain AA, docosapentaenoic acid or docosahexaenoic acid (DHA) in sn-2, which are released upon PLA<sub>2</sub> activity<sup>70-72</sup>.

The different glycerophospholipid subclasses are synthesized through specific *de novo* pathways that are summarized in **Figure 14**. This *de novo* biosynthesis takes place in the ER, peroxisomes and mitochondria, although the final remodeling steps can occur in either the ER or mitochondria. Starting from a glycerol molecule that is phosphorylated to glycerol-3-phosphate, a lysophosphatidic acid (LPA) is formed following the binding of a FA by glycerol-3-phosphate acylCoA:glycerol-3-phosphate acyltransferases (GPATs), which prefer saturated or mono-unsaturated FAs. Then, a second FA is esterified in the LPA yielding PA via acyl-CoA lyso-PA acyltransferases (LPAATs). The formed PA is further metabolized to form two different glycerol derivatives. One, DAG (or DG, they are named interchangeably in this work), is formed after the dephosphorylation of PA by phosphatidic acid phosphatase (PAP). This DAG is intermediary for the synthesis of TG by the addition of an acyl chain by diacylglycerol acyltransferase (DGAT) or by the transfer of an acyl chain from PC to DAG by phospholipid:diacylglycerol acyltransferase (PDAT). In addition, PC, PE and PS are also produced from DAG. PS is also formed from PC and PE. The other glycerol derivative is cytidine diphosphate-DAG (CDP-DAG) that is metabolized to form PI, PG, CL or PS.

The biophysical properties of the cell membranes depends on the characteristics of the phospholipids within these structures. This lipid variety is observed among different tissues and even between organelles within the same cell, being extremely important since it is reflected in the specific function of each compartment. Concretely, the lipid diversity is given by the distinct head groups, chain length and insaturations of the acyl chains that determine the fluidity, permeability, stability, curvature and subdomain architecture of the bilayers. It is reflected in the vesicular trafficking, signal transduction and molecular transport of the cells. Therefore, the phospholipid content of the membranes directly affects all these cellular processes. The remodeling process of the *de novo* synthesized GPLs is performed in Lands' cycle. As the enzymes of *de novo* synthesis pathways have little substrate specificity for concrete FAs, the generated GPLs may not contain the acyl chains suitable for a correct function of the membranes. Hence, the glycerophospholipids modify their FA chains by a series of deacylation and reacylation reactions. The saturated FA esterified in sn-1 position are believed to be generally derived from *de novo* synthesis, whereas the unsaturated FA that is generally observed in the sn-2 position is introduced in this remodeling process. For this, phospholipase A2 (PLA<sub>2</sub>) specifically, cleaves the acyl chain at sn-2 of the GPL. Thus, important signaling molecules are generated, as lyso-phospholipids and free fatty acids are released, including the so important arachidonic acid (20:4). The latter can be converted to eicosanoids, which participate in a plethora of physiological and pathological processes, including inflammation, immune response, sleep regulation and pain perception. Then, the lyso-GPL can be reacylated by incorporating a different fatty acid to the previously cleaved position and forming a new phospholipid via specific acyl-CoA:lysophospholipid acyltransferases (LPLAT), as are different enzymes specific for each PL subclass. Therefore, this process can replace oxidized fatty acids and helps to generate

a diverse and asymmetrical content of acyl chains within the cell membranes, which is required for the correct function of the bilayers<sup>76–79</sup>.

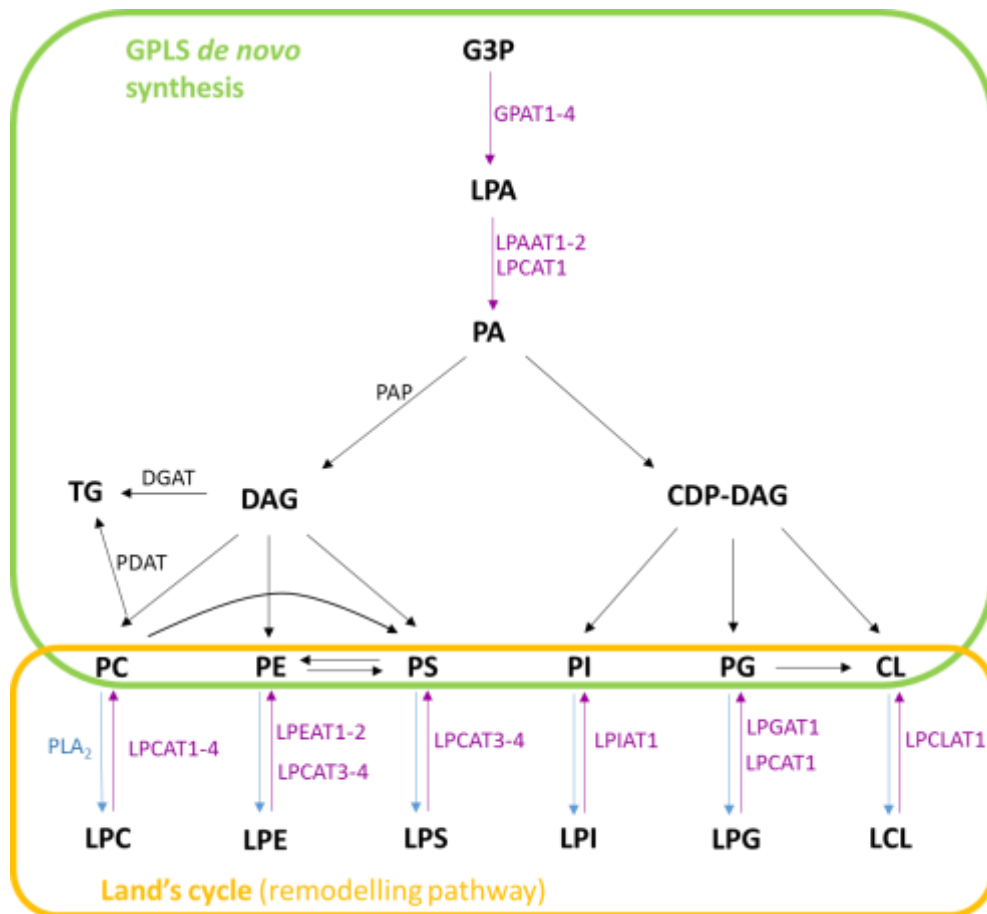


**Figure 14. Glycerophospholipid biosynthesis.** The combination of the different *de novo* synthesis pathways and Lands' cycle gives rise to phospholipid diversity. The blue arrows indicate PLA<sub>2</sub> and purple arrows acyltransferases. G3P, glycerol-3-phosphate; GPAT, glycerol-3-phosphate acyltransferase; LPA, lysophosphatidic acid; LPAAT, lysophosphatidic acid acyltransferase; LPCAT, lysophosphatidic acid acyltransferase; CDP-DAG, cytidine diphosphate-diacylglycerol; LPE, lysophosphatidic acid; LPC, lysophosphatidic acid; LPS, lysophosphatidic acid; LPI, lysophosphatidic acid; LPG, lysophosphatidic acid; LCL, lysophosphatidic acid; LPEAT, lysophosphatidic acid acyltransferase; LPIAT, lysophosphatidic acid acyltransferase; LPGAT, lysophosphatidic acid acyltransferase; LPCLAT, lysophosphatidic acid acyltransferase.

**Sphingolipids (SPLs)** are a family of complex lipids that share a common structural feature, a sphingoid base backbone, which is composed of a set of aliphatic amino alcohols. The most common one is sphingosine, an 18-carbon length aliphatic chain with a double bond in position 4, hydroxyl groups in positions 1 and 3, and an amine group in position 2. The sphingoid bases are produced *de novo* by the condensation of the amino acid serine and a long-chain fatty acyl-CoA of different lengths and number of insaturation. Sphingosine is the most common sphingoid base and is synthesized by the condensation of serine with palmitic acid. In addition, the FAs that are bound to the sphingoid bases in this lipid class differs slightly from the ones of the GPLs, since they can be long chains of up to 26 carbons, and can be odd- or even-numbered. However, in the sphingolipids of the epidermis there can be FAs of 28 to 36 carbons. Besides, polyunsaturated FAs are rarely found within these lipids<sup>80</sup>.

There are different bioactive lipids within sphingolipid family, such as ceramides, sphingosine 1-phosphate (S1P), sphingosine and sphingoglycolipids. They participate in different cellular processes closely related to carcinogenesis, as they regulate inflammation, senescence, apoptosis, angiogenesis, cell proliferation, survival, migration and differentiation<sup>63</sup>.

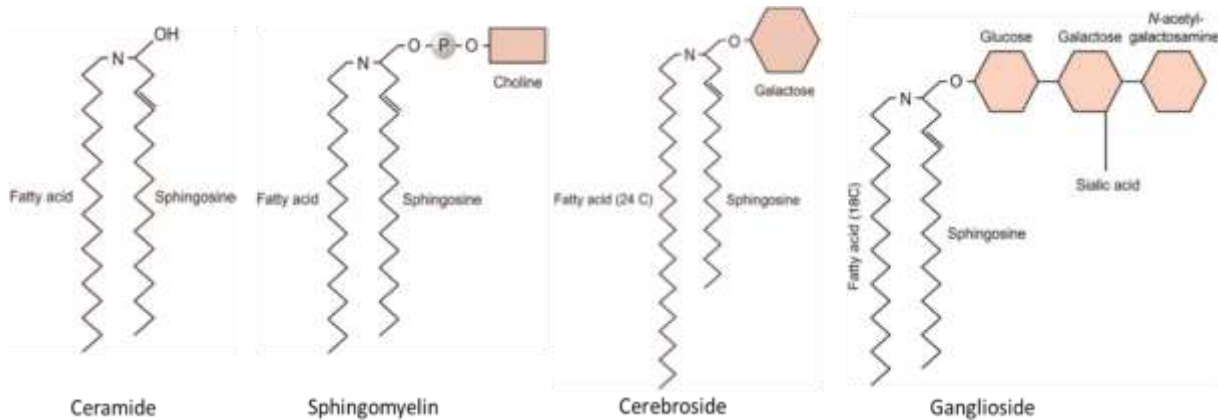


Figure 15. Schematic representation of the general structure of sphingolipids<sup>54</sup>.

- Ceramides (Cer) are formed by the addition of a fatty acid to a sphingoid base through an amide bond. The acyl-chains of these molecules can be very distinct depending on their biological origins, although they are usually saturated or mono-unsaturated acyl chains. Despite their very low abundance in tissues others than the skin, they have important biological functions on their own, since they are important lipid second messengers. Additionally, ceramides can be precursors of more complex sphingolipids, which perform a wide range of functions in cells<sup>81</sup>. Furthermore, ceramides perform structural functions in the membranes, as they affect the permeability of the bilayers by interacting with the ion channels of the membranes. Although ceramides are minor components of the membranes, they are accumulated in rafts participating in several signaling events, generally activating catabolic enzymes and slowing down anabolic processes. Thus, they are significant players in the regulation of cell transformation, differentiation, proliferation, migration, cell death, autophagy, senescence and apoptosis. Indeed, the mechanism of action of many chemotherapeutic agents and radiation treatments includes the ceramide-mediated induction of cell death<sup>81-83</sup>.

Interestingly, there is a great accumulation of ceramides in the stratum corneum of the skin, making up to 50% of all the lipids found in this structure. Here, ceramides exist as both free molecules and esterified to structural proteins. Moreover, they present distinct features, as they contain larger carbon chains, which help them to participate in the barrier properties of the skin, since they confer lower permeability to the skin<sup>82</sup>.

The biosynthesis of ceramides is complex, and can be performed by distinct pathways (**Fig. 16**). First, they can be *de novo* synthesized in the endoplasmic reticulum. It begins with the condensation of a serine and palmitoyl-CoA and subsequent CoA release by serine palmitoyltransferase (SPT), yielding 3-keto-dihydrosphingosine. Next, this is reduced by 3-ketosphinganine reductase to form sphinganine (dihydrosphingosine). The latter is condensed with a very-long chain FA, turning it to dihydroceramide by the action of dihydroceramide synthase (CerS). There are six different isoforms of CerS,

depending on the carbon-chain length of the ceramide they synthesize. For instance, CerS3 participates in the synthesis of very-long-chain (28-32 C) ceramides with polyunsaturated FAs, that are highly expressed in the skin<sup>84</sup>. Finally, a double bond is introduced in the position 4 of the sphingoid base via a dihydroceramide desaturase, to form the final ceramide. While most of the ceramide needed as intermediary is synthesized in the cytoplasmic leaflet of the endoplasmic reticulum, the production of more complex SPLs is carried out in the Golgi apparatus. Therefore, ceramides are transported to the Golgi apparatus by a key cytoplasmic protein, the ceramide transporter (CERT)<sup>82,85,86</sup>.

Another route for ceramide biosynthesis is the catabolism of complex SPLs inside the lysosomes, the route called salvage pathway. This route generates ceramide much faster than the *de novo* synthesis. Thus, it is of striking importance for rapid signaling pathways. Here, S1P is dephosphorylated via sphingosine kinase and an acyl-CoA is bounded to the formed sphingosine by the action of ceramide synthase forming a ceramide molecule<sup>86</sup>. The third route for ceramide synthesis is the SM cycle, where SM is catabolized by sphingomyelinases (SMases) yielding a ceramide and phosphocholine. There are three different types of SMases according to their pH-dependent optimal activity: acid, neutral and alkaline SMases<sup>87</sup>. Besides, glycosphingolipids can also be hydrolyzed by glycosidases yielding ceramide, although this is not a very important pathway in animal tissues.

Then, the released ceramides are further catabolized by ceramidases, yielding a sphingosine base and a free FA. Markedly, there are five different ceramidases, with different subcellular localizations and FA specificity, thereby affecting different cellular and signaling events. Some of the sphingoid bases generated in this pathway exit the lysosomes and are reutilized for ceramide synthesis via CerS. Likewise, the released sphingosine can be phosphorylated by sphingosine kinases to form sphingosine-1-phosphate that can be hydrolyzed by lyases yielding PE and fatty aldehyde. It is estimated that this pathway accounts for the synthesis of the 50-90% of S1P<sup>82,85,86</sup>.

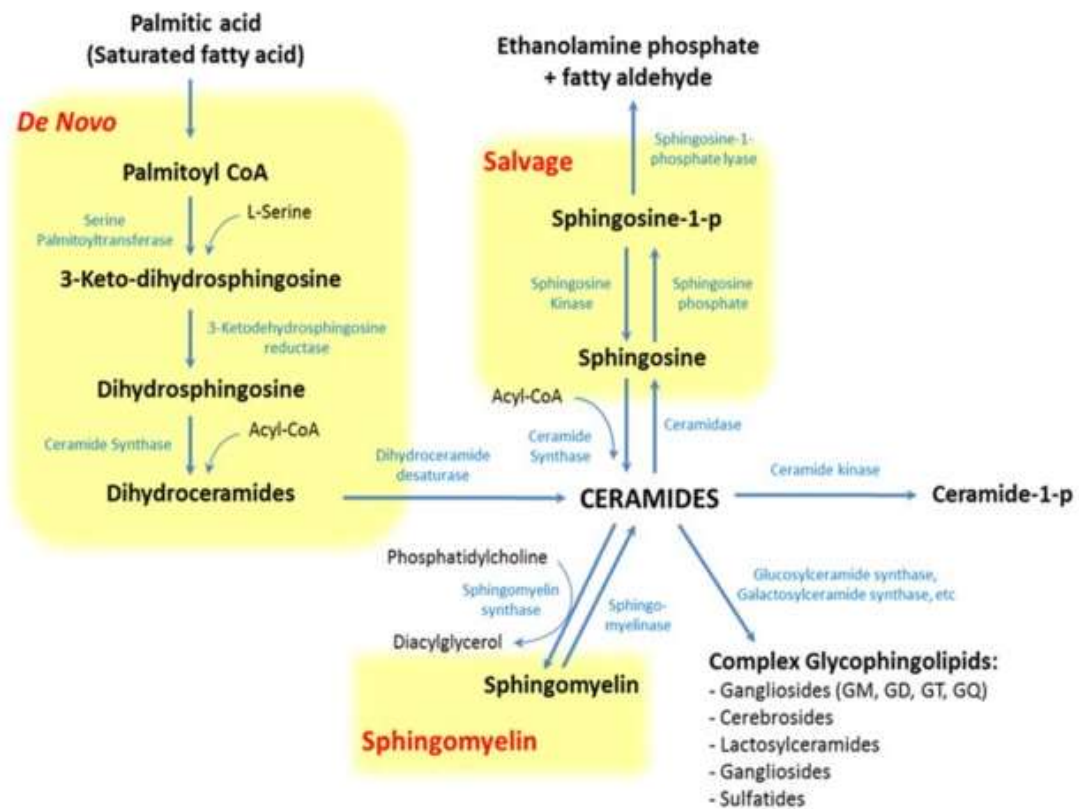


Figure 16. Representation of the metabolic pathways of sphingolipid metabolism<sup>86</sup>.

- Sphingomyelin (SM) is the most abundant SPL, and it is ubiquitously distributed in cell membranes, especially in the outer side. It is formed by the addition of a phosphocholine to the position 1 of the sphingoid base of a ceramide. Normally, the base is a sphingosine, and the side chains are long FAs either saturated or monounsaturated odd-numbered chains<sup>87</sup>.

The synthesis of SM takes place in the Golgi apparatus and plasma membrane (**Fig. 16**), by the linkage of a ceramide and a phosphocholine donated from a PC to a ceramide, and releasing a DAG molecule and a sphingomyelin. This reaction is catalyzed by sphingomyelin synthase (SMS). Additionally, they can also be synthesized by the acylation of a lyso-sphingomyelin. When the biosynthesis takes place in the Golgi apparatus, the ceramide synthesized in the endoplasmic reticulum is transported to Golgi by CERT in an ATP-consuming process. Then, much of the SM produced is transported to the plasma membrane by a vesicular transport mechanism. On the other hand, they are hydrolyzed by SMases releasing phosphocholine and ceramide<sup>81</sup>.

SMs are more abundant in Golgi and plasma membranes, presenting a lower concentration in mitochondria. They are usually located close to cholesterol forming the lipid rafts of the membranes. In fact, several evidences suggest that the metabolisms of these two molecules are connected, and SM levels may control the distribution of cholesterol within the cells. Moreover, SMs control the formation and function of ion channels. Interestingly, they inhibit the activity of Phospholipase A<sub>2</sub>, an important enzyme in eicosanoid production and phospholipid remodelling. SM is the most abundant sphingolipid in the nucleus, and participates in several process there. It is significant for the chromatin assembly and dynamics, and it is an important component of the nucleus matrix<sup>82</sup>.

- Glycosphingolipids are divided in two groups: Cerebrosides, and gangliosides. Cerebrosides in particular are monoglycosylceramides that are formed by the addition of a carbohydrate molecule to a ceramide. Although they can have different sugars in their structure, glucose (glucosylceramide –GlcCer) and galactose (galactosylceramide –GalCer) are the most common. They have an important structural role in the membranes, especially in the brain. Like SMs, they are usually accumulated in the outer leaflet of plasma membrane together with cholesterol forming lipid rafts, where they bind to enzymes and receptors. They can also be intermediaries of complex glycosphingolipids. Glucosylceramide, although is found in different tissues such as spleen, erythrocytes and nervous tissue, is a major constituent of the skin, and it is required for axonal growth especially in the brain. Furthermore, it has been demonstrated that they are essential for intracellular membrane transport, cell proliferation and survival. On the other hand, galactosylceramides are mainly present in nervous tissue, having an essential role in oligodendrocyte differentiation and myelin structure formation, stability and function. In addition, they have been found to be potent activators of the immune system<sup>88,89</sup>. At the cellular level, cerebrosides are important for cell adhesion in melanoma cells, therefore participating in cell growth and differentiation<sup>89</sup>.

One to five molecules of sialic acid attached to a lactosylceramide form gangliosides. Lactosylceramides are molecules that contain a galactose and a glucose linked to a ceramide. Like cerebrosides, gangliosides are accumulated in the outer leaflet of the plasma membrane forming rafts, and are also important components of the nuclear membrane<sup>90</sup>.

**Sterol** lipids are a family of polycyclic compounds, being cholesterol the most abundant member. Cholesterol is a rigid planar four-ring molecule with a carbon side-chain. It is ubiquitously distributed among all the tissues, and it accumulates mainly in the plasma membrane (30-50% of the lipids in the bilayer). It can be present in a free form, amphipathic form or esterified to long-chain FA forming cholesterol esters. Cholesterol plays a fundamental role in cells, as it is an important structural component of cell membranes, influencing the fluidity of the bilayers as it intercalates between the phospholipids. Moreover, it is the precursor of all steroid hormones and other important metabolites such as Vitamin D and bile acids. Indeed, it is vital for cell signaling, transport, morphogenesis, lipid absorption and digestion, and nerve conduction, among others<sup>91</sup>. Cholesterol esters on their side, are completely hydrophobic molecules and instead of accumulating in the membranes, they are present in the lipid droplets storing cholesterol.

The mevalonate pathway drives the biosynthesis of sterol isoprenoids, such as cholesterol, steroid hormones and bile acids, and nonsterol isoprenoids. This is a very complex process, as at least 30 enzymatic reactions take place in this network. First, the synthesis of the intermediary mevalonate is achieved, which takes place in two consecutive enzymatic reactions, by the union of acetyl-CoA and acetoacetyl-CoA and the action of HMG-CoA synthase, and the subsequent reduction of the previously formed HMG-CoA by HMG-CoA reductase (HMGR)<sup>92</sup>. The latter is the rate-limiting step in mevalonate pathway. If there is low presence of sterol isoprenoids in the cell, the sterol regulatory element binding protein (SREBP) transcription factors are activated and trigger the transcription of HMGR gene. Besides HMGR, SREBPs activate the transcription



of some of the enzymes of the mevalonate pathway<sup>93</sup>. Moreover, SREBPs have also been linked to the increased expression of phospholipid synthesis enzymes<sup>94</sup>.

Next, mevalonic acid undergoes two consecutive phosphorylations, yielding two isoprenes. These are consecutively condensed to give squalene. Then, squalene undergoes several enzymatic reactions to finally produce cholesterol.

Other lipid classes that are not studied in this thesis are prenol lipids, saccharolipids and polyketides.

**Prenol lipids** are synthesized by the subsequent condensation of the five-carbon precursors isopentenyl diphosphate and dimethylallyl diphosphate that are produced in the mevalonate pathway. They contain an isoprenoid tail linked to quinonoid core<sup>83</sup>. Carotenoids are important components of this lipid class, as they are simple isoprenoids that act as antioxidants and precursors of vitamin A. Moreover, vitamin E and vitamin K are other significant lipids within this subclass.

**Saccharolipids** are formed by a direct link between a FA and a sugar molecule. They are mainly found in bacteria and plants<sup>83</sup>.

**Polyketides** are synthesized after the polymerization of acetyl and propionyl subunits. A large number of the members of this lipid subclass are secondary metabolites and animal products. Among them, there are several anti-microbial, anti-parasitic and anti-cancer agents<sup>59</sup>.

#### 2.1.2. Lipid nomenclature

In this work, the shorthand notation has been used. This approach provides a standard and practical nomenclature that is based on LIPID MAPS terminology. For this, every lipid class is provided with an abbreviation that defines its backbone, the head group, and the presence of sugar moieties. In addition, the information about the structure is provided by the description of the acyl chains, which are related indicating the carbon chain length and the number of insaturations<sup>83,95</sup>. Therefore, every lipid species is named by the abbreviation of its lipid subclass followed in parentheses with the number of carbons and the number of insaturations within the acyl-chain, separated by a colon. However, in this nomenclature, the type (double or triple bond), position and geometry of the insaturations are missed. For example, a 20-carbon long fatty acid with three insaturations would be denominated as FA(20:3).

Furthermore, if the lipid is a glycerophospholipid with two FA chains, first, the FA esterified in carbon 1 (sn-1) is named and then the FA esterified in carbon 2 (sn-2), separated by a slash. Thus, a glycerol backbone with FA(16:0) esterified in carbon one, FA(20:4) in carbon two and head group of phosphocholine in carbon three would be named as PC(16:0/20:4). However, sometimes it is not possible to define the two FA chains, and the lipids are named as the total sum of carbons and insaturations of both acyl-chains. In this case, it would be noted as PC(36:4).

In the case that the glycerophospholipid has lost one of its FA, the term lyso is used. This is for example LPE(18:0), that stands for lyso-phosphatidylethanolamine with an esterified 18:0 FA. Using this technology it is not possible to reveal in which carbon of the glycerol backbone is esterified the FA.

Besides lipids with esterified FAs, there are ether lipids, which can have the fatty-alcohol linked through either an O-alkyl bond documented as O before the number of carbons and insaturations of the chain, or O-alk-1-enyl bond written as P<sup>95</sup>. For instance, a lipid molecule with

an ethanolamine head group, a fatty-alcohol derived from FA(18:0) linked with an alkenyl bond and a FA(20:4) esterified, it would be named as PE(P-18:0/20:4).

Sphingolipids for their part can be d- or t- in sn-2 depending on the hydroxyl groups present in the sphingoid base: d- for di, and t- for tri. Then, it comes the number of carbons:insaturations of the sphingoid base, followed by a slash and the carbons:insaturations of the FA bound to the sphingoid base<sup>95</sup>. Hence, a sphingomyelin molecule with a di-hydroxyl 18:1 sphingoid base, and with a FA(18:2) linked to its structure, it would be denominated as SM(d18:1/18:2).

**Table 4. Abbreviations of the lipid classes detected in this work.**

Lipid Class	Abbreviation
<b>Free Fatty Acid</b>	FFA
<b>Glycerolipids</b>	GL
Diglycerides	DG
Triglycerides	TG
<b>Glycerophospholipids</b>	GPL
Phosphatidic Acid	PA
Phosphatidylcholine	PC
Lysophosphatidylcholine	LPC
Phosphatidylcholine ether	PC(P/O)
Phosphatidylserine	PS
Phosphatidylethanolamine	PE
Lysophosphatidylethanolamine	LPE
Phosphatidylethanolamine ether	PE(P/O)
Phosphatidylinositol	PI
Phosphatidylglycerol	PG
<b>Sphingolipids</b>	SPL
Ceramides	Cer
Sphingomyelin	SM
Hexosylceramide	HexCer
<b>Sterols</b>	
Cholesterol esters	CE

## 2.2. Lipidomic analyses

The heterogeneous nature of melanoma tumors hampers to find a completely accurate biomarker and treatment option for melanoma. Furthermore, the variability of the carcinogenic process is such that even tumors with the same histologic features, share different genetics, proteomics, metabolomics and epigenetics, thus presenting a distinct proliferative and metastatic profile. A better understanding of the molecular changes within neoplasms is of vital importance. In line with this, the study of the lipid content of cells and their metabolism has aroused great interest in recent decades.

Lipidomics was first defined in 2003 as an analytical approach that aims to characterize and quantify the lipid content of a sample, as well as identify the interactions of these molecules with other biomolecules such as other lipids, proteins or genetic material. From then on, lipidomic analyses have evolved as a promising field in cancer research and biomarker discovery. To date, these approaches are frequently used to detect and classify tumor cell lines and tissues, in order to eventually differentiate normal and tumor tissues<sup>96-99</sup>.

Owing to the physical and chemical diversity of lipids, there is no single analytical process that studies the entire lipidome of a cell or sample in a single attempt. However, several analytical procedures have been developed recently that allow the identification of a broad spectrum of lipids. The rapid evolvement of this field has been tightly connected to the great advances made in mass spectrometry techniques. Although these studies can be performed using NMR (nuclear magnetic resonance), Raman spectroscopy and other spectroscopic approaches, most lipidomic methodologies are mainly based on mass spectrometry methods (MS), which can be performed either directly on the samples or combined with a previous liquid chromatography. A common workflow in lipidomic analyses comprises lipid extraction from the biological sample, possible chromatographic separation, soft ionization and MS-based analysis, and data processing.

In this work, we have used two different lipidomic methodologies, that are two of the most used mass spectrometry strategies for lipidomic studies: UHPLC coupled to ESI-MS/MS tandem methodology, and MALDI-MS methodology<sup>96-99</sup>.

### 2.2.1. UHPLC-ESI-MS/MS methodology

In this approach, lipid extracts of the cell lines studied were required, so, the first step was to optimize the best extraction conditions for our samples. Before choosing the most suitable extraction method, the extraction percentage of the lipids in the sample must be assessed performing a recuperation experiment comparing different methodologies. For this, a known quantity of different lipid-standards that represent the lipid families present in the study samples are added to the samples before performing the extraction. In addition, a control condition is needed. Here, an intact sample is extracted and the lipid-standards are added after the extraction. In this way, the intensity obtained for the standards would be representative of the total amount of standard added. Then, the intensity achieved for the standards in the samples is compared with the intensity of the standards of the control condition. In this way, the intensity difference represents the percentage of sample that is recovered from the extraction, this is, the recovery rate. The the Bligh & Dyer method shows overall better recovery percentages than the protein precipitation method with isopropanol (**Table 5**). Therefore, Bligh & Dyer method was chosen as the gold standard method for the lipid extraction of the small biological samples used in this work.

**Table 5. Recovery rates (%) of the different standards performing the lipid extraction of a sample using Bligh & Dyer method and protein precipitation with isopropanol.**

Lipid class	Lipid Standard	Recovery rate (%)	
		Bligh & Dyer	Isopropanol
Glycerolipids	TG(14:0-16:1-14:0)	97	84
	TG(16:0-18:0-16:0)	94	66
	TG(15:0-18:1-15:0)	93	88
	TG(17:0-17:1-17:0)	100	88
Glycerophospholipids	PC(17:0/14:1)	102	95
	LPC(17:1)	82	91
	PI(17:0/14:1)	46	86
	PG(17:0/14:1)	70	95
Sphingolipids	SM(d18:1/12:0)	96	87
	Cer(d18:1/25:0)	105	116
	Cer(d18:1/12:0)	91	91
	GlcCer(d18:1/12:0)	94	93
	LacCer(d18:1/12:0)	89	103

In the Bligh & Dyer method, a two-phase separation is achieved, using chloroform and methanol-water solvents. In the non-polar solvent, this is chloroform, the hydrophobic lipids are dissolved and thereby extracted, while the polar components are concentrated in the polar methanol solvent in order to break the hydrogen bonds or electrostatic forces that bind them to the proteins of the membrane. In addition, the alcohol-solvent generates the inactivation of many phosphatidases and lipases, preventing the enzymatic degradation of the lipids of the sample<sup>100</sup>. Therefore, this procedure enables the separation of the lipids that contain glycerol, steroids, ceramides and sphingomyelins in the chloroform phase, whereas the polar lipids, such as phosphorylated PIs, complex glycolipids, specially gangliosides, and non-lipid components such as sugars are retained in the aqueous phase<sup>101</sup>.

As pointed out in the previous section, the cellular lipidome is a very complex mixture of lipids, considering that within each lipid class there is lipid species galore. Thus, chromatographic pre-separation of the lipid families is often used, since the correct identification of isobaric molecules can be challenging. Therefore, different chromatographic approaches coupled to MS are widely used in lipidomic studies.<sup>96–99</sup>

The next step in this approach was to separate the lipid classes using chromatographic techniques. Concretely, ultra-high pressure liquid chromatography (UHPLC) was used, as it is a very advantageous technique for the separation of amphipathic lipids based on their physicochemical properties. Indeed, when using reversed-phase UHPLC, lipids of the same class can be separated based on their lipophilicity, which is determined by their acyl chains' length and number of double bounds. For instance, the elution time is faster for lipids with short acyl-chains and polyunsaturated acyl structures<sup>102</sup>. Moreover, UHPLC strategy is very convenient for separating phospholipids in the different subclasses<sup>96</sup>. Since the chromatograph is coupled to the spectrometer, as soon as the components of the mixture are separated according to their retention time, they are introduced in the spectrometer and identified via MS-based analyses.

Mass spectrometry techniques allow the identification of different charged molecules (ions) according to their mass-to-charge ratio ( $m/z$ ), providing both structural and quantitative information of the analytes (ions). The essential parts of a spectrometer are the ion source, the

mass analyzer, the detector and the data system<sup>103</sup>. The extracted lipids, with or without previous separation by UHPLC approaches, enter the ion source where they are ionized, thereby acquire positive or negative charge. Afterwards, the ions pass through the sampling cone and reach the analyzer. The aim of the analyzer is to solve the generated ions according to their mass-to-charge relationship. For example, when quadrupole-time-of-flight (Q-TOF) analyzer is used, the quadrupole selects the ions and they are sent to the collision cell for argon fragmentation. These molecules reach the time-of-flight analyzer, which applies an electric field to accelerate all the ions to the same potential, and the time that takes each of the ions to reach the detector, which depends on its mass, is measured. Ions with a higher mass arrive later at the detector. Eventually, the detector records the information of the mass of the ions and their abundance in the mixture, which is then sent to the data system where it is graphically represented as mass spectra. Each peak of the graph represents a specific mass present in the mixture, and the amplitude of each peak stands for the relative abundancy of that ion.

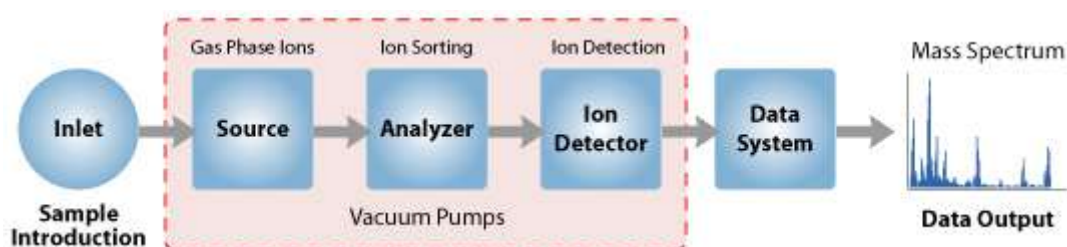


Figure 17. Schematic representation of the different components of a mass spectrometer<sup>103</sup>.

The great progress made in the lipid research field has been largely due to the advances achieved in the soft ionization MS techniques. These include ESI (electrospray ionization) and MALDI (matrix-assisted laser desorption and ionization). ESI uses electrical energy to transfer the ions present in the extraction solvent or mobile phase of UHPLC to a gaseous phase such as an aerosol. In order to evaporate the solvent and obtain the aerosol, the solution is pulverized through a quartz capillary with a high potential, together with a stream of hot nitrogen that help to evaporate the solvent from the charged droplets. Eventually, the solvent-free sample ions pass through the sampling cone and arrive at the analyzer and the detector. The UHPLC-ESI-MS approaches increase greatly the sensitivity and accuracy for detecting low abundant lipids. Additional information about the structure of the molecule can be provided using tandem MS/MS techniques<sup>104</sup>. Here, two different analyzers are used; first the precursor ion is revealed, and then this molecule is fragmented in a collision cell, and thereby detected by a second mass analyzer. In this way, the structure of the precursor molecule is more efficiently identified<sup>96,98</sup>. It is important to highlight that ESI is the preferential ionization method for studying lipids in solution<sup>105</sup>.

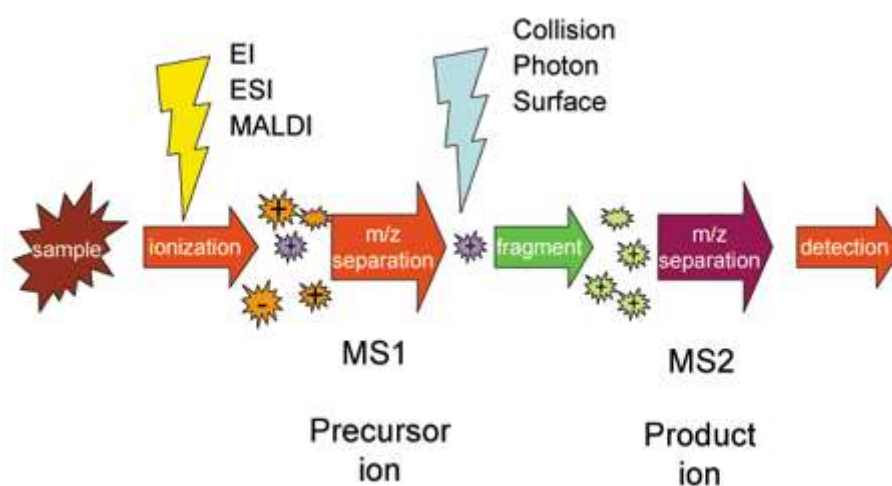


Figure 18. Workflow of tandem MS/MS strategy<sup>104</sup>.

#### 2.2.2. MALDI-MS methodology

The second analytical procedure employed was based on lipidomic analysis of functional cell membranes using MALDI-MS methodology. For this, the first step was to extract the cell membranes of the cell lines studied and immobilize them fabricating a functional cell membrane microarray, using a technology property of IMG Pharma Company. Then, for the lipidomic study, MALDI-MS strategy was performed.

MALDI-MS technique is frequently used for biomarker discovery. It is a laser-based soft-ionization technique, where a thin layer of low-molecular-weight organic matrix is applied on top of the sample. This matrix absorbs the laser radiation, and emits molecular ions and fragmented ions. One of the critical steps in this analytical process is the sample preparation. Indeed, matrix selection and deposition is strikingly important. It has been demonstrated that the best matrix deposition method includes matrix sublimation to ensure a regular distribution of it along the sample, and the use of matrixes that form small crystals. MBT (2-mercaptobenzothiazole) and DAN (2,5-diaminonaphtalene) for positive and negative ion detection, respectively, have shown great specificity and a good identification of the different lipid species<sup>106</sup>. This analytical approach is suitable for polar lipids including phospholipids and sphingolipids, and some non-polar lipids such as DGs and TGs<sup>98,107</sup>.

### 2.3. Cancer metabolism

Cancer cells undergo molecular changes that support the acquisition and maintenance of the carcinogenic phenotype, what gives them the advantage to survive, proliferate and grow in the stressful conditions generated by the tumorigenesis process<sup>108</sup>. In order to support the anabolic and energetic needs of tumor cells, the metabolic program of the cells is accurately rewired, what is directly regulated by translational and posttranslational modifications.

In brief, under normal conditions in healthy cells, the absorbed glucose is mainly transformed into pyruvate in the cytosol and metabolized by the oxidative phosphorylation (OXPHOS) in the mitochondria, producing 36-38 ATP molecules per molecule of glucose<sup>109</sup>.

Conversely, malignant cells use the hypoxic response used by normal tissues, regardless of the availability of oxygen (**Fig. 19**). This is defined as the Warburg effect, which is the first metabolic alteration detected in cancer cells and was described in the first half of the 20<sup>th</sup> century by Otto Warburg. Significantly, it states that the main route of glucose metabolism in cancer cells moves from oxidative phosphorylation to lactate fermentation, decreasing significantly the production of ATP molecules<sup>110-112</sup>. Melanoma in particular, has been defined as a very glycolytic cancer, as 60-80% of the absorbed glucose is converted into lactate in normoxia, increasing to 90% or more in hypoxia situations<sup>113</sup>. The physiological consequences of the metabolic plasticity observed in cancer cells are bioenergetics alterations and augmented synthesis of biomolecules, since the carbons derived from glucose are not used for obtaining energy but as biosynthetic building blocks for macromolecules such as lipids, amino acids and nucleotides.

Until recently, it was thought that cancer cells had impaired mitochondria, so the electron transport chain could not generate ATP, believing that this was the reason why these cells use aerobic glycolysis. However, it has been shown that mitochondria operate properly and glutamine is the principal carbon supplier of tricarboxylic acid cycle (TCA), instead of glucose<sup>110-112</sup>. In this way, glutamine is considered an important source of energy for proliferating cells. Additionally, glutamine also supplies carbons for the synthesis of lipids and the amino-nitrogens needed for the synthesis of amino-acids, nucleotides and lipids<sup>110,114,115</sup>.

Another source of energy for cancer cells is the oxidation of fatty acids. Here, these molecules are shortened by a series of catabolic reactions, generating acetyl-CoA that is used to replenish the TCA cycle, generating twice as much ATP as carbohydrates, and NADPH. The use of this energy source is emphasized when the availability of nutrient and oxygen is scarce, and the highest levels of use of fatty acid oxidation have been related to aggressive tumors<sup>115,116</sup>.

Aside ATP, NADPH is also needed to support the increased anabolic pathways in cancer cells. Moreover, NADPH also protects cancer cells from oxidative stress. In addition to the mitochondrial fatty acid oxidation (FAO), the pentose phosphate pathway (PPP) also provides NADPH after the oxidation of glucose<sup>117</sup>.

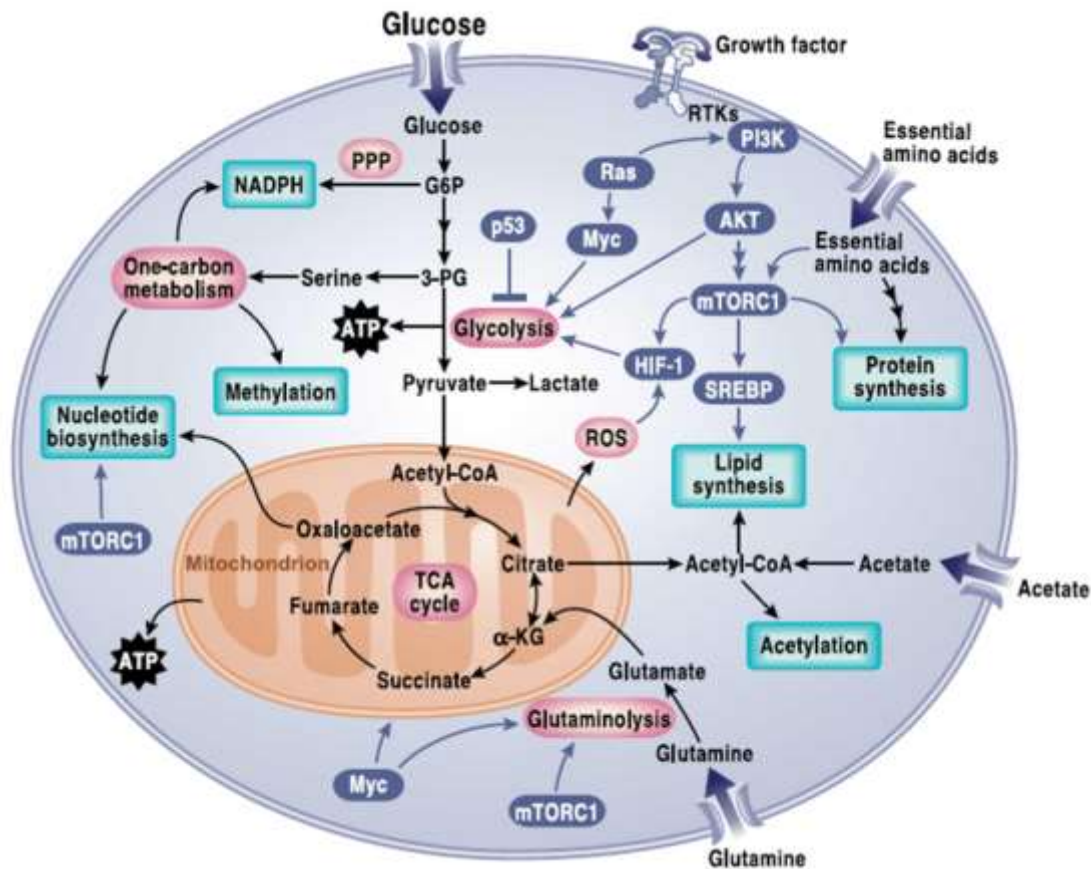


Figure 19. Schematic representation of the signaling pathways that regulate metabolic rewiring in cancer cells<sup>108</sup>. The aberrant activation of different metabolic pathways in cancer cells increases the biosynthesis of lipids, nucleotides, and proteins. In addition to the increase of glucose absorption and glycolytic flux. Abbreviations: PPP –pentose phosphate pathway; G6P –glucose-6-phosphate; 3-PG -3-phosphoglycerate; ATP –adenosine triphosphate;  $\alpha$ -KG – $\alpha$ -ketoglutarate; RTK –receptor tyrosine kinase.

### 2.3.1. Lipid metabolism and cancer

The alteration of lipid metabolism has gained attention in recent years. Compelling evidence suggests that both *de novo* biosynthesis and oxidation of these macromolecules are increased in cancer. The rewiring of lipid metabolism results in disrupted energy production, distinct cell signaling pathways, structural alterations in cell membranes, and aberrant gene expression and protein distribution, affecting significant cellular functions, such as growth, proliferation, apoptosis, autophagy, differentiation, and resistance to drug and chemotherapy, among others<sup>49</sup>.

Malignant cells show great need for lipids including cholesterol, so both the synthesis and the uptake of these molecules are increased in cancer, storing the excess in lipid droplets (LD) within the cells, which is considered a cancer trait. Melanoma particularly shows a great necessity of FAs for its progression and metastasis, using them for energy extraction by FAO or membrane phospholipid synthesis, among other functions. Aggressive cells show higher levels of expression of the genes involved in lipid biosynthesis, catabolism and intracellular storage of lipids. Besides, it has been reported that lipid metabolism participates not only in the first steps of the metastatic process, but also in peripheral dissemination and seeding. In fact, both the



pharmacological and molecular blockade of this process with siRNAs has led to cell apoptosis and a decreased primary tumors volume<sup>114,118</sup>.

The metabolic rewiring of cancer cells drives the aberrant activity of SREBP transcription factor, the master regulator of fatty acid, phospholipid, triglyceride and cholesterol metabolism. SREBP controls lipid metabolism at transcriptional, translational and post-translational levels. This transcription factor promotes the upregulation of the expression and activity of several lipogenic and lipolytic enzymes. For instance, FAS (fatty acid synthase), ACC (acetyl-CoA carboxylase), ACLY (ATP citrate lyase), and SCD (stearoyl-CoA desaturase) enzymes upregulation is a common phenotype observed in a wide range of cancers, including melanoma. As it is represented in the **Figure 20**, these enzymes participate directly in the *de novo* biosynthesis of FAs, and in the modification of the new FA molecule by elongating its carbon chain and introducing insaturations<sup>94</sup>. It is noteworthy that the pharmacological inhibition of these enzymes reduces the invasion, migration and survival of cancer cells *in vitro*<sup>114,119</sup>.

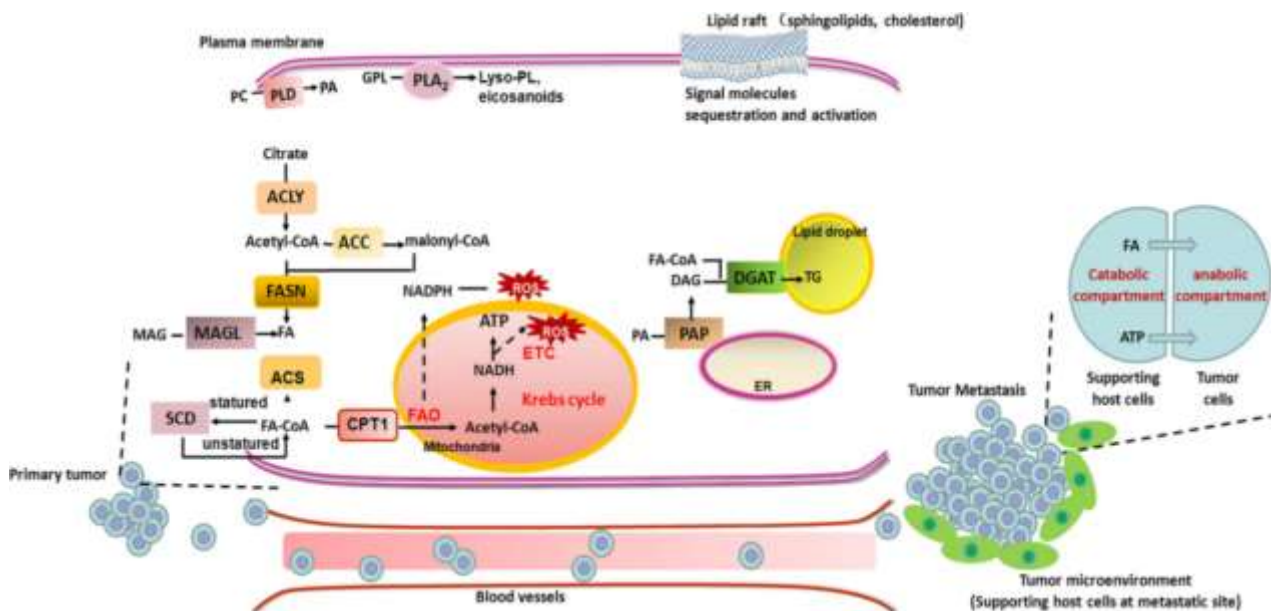


Figure 20. Schematic representation of the lipid metabolism rewiring in cancer cells<sup>120</sup>.

Although FA synthesis and oxidation are a priori incompatible processes, they coexist in cancer cells taking advantage one from the other. FA oxidation produces acetyl-CoA accumulations in the cells, which can be used for FA synthesis initiation. Furthermore, the ATP and NADPH generated in the oxidation are profited for anabolic purposes. The cells eliminate toxic lipids hydrolyzing them and, at the same time, FA synthesis generates the concrete lipid species required for the malignant transformation of the cells<sup>120</sup>.

The metabolism of the different phospholipid subclasses is also altered in cancer, as the biosynthesis of phospholipids is stimulated, thereby increasing their content in tumor cells<sup>121,122</sup>. Overwhelming evidences suggest that the enzymes that participate in the Kennedy pathway are overexpressed in tumor tissues. Concretely GPAT2, part of the GPAT family of enzymes that catalyze the first reaction of this stepwise process is overexpressed in some cancer tissues<sup>77</sup>. Choline kinase (CK), which is responsible for the first step of PC biosynthesis, has an increased

presence and activity in cancer cells, including breast, ovarian, lung, colon, prostate, endometrial, pancreatic cancer and melanoma<sup>123</sup>. It participates in tumor development, progression and metastatic dissemination in several cancers<sup>122</sup>. In line with this, numerous CK inhibitors are under study for clinical development, after showing great efficacy *in vitro* and *in vivo* in different cancer cell lines<sup>55,124</sup>. In order to maintain a high PC biosynthetic rate, the absorption of free choline by cancer cells is also stimulated. The proteins that participate in the transportation of choline inside the cells appear upregulated in different cancer cells, including melanoma. In fact, the inhibition of these proteins through different mechanisms has reduced tumor cell proliferation, increased apoptosis and blocked tumor progression<sup>123</sup>. Besides, the catabolism of PCs is also enhanced in tumor cells. This is strikingly important in tumor progression, and is performed by phospholipases A, C and D, yielding very important second messengers such as, DAG, PA, LPA, FFAs, Lyso-PC, free choline and phosphocholine<sup>121</sup>.

In spite of lacking evidences of the exact role of the plasmalogens in cancer, a large body of work demonstrates the overexpression of various enzymes that take part in the biosynthesis of ether lipids in cancer tissues. Moreover, it has been demonstrated that ADAPS is overexpressed in several cancers, what is turned into higher levels of alkyl ether lipids, favoring cancer progression<sup>74</sup>. Indeed, the knockdown and inactivation of this enzyme has been associated to impaired cancer progression, whereas its overexpression and thus increased ether lipids content has been associated to increased tumor cell growth, motility and survival<sup>70,125</sup>.

FAO not only occurs in mitochondria, but also in the peroxisomes. Although the oxidative mechanism is identical in both organelles, the enzymes involved in each organelle are different as they metabolize different FAs. Indeed, branched and very long-chain fatty acids (>26 carbons) can only be hydrolyzed in the peroxisomes, where the first oxidative reactions take place, breaking the long-chains into smaller ones, which are then shuttled to the mitochondria to continue the oxidation<sup>74,75</sup>.

In addition, the specific lyso-phospholipid transferases (LPATs) and PLA<sub>2</sub> that participate in the Lands' cycle are overexpressed in several cancers, such as, liver, colon, prostate, lung, gastric and breast cancers<sup>77</sup>. The increased production of important signaling molecules such as lyso-PLs and free fatty acids, is turned to enhanced proliferation, migration and metastatic capacity in several cell lines<sup>96</sup>.

With regard to sphingolipids, a common scenario in several cancers is characterized by the increased activities of glucosylceramide synthase (GCS), SM synthase (SMS), ceramide kinase (CERK), acid ceramidase (aCDase) and/or sphingosine kinase (SK), which increases the expression of pro-carcinogenic SPLs<sup>84</sup>. In general, the accumulation of ceramides in the cells triggers apoptosis, although it has been demonstrated recently that this is ceramide-type specific. For instance, cancer cells present low levels of C18 ceramides due to the decreased expression of CerS1, whereas the increased expression of CerS2 is translated into accumulation of long-chain ceramides (22-24 carbons-length) in cancer cells<sup>84,85</sup>. Particularly in melanoma, low expression of CerS6 was correlated with poor prognosis. To gain insight into the importance of this enzyme in melanoma progression, its expression was silenced and the cell lines showed increased progression and invasion<sup>126</sup>. Moreover, the *in vitro* overexpression of CerS5/6 that induces C16 ceramide production and accumulation, enhanced apoptosis in cancer cells. Interestingly, upon satisfactory chemotherapeutic treatments, long-chain ceramides tend to accumulate and CerS4, 5 and 6 are found overexpressed<sup>85</sup>.

On the other hand, melanoma among other cancers show high levels of acid ceramidases. Compelling evidence suggest that lysosomal aCDase participates in the transition from proliferative to invasive phenotype in melanoma cells. In line with this, higher expression of aCDase in melanoma cells has been related to a proliferative state, whereas lower expression has been correlated to enhanced motility and invasive capacity<sup>127</sup>. Furthermore, aCDase overexpression has been proven to confer resistance to chemotherapeutic agents, highlighting the importance of these enzymes in the carcinogenic process<sup>128</sup>.

According to the role of SM in cancer, SM synthase (SMS) downregulation has been correlated to poor outcome in melanoma, thereby decreasing SM levels in primary and metastatic melanoma<sup>129</sup>. Interestingly, acid SMases have been proven pivotal in the metastatic process of melanoma<sup>84</sup>.

The mevalonate pathway is another lipogenic route that has increased activity in cancer. As explained previously, several evidences suggest that many cancer types present high activity of SREBP transcription factors that promote the expression of the enzymes of the mevalonate pathway. When the pathway is activated, the cells synthesize cholesterol that is accumulated in high levels in different tumor tissues, such as breast cancer<sup>130</sup>. Cholesterol esters on their side, are synthesized by acyl-CoA:cholesterol acyl transferase (ACAT), which is found overexpressed and correlates with tumor grade in different cancers such as clear cell renal carcinoma<sup>131</sup>. Interestingly, statins, that lower plasma cholesterol levels and are so largely used in clinic, have been proven to reduce cancer cell proliferation, induce apoptosis and make cancer cells more sensitive to chemotherapeutic agents *in vitro*. In fact, the administration of statins together with chemotherapeutic agents has shown greater efficacy than drugs alone. However, these effects are still under study since they appear to be very specific to the cancer type<sup>132</sup>.

In summary, it has largely been demonstrated that cancer cell metabolism, and concretely lipid metabolism, are altered in cancer. This metabolic rewiring supports the acquisition of the malignant traits that cancer cells possess. Therefore, the inhibition of the key enzymes that participate in lipid metabolism arises as a promising treatment option for cancer patients.

### 3. Phospholipase D and cancer

Phospholipases form a ubiquitous family of enzymes that participate in the catabolism of glycerol-based phospholipids. The members of this family can be divided in four major classes, each of which hydrolyses different phospholipid molecules in a specific position (**Fig. 21**). They are pivotal both in physiological and pathological conditions, since they are necessary for the remodeling and homeostasis of the plasma membrane. Indeed, they have been largely related to carcinogenesis and other diseases, as the released molecules are bioactive lipids that regulate diverse intracellular and intercellular signaling pathways, which affect cell proliferation, survival, migration, vesicle trafficking and cell death, among others. Moreover, many of the different members of this family have been found to be overexpressed in several cancers<sup>133</sup>.

Enzymatic action of the diverse phospholipases:

- PLA: Phospholipase A<sub>1</sub> and A<sub>2</sub> can cleave the ester bond of the GPL at sn-1 or -2 position respectively, releasing a free fatty acid and a lysophospholipid.
- PLB: presents both PLA<sub>1</sub> and PLA<sub>2</sub> activities.
- PLC: cleaves the bond between the phosphate and the glycerol at sn-3, producing a DAG and a phosphorylated head group.
- PLD: cleaves the bond between the phosphate and the polar head group of the glycerophospholipid, releasing a PA and a free polar head group.

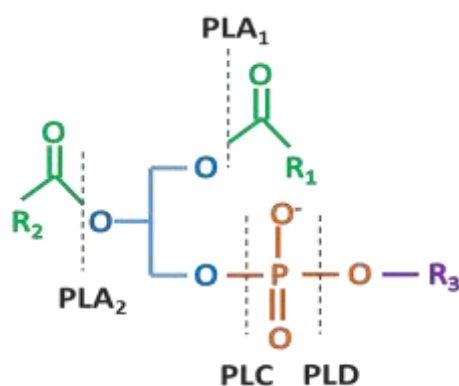


Figure 21. Cleavage sites of the different phospholipases.

In particular, the PLD subclass is composed of six different isoforms in mammal cells. So far, PLD1 and PLD2 are the best-studied members. Although both show the same catalytic activity, that is, they hydrolyze preferentially a PC yielding PA and free choline, their tissue and subcellular location is different. PLD1 is found mainly in the inner leaflet of different perinuclear membranes, such as secretory granules, endosomes, lysosomes and Golgi apparatus. Once activated, it is transported to the plasma membrane. There, it exerts its hydrolytic activity influencing membrane trafficking, mitosis and signal transduction. This isoform has been linked to cancer, thrombotic disease and autoimmunity. Conversely, PLD2 is found primarily in the plasma membrane and has been related to strong catalytic activity. Indeed, the lipase activity exerted by PLD2 has been linked to cytoskeleton reorganization, regulated secretion and cell cycle control. Similar to PLD1, PLD2 has also been reported to be related to cancer, as well as hypertension and Alzheimer's disease. Additionally, PLD3, PLD4, PLD5 and PLD6 isoforms are also found in mammal cells. However, not much is known about their functions. It has been shown that PLD3, PLD4 and PLD5 isoforms are anchored in the plasma membrane by a

transmembrane domain. However, PLD6 has been described as a dimeric protein that can be found on the external surface of the mitochondria<sup>133</sup>.

PLD1 and PLD2 share a 50% homology among their sequences, although PLD2 is shorter. A common structural feature that they share is a conserved motif of phosphatidyltransferase HKD that is duplicated and encodes the catalytic site of these enzymes. This domain is characterized by the amino acid sequence HxKx<sub>4</sub>Dx<sub>6</sub>, with histidine, lysine and aspartic acid, where x represents any amino acid residue. Moreover, at the amino terminal region of both PLD1 and PLD2 there is a tandem of PX (phox homology) and PH (pleckstrin homology) domains. This tandem participates in the interactions with the lipids of the membranes and controls the subcellular localization of the enzymes. However, these domains do not participate in the catalytic activity of these proteins<sup>134</sup>. With respect to the remaining PLD isoforms, neither PLD3, PLD4, PLD5 nor PLD6 possess PH and PX domains within their sequence. Furthermore, all but PLD6 have two HKD motifs, that has a single HDK domain<sup>135</sup>.

PIP<sub>2</sub> (phosphatidylinositol 4,5-biphosphate) is a fundamental cofactor for the catalytic activity of PLDs, hence, a PIP<sub>2</sub> binding region has been found. Bruntz et al. mutated this region, showing that the catalytic activity suffered a significant decrease, while the subcellular location was not affected. In addition, it has been postulated that the role of PIP<sub>2</sub> could be to recruit PLD to a concrete membrane domain and stimulate PC catalysis by facilitating the binding of the substrate to the active site<sup>134</sup>.

Despite being the lipase activity the best-known activity of PLDs, these enzymes also show protein-protein interactions. The catalytic activation of these enzymes occurs in two different pathways. On the one hand, lipase activity is driven by phosphorylation through receptor tyrosine kinases (RTKs), such as EGFR or PDGFR, and non-receptor tyrosine kinases including protein kinase C (PKC), Src and janus kinase 3 (JAK3)<sup>135</sup>. In this way, different extracellular mitogenic signals stimulate the activation of PLD: chemokines (IL-8), insulin, growth factors (epidermal growth factor (EGF), platelet-derived growth factor (PDGF), vascular endothelial growth factor (VEGF)), fatty acids, sphingosine-1-phosphate (S1P), among others<sup>136</sup>. On the other hand, the guanine nucleotide exchange factor (GEF) activity is a unique feature of the PLD2 isoform. This is implicit in cell motility, and the regulation of PLD2 activation is carried out through small GTPases such as Rac2, Arf, Rho and Ras, among others. Furthermore, it has been found that PA controls the GEF activity of PLD2, what adds greater sophistication to the regulation of this enzyme<sup>135,137</sup>.

Upon activation, the formed PA can be subsequently converted to lyso-PA by PLA<sub>2</sub> or to DAG by PA-phosphohydrolase. Therefore, PLD is a key enzyme in cell signaling, as the molecules produced are important lipid mediators involved in several cellular signaling pathways. In fact, one of the important features of PA is its interaction with some proteins, many of which participate in cellular signaling pathways. For instance, mTOR, Akt and Raf-1 (member of ERK signaling pathway) proteins interact with PA, which implies the influence of PLD on cell proliferation, growth, and survival<sup>133</sup>.

Specifically in cancer, in addition to the regulatory transcriptional mechanisms, post-transcriptional mechanisms also contribute to the enhanced expression and activity of these enzymes<sup>138</sup>. Thus, both the expression and the activity of PLD1 and PLD2 are upregulated in several types of neoplasms, including breast, kidney, colon, gastric, brain, thyroid, as well as melanoma<sup>139</sup>. PLD2 in particular, correlates with poor prognosis in colorectal and renal neoplasms<sup>140</sup>. Overexpression of PLD and increased activity affect a wide range of processes

involved in tumor progression and metastasis by different signaling pathways. The increase in PLD activity due to mitogenic signals (EGF, PDGF) and the expression of the oncogenes (Ras, Raf, Src) has been linked to the activation of MAPK, RAS and mTOR<sup>140,141</sup>. Moreover, HIF increases the expression of PLD2<sup>142</sup>, and PLD activity contributes to rapamycin resistance and survival of human bladder, breast and lung cancers through mTOR<sup>143,144</sup>. In this regard, PLDs are important to maintain altered cancer metabolism, supporting the biosynthetic and bioenergetic demands of cancer cells. For instance, PLD enzymes increase the uptake of glucose by Glut-4 and the formation of LD. In line with this, PLD interacts with both the tumor and the microenvironment, favoring proliferation and stimulating angiogenesis<sup>142</sup>.

One of the effects of PLDs on cancer that stands out over the others is their role in the metastatic process. Both the PA produced by their lipase activity and their protein-protein interactions with different signaling molecules such as Grb2, Rac2, WASP, S6K and JAK3, among others, are key to induce cell motility. However, the expression levels of PLD1 in the metastatic sites do not differ significantly with those of the primary renal tumors. Therefore, it is suggested that although PLD1 also contributes to the metastatic process, PLD2 might play a pivotal role in tumor cells for metastatic dissemination<sup>140</sup>. Moreover, it is postulated that PLD1 exerts its function mainly in the tumor microenvironment, whereas the activity of PLD2 is intrinsic to tumor cells. In line with this, some information can be gleaned from different studies. Once the migratory cells enter the circulatory system, they attach to the platelets in order to protect them and direct them to the secondary tissue. It has been demonstrated that the activity of PLD1 is pivotal for the aggregation of tumor cells to the platelets via integrins. To gain insight into the role of PLD1 in this process, PLD1 knockout mice were intravenously injected with wild type melanoma cells, noticing a 50% decrease in the formation of metastases in these mice. Besides, the deletion of PLD1 in endothelial cells led to a decrease in neovascularization of tumors<sup>145</sup>.

On the other hand, PLD2 has been strongly linked to metastatic dissemination. PLD2 activity supports the proliferation and invasiveness of different cancers, such as lymphoma<sup>146</sup> and breast cancer<sup>139</sup>. Moreover, PLD2 has been demonstrated to induce the metastatic process by phosphorylation of FAK, and activation of Akt and mTOR<sup>146</sup>. In fact, PLD2 supports matrix substrate degradation, invadopodia formation, tumor cell migration, invasion and metastatic spread of breast cancer cells. It increases the secretion of matrix metalloproteinases from tumor cells and promotes the rearrangement of the actin cytoskeleton<sup>147</sup>, while its inactivation impairs cell proliferation, adhesion, migration and invasion<sup>146</sup>. In breast cancer, overexpression of PLD2 resulted in increased tumor growth, chemoresistance and reduced apoptosis in mice, whereas silencing of PLD2 significantly impaired tumor growth and lung metastases<sup>139</sup>.







# **HYPOTHESIS & OBJECTIVES**



### 1. Hypothesis

Melanoma is the cancer that arises upon the malignant transformation of the melanocytes of different locations, although skin melanoma stands for the most common one. Its incidence has increased steadily during the last decades, and is considered the seventh most diagnosed cancer in Europe. Although it only represents the 4% of all diagnosed skin tumors, it is responsible for 80% of the deaths caused by these cancers<sup>1</sup>. It should be noted that it is predicted that 150,000 new cases will be diagnosed in Spain during 2019<sup>3</sup>.

The great heterogeneity observed in melanoma tumors has hindered the identification of truly effective biomarkers or treatments, and mortality rates are still very high, especially for metastatic melanoma. Therefore, it stands to reason that there is great need to identify new biomarkers that can be used as therapeutic targets or help in the early detection, diagnosis and prognosis, as it is evident that the recovery rates are higher the earlier the tumor is detected.

In this regard, cellular metabolism has been established as a cancer trait. It is known that the rewiring of metabolic pathways that these cells undergo supports the malignant phenotype acquired by the tumor cells. Specifically, the implication of lipid metabolism in the carcinogenic process has gain insight in the cancer research field. The metabolism is known to be altered in cancer cells, which induces modifications in the composition and quantity of some lipids. Furthermore, it has been hypothesized that these alterations in the composition and quantity of lipids and their metabolism can lead to the malignant transformation of non-pathological melanocytes to melanoma. Thence, the specific lipid species identified with an aberrant expression in melanoma compared to non-pathological melanocytes could be important potential biomarkers for this disease and help to shed light in their involvement in the development and progression of melanoma. Moreover, the variations in the lipid content go together with the alterations in the expression and activity of the enzymes that participate in the metabolism of these molecules. For instance, phospholipase enzymes participate in the catabolism of the glycerophospholipids, and the different isoforms of this family of enzymes has been largely related to cancer. Indeed, PLD2 has been shown to contribute in the carcinogenic process and metastatic dissemination of different cancers.

## 2. Objectives

The main objective of this doctoral thesis was to identify new melanoma lipid biomarkers that will aid in the early detection, diagnosis and prognosis of melanoma. For that purpose, different lipidomic approaches were applied. In addition, it was expected that the results obtained in this work would gain insight into the molecular and cellular mechanisms involved in development and progression of melanoma.

For this, the main objectives are itemized in the following specific objectives:

- Analyze the lipidome of healthy melanocytes, nevi melanocytes, primary melanoma and metastatic melanoma cell lines, using lipid extracts obtained from various cell lines.
- Implement an effective new biotechnological tool with translational potential for lipidomic biomarker detection.
- Identify specific lipid species with diagnostic and prognostic value for melanoma.
- Determine the functional implications of PLD2 enzyme in pro-tumorigenic and metastatic activities in melanoma cells.

# **MATERIALS & METHODS**



## 1. Materials

### 1.1. Reactants

Table 6. List of the reactants used for the experiments and the supplier.

Product	Supplier
RPMI 1640 Glutamax	Life Technologies
Mc Coy's 5A	
Medium 254	
Human Melanocyte Growth Supplement (HMGS)	
Penicillin (100 UI/mL) – Streptomycin (100 µg/mL)	
TryPLE Select (1x)	
0,05% Trypsin-EDTA (1X)	
Hank's Balanced Salt Solution	
Opti-MEM I (1X)	
Fetal Bovine Serum (FBS)	
Nitrocellulose Blotting Membrane	
DMEM	Sigma-Life Science
L-Glutamine	
Phosphate Buffered Saline tablet	
Dimethyl Sulfoxide (DMSO)	
Trypan Blue solution	
HEPES	
Hyaluronidase from sheep testes	
Dispase II	
Monoclonal Anti-Fibroblast Surface Protein Antibody	
BSA	
RIPA Buffer	
Protease Inhibitor Cocktail 3	
Phosphatase Inhibitor	
Collagenase A	
Trypsin	
Complement sera from rabbit	
DL-Dithiothreitol	
Bovine serum albumin	
Bicinchoninic Acid Solution (BCA)	
Sodium Dodecyl Sulfate (SDS)	
Ponceau S	
TWEEN® 20	
Trizma® Base	
Triton® X-100	
Bromophenol Blue	
Aprotinin	
Leupeptin	
EMEM	ATCC
Venor® GeM One Step Test Kit (Mycoplasma)	Minerva Biolabs
XTT Cell Proliferation Kit II	Roche Molecular Biochemicals
PLD2 Expression Plasmid	OriGene
TransIT®-2020 transfection reagent	Mirus Bio
PLD2 protein siRNA	Ambion – Thermo Fisher Scientific

Negative control siRNA	
DharmaFECT 1 transfection reagent	Dharmacon
Primocin™	InvivoGen
Copper (II) Sulfate Pentahydrate	AppliChem - PanReac
Glycine	
Methanol	
30% Acrylamide/Bis-acrylamide 29:1	Bio-Rad
Temed	
Precision Plus Protein™ Dual Color Standards	
Ammonium Persulfate	
30% Glycerol Solution	
Non-fat powder milk	Nestle
SuperSignal™ West Femto Maximum Sensitivity Substrate	Thermo Scientific
SuperSignal™ West Pico Chemiluminescent Substrate	
Fluoromount G (for immunofluorescence)	Electron Microscopy Sciences
Paraformaldehyde 16% Solution, EM Grade	
[ <sup>3</sup> H] Butanol	American Radiolabeled Chemicals Inc.
Phosphatidylinositol 4,5-bisphosphate (PIP2)	Avanti Polar Lipids
Short side-chain phosphatidylcholine (PC8)	
Methanol for UHPLC	Fisher Scientific
Chloroform for UHPLC	
Toluene for UHPLC	
Methylene Chloride for UHPLC	
Acetonitrile for UHPLC	
Formic acid for UHPLC	
Isopropanol for UHPLC	

### 1.2. Commercial cell lines

The commercial cell lines used can be classified into three main groups: normal skin melanocytes (HEMn-LP, HEMn-MP, HEMn-DP), primary melanomas (A375, MEL-HO, Sk-Mel-28, Sk-Mel-31, G-361, ME4405) and metastatic melanomas (Hs294t, RPMI 7951, A2058, Sk-Mel-3, COLO-800, HT-144, WM-266-4, Sk-Mel-2, VMM1). In the following table, there is a detailed information of each cell line.



Table 7. Detailed description of the commercial cell lines used in this study.

Cell line	Code	Type	Tissue	Age	Sex	Company
<b>HEMn-LP</b>	C-002-5C	Lightly pigmented melanocytes	Foreskin	Neonate	Male	Cascade Biologics, Inc.
<b>HEMn-MP</b>	C-102-5C	Moderately pigmented melanocytes	Foreskin	Neonate	Male	Cascade Biologics, Inc.
<b>HEMn-DP</b>	C-202-5C	Darkly pigmented melanocytes	Foreskin	Neonate	Male	Cascade Biologics, Inc.
<b>A375</b>	ATCC CRL-1619	Primary melanoma	Skin	54	Female	ATCC
<b>MEL-Ho</b>	ACC-62	Primary melanoma	Skin		Female	Innoprot S.L.
<b>Sk-Mel-28</b>	ATCC HTB-72	Primary melanoma	Skin	51	Male	ATCC
<b>Sk-Mel-31</b>	ATCC HTB-73	Primary melanoma	Skin	33	Female	ATCC
<b>G-361</b>	ATCC CRL-1424	Primary melanoma	Skin	31	Male	ATCC
<b>ME4405</b>	CVCL_C680	Primary melanoma	Skin	83	Female	
<b>Hs294t</b>	ATCC HTB-140	Metastatic melanoma	Lymph node	56	Female	ATCC
<b>RPMI 7951</b>	ACC-76	Metastatic melanoma	Lymph node	18	Female	Innoprot S.L.
<b>A2058</b>	ATCC CRL-11147	Metastatic melanoma	Lymph node	43	Male	ATCC
<b>Sk-Mel-3</b>	ATCC HTB-69	Metastatic melanoma	Lymph node	42	Female	ATCC
<b>COLO-800</b>	ACC-193	Metastatic melanoma	Subcutaneous	14	Male	Innoprot S.L.
<b>HT-144</b>	ATCC HTB-63	Metastatic melanoma	Subcutaneous	29	Male	ATCC
<b>WM-266-4</b>	CRL-1676	Metastatic melanoma	Skin	55	Female	ATCC
<b>Sk-Mel-2</b>	ATCC HTB-68	Metastatic melanoma	Skin	60	Male	ATCC
<b>VMM1</b>	ATCC CRL-3225	Metastatic melanoma	Brain			ATCC

## 2. Methods

### 2.1. Cell culture

Cell culture is a widely used research tool to study the physiology and biochemistry of cells, as well as the toxicity and effects of different drugs and compounds in cells. This research model is established after the isolation of cells from a tissue and their maintenance in a beneficial artificial environment.

Cell cultures must be maintained in a controlled atmosphere of temperature, pH and humidity. In this way, they are kept inside an incubator, which creates a humid atmosphere with 5% CO<sub>2</sub> and a temperature of 37°C, promoting cell growth. The manipulation of these cells must be done inside a laminar flow cabinet to provide a sterile environment and avoid contamination by bacteria, virus or yeast. Furthermore, all the solutions and materials used with the cells must be sterile and pre-heated at 37 °C.

The culture conditions vary depending on the origin of each cultivated cells. According to their nutritional needs, each cell type is maintained in a medium of defined chemical composition that supplies growth factors, essential nutrients (amino acids, vitamins, carbohydrates, and minerals), hormones and gases (O<sub>2</sub>, CO<sub>2</sub>).

In this work, two different types of cultures were used. On the one hand, **primary cells** isolated directly from a nevus and established as a culture. Most of the primary cells have a limited lifetime, except primary cells isolated from tumors. On the other hand, we have also used commercially available **tumor cells**.

Table 8. Complete cell culture media composition for each cell line.

Cell line	Culture media
<b>HEMn-LP</b>	Medium 254 1X Human Melanocyte Growth Supplement
<b>HEMn-MP</b>	
<b>HEMn-DP</b>	
<b>Nevus 1-9</b>	
<b>A375</b>	DMEM 10% FBS 2 mM L-glutamine 100 UI/mL Penicillin 100 µg/mL Streptomycin
<b>ME4405</b>	
<b>Hs294t</b>	
<b>RPMI 7951</b>	
<b>A2058</b>	
<b>HT-144</b>	
<b>Sk-Mel-28</b>	EMEM 10% FBS 100 UI/mL Penicillin 100 µg/mL Streptomycin
<b>Sk-Mel-31</b>	
<b>WM-266-4</b>	
<b>Sk-Mel-2</b>	
<b>MEL-Ho</b>	RPMI 1640 GlutaMAX™ 10% FBS 100 UI/mL Penicillin 100 µg/mL Streptomycin
<b>COLO-800</b>	
<b>VMM1</b>	
<b>G-361</b>	Mc Coy's 5A 10% FBS 2 mM L-glutamine 100 UI/mL Penicillin 100 µg/mL Streptomycin
<b>Sk-Mel-3</b>	

#### 2.1.1. Defrosting cells

In order to initiate a cell culture from a purchased cell line or a stock created in the laboratory, first, the cells were revived. For that, the vial containing the cells was heated to 37 °C and immediately mixed with 1/10 parts of complete cell media. The suspension was centrifuged at 200 g for 5 minutes at 4 °C. Then, the supernatant was discarded and the cell pellet was re-suspended in 1 mL of complete cell media. Finally, the cell suspension was seeded in a 25-cm<sup>2</sup> culture flask with 4 additional mL of complete media.

#### 2.1.2. Cell subculture

The cultured cells are growing actively, so after a few days they arrange in a monolayer and consume the nutrients present in the culture media releasing waste products of cell metabolism. Therefore, when 90% confluence was reached, the cells were harvested and plated at a lower density with fresh complete media, to maintain the cell culture over time.

To subculture the cells, cell culture media was removed and the cells were washed with phosphate saline buffer (PBS) without calcium and magnesium to favor the activity of the dissociating agent. Then, the cells were detached by the action of the trypsin-EDTA solution for approximately 5 minutes at 37 °C. Once the cells were detached, fetal bovine serum (FBS) was added to inactivate the dissociation agent trypsin and the solution was centrifuged at 200 g for 5 minutes. Subsequently, the supernatant was discarded and the cells re-suspended in 1-2 mL of fresh culture media. For cell counting, the cells were mixed 1:1 with trypan blue, which is a vital stain that selectively colors the dead cells in blue while the living cells remain uncolored. Then, using the TC20 Automated Cell Counter (BioRad), the total number of cells and their

viability were determined. In this way, the volume of cell suspension necessary in each experiment was calculated, together with the viability of the cells, which must be higher than 90% to carry out any analysis.

#### 2.1.3. Freezing cells

The cells cannot be maintained eternally in culture, since they are prone to suffer genetic alterations, microbial contamination, etc. Therefore, it is extremely important that the cells are frozen at low passage and a seed stock is made for long-term preservation in liquid nitrogen. Thus, if the cells were maintained in culture for about 20 passages or were contaminated, they were replenished from frozen stock.

Following the same procedure as for subculturing cells, after centrifugation, the cell pellet was re-suspended in freezing media (10% DMSO, 90% FBS) at the recommended cell density. Then, the cells were frozen slowly by lowering the temperature by approximately 1 °C per minute using a “Mr. Frosty” cryo-freezing container in a -80 °C freezer. After 24 h, the frozen vials were transferred to liquid nitrogen for long-term storage.

#### 2.1.4. Mycoplasma detection

While bacterial and yeast contaminations can be easily detected in cell cultures, mycoplasma contamination is difficult to recognize, since they are not detectable by the eye or by light microscopy. Moreover, antibiotics used regularly in cell culture are not effective for these microorganisms. It is expected that between 10% and 85% of the cell lines used in any laboratory are contaminated (InvivoGen). This contamination can have many effects on cells, such as chromosomal aberrations, alterations in the proliferation rate, cell metabolism and cell viability. Hence, cell cultures must be tested every 3 months.

For this, Venor® GeM One Step Test was used, which through PCR technique detects 10 different species of mycoplasma in culture media that have been in culture for at least 48 h. If it was positive for mycoplasma, the cells were discarded and new cells were revived from the stock in liquid nitrogen.

#### 2.1.5. Cell pellet collection

Once sufficient amount of cells was reached, they were harvested and collected to store the cell pellet and use it later for the extraction of proteins, lipids and cell membranes.

When 90% confluence was achieved, as in the cell subculture, the cells were harvested with trypsin and centrifuged at 200 g for 5 minutes. Then, the supernatant was removed, the pellet was re-suspended in 1 mL of PBS and the cells counted. This suspension was centrifuged again at 300 g for 5 minutes. After discarding the supernatant, the cell pellet was introduced in liquid N<sub>2</sub> for rapid freezing, and immediately after, they were stored at -80 °C until use.

#### 2.1.6. Cell transfection

Cell transfection is the procedure by which foreign genetic material is introduced into eukaryotic cells for two different purposes. On the one hand, to induce gene expression to increase the cellular levels of a recombinant protein a plasmid or mRNA is used. On the other hand, knockdown of a certain gene to reduce the expression of a protein RNA interference is used. Furthermore, the transfection can be stable since the foreign material integrates the genome or transient for a limited time of 24 to 96 hours. This process can be achieved through different chemical, biological or physical methods. In this study, lipid-based reagents forming nucleic acid-lipid complexes were used via electrostatic interactions between the negatively charged nucleic acids and the cationic lipids. These complexes were captured by the cells as they fused together

with the phospholipids of the cell membrane and delivered the genetic material inside the cell. Once inside the cell, the transfected DNA was translocated into the nucleus while the RNA remained in the cytoplasm.

- PLD2 protein overexpression:

A commercially available expression plasmid was employed to increase the synthesis of PLD2 protein in melanoma cells. The plasmid increased the amount of messenger RNA of PLD2 gene and this resulted in higher levels of PLD2 protein in the cells.

Melanoma cells were seeded in a 6-well plate, and when they reached 60-70% confluence, they were transfected with the expression vector. At this point, new complete media was added to the cells along with the transfection mixture. The latter was composed of 1 µg of DNA and 2 µL of TransIT®-2020 transfection reagent mixed in 300 µL of Opti-MEM™ for 20 minutes prior to adding it to the cells. In another well, the cells were only incubated with the transfection reagent plus a scramble plasmid, which was used as a control condition of the transfection.

After 48 hours of incubation, the transfection media was removed and the cells were ready for any experiment. The efficacy of the overexpression was verified by western blot.

- PLD2 protein silencing:

In order to knockdown the expression of the PLD2 protein, a commercial siRNA was used. This methodology is based on a double-stranded RNA molecule of 20-25 base-pair in length that interferes with the messenger RNA of a certain gene that blocks its translation into protein and degrades it.

When the cultured cells reached 60-70% confluence in 6-well plates, the cell medium was removed and fresh complete medium was added. Immediately, the transfection mix was formulated as follows: 150 µL Opti-MEM™ and 50 nM of siRNA were mixed in a glass tube; in another tube, 150 µL Opti-MEM™ and 9 µL RNAiMax transfection reagent were mixed. After 5 minutes of incubation, both tubes were mixed and incubated for another 5 minutes before adding the solution to each well. After 48 hours of incubation, the cells were ready for any experiment. For the transfection control condition, an irrelevant siRNA molecule was used, which has been shown to have no effect on proliferation, viability or cell morphology. The silencing efficacy was verified by western blot.

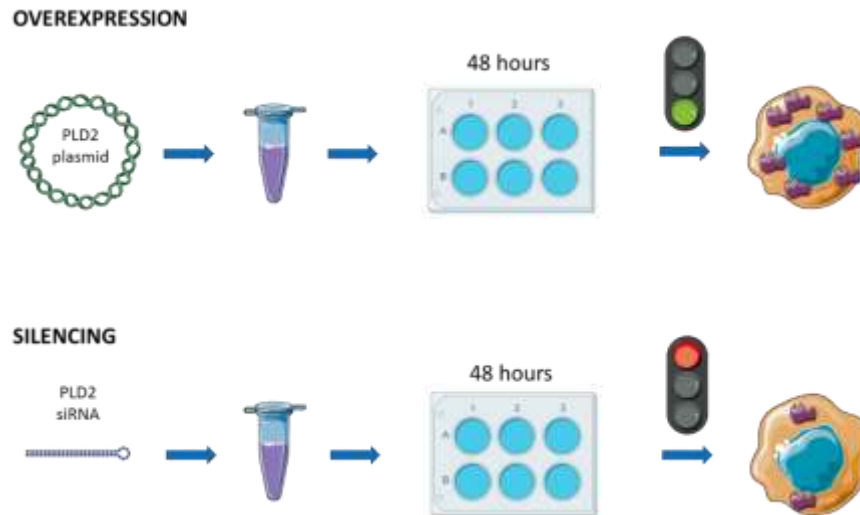


Figure 22. Workflow schema of PLD2 overexpression and silencing.

#### 2.1.7. Cell proliferation assay

In order to study cell proliferation, the XTT Cell Proliferation Kit II was used. This is a colorimetric assay whereby only viable cells are metabolically active to reduce the tetrazolium salt XTT of yellow color in an orange colored formazan dye, which can be detected at a wavelength of 490 nm by a spectrophotometer. The amount of formazan generated is directly proportional to the number of viable cells.

First, the cells were seeded in triplicates in flat-bottom 96 well-plates and left overnight to allow their adhesion to the surface. Then, they were starved for 2 hours using a culture media supplemented with 1% FBS to synchronize the cell cycle of all the cells present in the culture. Afterwards, the starving medium was removed and complete medium was added to the cells. 24 hours later, the XTT mixture was added to the cells at a ratio of 1:50. After 4 hours of incubation, the absorbance of each well was measured at a wavelength of 490 nm in a spectrophotometer. The proliferation rate of the cells studied was calculated as a percentage in relation to the control.

#### 2.1.8. Cell invasion assay

Metastatic cells have the ability to detach from the primary tumor and by degrading the extracellular matrix invade the surrounding stroma. To evaluate the invasion capacity of the cells, an *in vitro* transwell invasion assay was performed. The upper chamber of the transwell is sealed with a polycarbonate filter with pores of 8  $\mu\text{m}$  diameter and coated with Matrigel<sup>®</sup> that resembles the extracellular matrix in tissues, since it contains collagen IV, laminin, entactin, heparan sulfate and proteoglycans. Invasive cells degrade the Matrigel<sup>®</sup> and pass through the pores to reach the underside of the filter.

First, starving media without FBS was added to the transfected cells for 2 hours. At the same time, Matrigel<sup>®</sup> plates were taken out of the fridge and allowed to reach room temperature. Then, the Matrigel<sup>®</sup> from the transwell inserts was rehydrated by adding starving media to the upper and lower chambers for 2 hours.

After this period, the starving medium of the inserts and the wells was carefully aspirated, without touching the Matrigel<sup>®</sup> layer. At that time, complete cell culture medium was added to

the bottom well. Simultaneously, the cells were harvested and added to the upper chamber at a concentration of  $7.5 \times 10^5$  cell/mL in starving media with 0.5% FBS. This was incubated for 20h in the culture incubator.

Eventually, the non-invasive cells that remained in the transwell insert were removed by aspirating the cell medium and scrubbing the filter with cotton swabs. Then, the media in the well was replaced with 4% paraformaldehyde (PFA) to fix the cells that invaded and reached the other side of the filter, as after 20 hours of invasion assay most of the cells are still on the filter and have not yet reached and attached to the bottom of the well. After 10 minutes and three washes of PBS, the invading cells were stained with 0.2% crystal violet for 8 minutes by adding the solution to the bottom well. Then, the transwell was washed with water as many times as necessary to remove all the non-specific staining. When the inserts were dry, they were observed in the microscope and 6 different fields were photographed at 20X. Finally, all the cells in each field were counted and the percentage of invasiveness of each group was calculated related to the control.

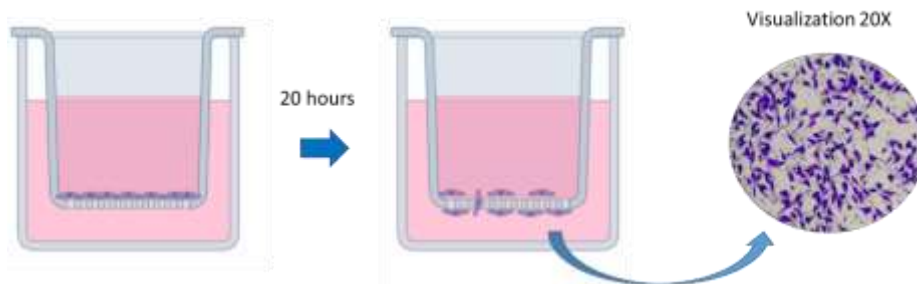


**Figure 23.** Scheme of the transwell *in vitro* invasion assay, and eventual visualization of the cells that invaded.

### 2.1.9. Cell migration assay

Similarly to invasion assay, the migratory capacity of melanoma cells was studied using boyden chambers. However, in this case, the transwell with  $8 \mu\text{m}$  pores was not coated with matrix.

First, the transfected cells were starved for 2h. After this period, the cells were harvested and added to the upper chamber at a concentration of  $5 \times 10^4$  cell/mL in 0.5% FBS media. At the same time, complete culture media was added to the bottom chamber.

After 20 hours of incubation, the non-migrated cells were carefully aspirated and the upper filter scrubbed with a cotton swabs. Then, the culture media in the bottom chamber was substituted with 4% PFA to fix the migrated cells in the bottom side of the filter. After 10 minutes and washing the cells 3 times with PBS, the cells were stained with 0.2% crystal violet for 8 minutes. Then, the transwell was washed with water until all non-specific staining was removed. Eventually, the filter was cut out with a scalpel and mounted on a microscope slide. As such, the migrated cells could be observed in a microscope at 20X and six different fields were photographed. Then, all the cells in each field were counted and the percentage of migration for each group was calculated according to the control.

## 2.2. Melanocyte isolation from human nevus

For this, human nevus from different patients were used, and the pertinent ethic statement was applied for the collection of these samples. The Euskadi Ethics Committee (Oncolmage, 14-10) approved this study and written informed consents were obtained from all the subjects.

As soon as the nevus was surgically removed in the operating room, a piece of it was placed in 10 mL of sterile cell culture medium with antibiotics. Henceforth, the handling was performed under aseptic conditions and all the solutions and materials used were sterile.

In order to eliminate surface contamination of the patient's skin, the tumor was introduced into ethanol 70° for 15 seconds several times and washed in PBS. Then, it was incubated overnight at 4 °C in an enzymatic solution of 0.25% trypsin, 20 mM HEPES and Primocin™ antibiotic solution in Hank's Balanced Salt Solution (HBSS).

Subsequently, the dermis and epidermis were separated in a petri dish using a scalpel; the epidermis was discarded, while the dermis was diced into millimeter pieces. These small portions were then incubated in an enzymatic solution of 0.05% Collagenase, 1.25 U/mL Dispase II and 0.1% Hyaluronidase for 2h while stirring in a water bath at 37 °C.

Once the fragments were partially digested, a mechanical digestion followed the isolation process. For this, the pieces were passed through a 40 µm pore filter that was adapted to a 50 mL tube, and the filtrate was centrifuged at 350 g for 5 minutes. Then, after discarding the supernatant, the cell pellet was re-suspended in Medium 254 and seeded in a petri dish. After an overnight incubation, the culture was washed several times with PBS until all the non-adhered cells (death cells, lymphocytes, erythrocytes, etc.) were removed and fresh medium was added.

In this culture, there were mostly melanocytes and fibroblasts. Willing to have a pure culture of melanocytes, when the cells reached confluence they were washed with 20 nM HEPES in HBSS solution and treated with an antibody (1:500) that recognized a protein present in the fibroblast membrane for 1 hour at 4 °C and gentle agitation. Without delay, the culture was cleaned three times with 20 nM HEPES in HBSS solution at 4 °C. Afterwards, anti-rabbit complement (1:2) diluted in a cold 20 nM HEPES in HBSS solution was added and incubated for 4 hours at 37 °C with vigorous shaking. In this way, the complement bound to the anti-fibroblast antibody caused the lysis of the fibroblasts. Eventually, the culture was rinsed several times to remove the remaining complement and Medium 254 was added to continue with the culture of pure melanocytes.

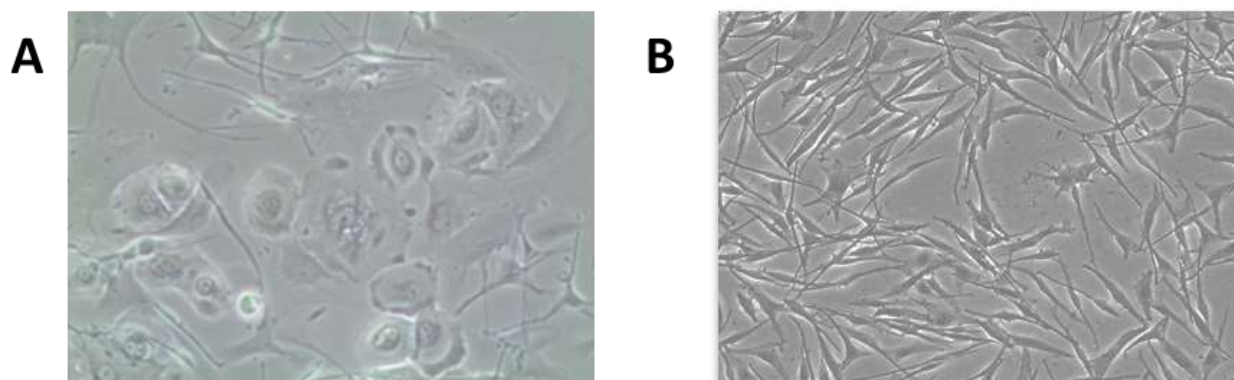


**Figure 24. Nevus melanocyte isolation process at different steps. A.** Co-culture of melanocytes, fibroblasts and keratinocytes. **B.** Culture of pure melanocytes., fibroblasts and keratinocytes. **B.** Culture of pure melanocytes.

### 2.3. Cellular lipids analysis

#### 2.3.1. Sample homogenization

The stored cell pellets were homogenized in 1 mL of PBS using the Polytron homogenizer applying 4 cycles of 10 seconds of homogenization and 10 resting seconds. During the process, the samples were kept on ice. At this point, 10  $\mu$ L of each sample was extracted for protein quantification by the BCA assay and the rest was saved for lipid extraction.

#### 2.3.2. Protein quantification

The protein concentration of each homogenate was determined using the BCA colorimetric assay (Bicinchoninic acid assay). This method is based on the Biuret test. The peptide bonds of the proteins in an alkaline solution reduce  $\text{Cu}^{+2}$  from copper (II) sulfate to  $\text{Cu}^+$ . The amount of  $\text{Cu}^+$  generated is proportional to the protein content. Two BCA molecules chelate with one  $\text{Cu}^+$  ion and form a purple complex that can be detected at the wavelength of 562 nm with a spectrophotometer<sup>148</sup>.

For this, a standard BSA curve (0-10 mg/mL) was used. Once all the study samples and the standard curve samples were ready, the working reagent was prepared, where 50 parts of bicinchoninic acid were mixed with one part of  $\text{CuSO}_4$  solution at 4% (copper sulfate pentahydrate). In a 96-well plate, in triplicate, 10  $\mu$ L of each condition was added to each well along with 200  $\mu$ L of the working reagent. This was incubated for 30 minutes at 37 °C in the dark.

Eventually, the absorbance of each well was read on a spectrophotometer at the wavelength of 562 nm. Based on the absorbance obtained for the standard curve, the protein concentration of each sample was calculated.

#### 2.3.3. Lipid extraction

Cell lipid extraction was carried out in the laboratory of Professor Begoña Ochoa. This assay was based on the Bligh & Dyer protocol<sup>101</sup>, using the same amount of protein for each sample. All the glass material used for this methodology must have been previously treated with a chromic mixture (10 g of potassium dichromate diluted in 1 L of  $\text{dH}_2\text{O}$  and 1 L of sulfuric acid) and thoroughly rinsed, in order to clean the glass material and remove all the residues.

Inside a ground neck flask, 0.4 mL of homogenate, 2 mL of chloroform and 4 mL of methanol were vigorously vortexed for two minutes. Immediately, 2 mL of  $\text{H}_2\text{O}$  and 4 mL of chloroform



were added, and the solution was stirred again for another two minutes. The mixture was then centrifuged at 200 g at 4 °C for 15 minutes, achieving phase separation. The lower phase was transferred to another glass tube and saved for later. The upper protein phase was re-extracted by adding 1.6 mL of chloroform, methanol and H<sub>2</sub>O. This solution was vigorously vortexed for 2 minutes and centrifuged at 200 g at 4 °C for 10 minutes. At this point, the upper aqueous phase was discarded and the lower phase mixed with the previous chloroform phase. Then, in order to evaporate the chloroform and concentrate the extracted lipids, the mixture was introduced in an evaporator/concentrator, and dry lipid-extracts were obtained. To prevent oxidation of the lipids, the tubes were closed under a stream of N<sub>2</sub>. As the aqueous phase was tossed away, the more polar lipids were not analyzed using this extraction method.

Next, the solvent was evaporated in an evaporator/concentrator system for about one hour, until the extract was dried. This extract was re-suspended in 900 µL of chloroform/methanol (2:1). The solution was transferred to a UHPLC vial and the solvent was again evaporated. Each tube with the lipid extract was closed under N<sub>2</sub> atmosphere and stored at -80 °C until use.

#### 2.3.4. Lipidomic analysis

The Central Analysis Service of the UPV/EHU (SGIKER) carried out this analysis. For the identification and quantification of lipids, an untargeted mass spectrometry technique was performed: UHPLC-ESI-Q-TOF (Ultra-high performance liquid chromatography coupled with time of flight quadrupole tandem mass spectrometer).

##### - Ultra-High Performance Liquid Chromatography (UHPLC):

For a better identification of the lipids, a reverse-phase UHPLC technique was used to separate the lipid families, with a non-polar stationary phase composed of silica beads and two different polar mobile phases (A and B), which were mixed at different percentages during the elution process.

First, the dry lipid extracts were reconstituted in 150 µL chloroform/methanol 2:1. Then, 7.5 µL of this solution was injected into the mobile phase and introduced into the chromatograph.

In order to ensure the accuracy of the results obtained in this experimental strategy different quality control samples and internal standards were analyzed together with the study samples. First, three blank samples were injected, consisting of CHCl<sub>3</sub> (2:1 v/v). Then, the 34 study samples were randomly introduced in the system, together with an internal standard solution of 1.92 µM PC (17:0/14:1) and 1.68 µM PI (17:0/14:1) diluted in CHCl<sub>3</sub> (2:1 v/v), which are detected in positive and negative ionization mode, respectively. In addition, 15 system Quality Control (QCsys) were introduced for the reconditioning of the system before the analysis of the study samples. QCs were prepared by reconstituting in 150 µL of CHCl<sub>3</sub> (2:1 v/v) the lipid extracts of four additional melanoma cell lines that were not analyzed in this experiment. Besides, QC samples (QCsample) were also analyzed. These were prepared by adding 15 µL of all the study samples, thus containing all the lipids that would be identified in the study samples. They were used to determine all the lipids that would be detected in the study samples, and also, as they were injected at the beginning, during the study sequence, and at the end of the analysis, to determine the analytical variability of the identified lipids, and normalize the results (see the injection order of all the samples in **Figure 25**).

At the beginning of the chromatography approach, the mobile phase was composed of phase A (acetonitrile and water 40:60) in 60% and phase B (acetonitrile and isopropanol 10:90) in 40%. Therefore, the first analytes eluted were the polar ones. Progressively, the concentration of

phase B was increased, until reaching 100%, when the non-polar compounds were eluted and directly entered the mass spectrometer.

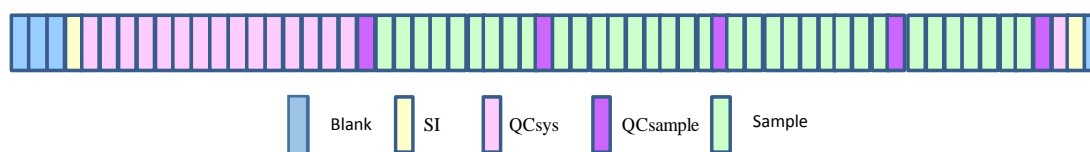


Figure 25. Injection order of the samples analyzed.

- ESI-TOF Mass spectrometry:

The lipid molecules were ionized in the ionization source using ESI methodology (ElectroSpray Ionization). The ions were then targeted through a tandem Q-TOF mass analyzer (Quadrupole/Time-of-flight) that separates the molecules according to their mass-to-charge ratio.

Eventually, the ions enter the detector, which records the information of both the precursor and the fragmented ions and their abundance in the mixture, which is then sent to the data system where it is graphically represented as mass spectra. Each peak of the graph represents a specific mass present in the mixture, and the amplitude of each peak represents the relative abundance of that ion.

Table 9. UHPLC-ESI-Q-TOF analysis conditions.

UHPLC	MS
<b>Column:</b> Acquity UHPLC HSS T3 2.1x 100 mm, 1.8 µm (Waters)	<b>Ionization mode:</b> ESI positive/negative
<b>Column Temperature:</b> 65 °C	<b>Adquisition mode:</b> MS <sup>E</sup> in resolution mode (FWHM≈20.000)
<b>Flux:</b> 500 µL/min	<b>Capillary voltage:</b> 0.7kV (ESI+) & 0.5 kV (ESI-)
<b>Mobil phase A:</b> Acetonitrile/H <sub>2</sub> O (40:60) with 10 mM NH <sub>4</sub> Ac	<b>Cone voltage:</b> 35 V
<b>Mobil phase B:</b> Acetonitrile/Isopropanol (10:90) with 10 mM NH <sub>4</sub> Ac	<b>Source temperature:</b> 120 °C
<b>Gradient:</b> 0-10 min, from 40 to 100%B; 10-11min, 100%B;	<b>Desolvation temperature:</b> 400 °C
<b>Temp. automatic injector:</b> 4 °C	<b>Desolvation gas:</b> 900 L/h
<b>Injection volume:</b> 7.5 µL	<b>Gas of the cone:</b> 30 L/h
	<b>Adquisition range:</b> 50 a 1200 u.
	<b>Scan time:</b> 0.5s

---

- Data analysis:

First, for the lipid assignment, in order to generate a data matrix, the R-software 3.1.1. was used. Then, for the identification of the lipids, the MSe Data viewer was employed to process the data obtained by the R software, and, finally, using the SimLipid software the lipid assignment was made.

Then, before performing any statistical analysis, the data obtained for each variable were normalized and logarithmically transformed to achieve a Gaussian distribution, and therefore avoid systemic bias in the multivariate analyses performed later.

To detect the differences between the samples studied, different multivariate data analysis were performed using the SIMCA 14.1 software. First, a **principal component analysis** (PCA) was conducted. This is a non-supervised analysis that finds patterns within the data without reference whether they belong to the same study group. It aims to find groups of similar samples, detect abnormal samples, relevant variables and the relation between variables and samples. For this, it transforms the data into fewer dimensions (Principal Components) that are representative of the features of the data, and better summarizes it using the fewer number of principal components possible. This is, only the more informative dimensions are used. To visualize the distribution of the data, score scatter plots of two principal components can be performed, where positively correlated samples are close to each other and the non-correlated data are far from each other.

In order to validate the PCA model, there are some model diagnostic tools. Like in a regression, the model fit is represented by  $R^2$ , and it informs how well the data can be mathematically reproduced by the computed model. Hence, if the correlation is good  $R^2$  is close to 1, and gets worse when  $R^2$  is smaller. However, it is not sufficient to have a  $R^2$  close to one to validate the model, as also its predictive ability is important. The latter is estimated by  $Q^2$ , which represents the lack of model fit of each sample to the PCA model. It measures the variation after applying the created model to the samples, this is, how much of a sample cannot be explained by the model. When  $Q^2 > 0.9$  the fitting to the model is considered excellent.

Besides, Hotelling's  $T^2$  analysis is also employed to evaluate the PCA model obtained. It measures the variation within the PCA model, by indicating how far each sample is from the center of the model. It sets a confidence limit where the samples can lie. In this study, if any result lies outside the limits of 95% of confidence interval after applying Hotelling's  $T^2$ , it will be considered a strong outlier. To visualize it, a score scatter plot of the two principal components was performed.

On the other hand, the detection tool of moderate outliers is DModX, which stands for distance to the model in X-space, with a maximum tolerable distance (DCrit) that is usually set in 0.05. Moderate outliers have DModX values larger than DCrits, so do not fit the model well.

The next step was to perform different supervised analyzes. First, a **partial least squares discriminant analysis** (PLS-DA) was carried out. This study analyzes the differences between each study group according to their lipidic profile, and is commonly used in metabolomic studies for classification and biomarker identification, as it sharpens the differences between the study groups. This model is especially useful when PCA method is not able to establish differences between the study groups. As the groups within the samples are already known, the aim of this analysis is to determine if the study groups are actually different, and what are the variables that stress the differences between the groups.

For the validation of the model, R<sup>2</sup>, Q<sup>2</sup> and Hotelling's T<sup>2</sup> ellipse plot are used as well as in PCA. Besides, permutation testing is also used in this case, which allows to determine the ability of the model to predict the Y response of new samples examined. Here, the variable Y was permuted 999 times in the two studied classes in each analysis.

Moreover, in order to validate the significance of the differences observed in the PLS-DA models, the p-values of each comparison were calculated using ANOVA approach.

The comparisons of the intensities detected for each lipid subclass were performed by adding the intensities obtained for all the lipid species pertaining to that lipid subclass. Then, the sums obtained for each study group were compared relating them to the value obtained for skin melanocytes. This is, the sum of the intensities of all the PCs in one group was divided by the sum of the intensities of all the PCs in skin melanocytes.

The next analysis was **orthogonal partial least squares discriminant analysis** (OPLS-DA). This model forces the variation between the groups, in order to detect the molecules that define the differentiation between the experimental groups. In fact, this method is used to identify the species that generate relevant changes in the lipidome. For this, a regression model is constructed between the multivariate data (X) and the class information (Y). To visualize the discriminating variables and thus select the potential biomarkers, score plots were used. In addition, jack-knife confidence intervals of the loading plots to reduce bias of parameter estimated and to determine variance were utilized, and also VIP (Variable Importance in Projection) plots. The latter graphs visualize the relative contribution of each lipid molecular species to the variance between each study group. High values of VIP score show great contribution of that lipid to the group separation.

The significantly different lipids detected were represented in Box-whisker plots, in order to study their relative abundance in each study group.

- Lipidomic analysis limitations:

The analytical procedure followed in this experiment only gives a hint of the tendency of the changes within the cells. First, in the extraction step, the more polar and hydrophilic lipid species were missed as they were dissolved in the aqueous phase, which was discarded. Concretely, all the phosphorylated lipids such as phosphorylated PIs, and complex glycolipids, specially gangliosides, were dissolved in the aqueous phase and therefore missed. These lipid species are thought to be very important in some malignant transformations, so, for a global lipidome analysis, in future experiments, the most polar lipids should be extracted using different methods.

In addition, this is a semi-quantitative analytical procedure, as internal standards for quantification have not been used. The comparisons carried out with these results are only the comparative of the intensities of each lipid species as the mean of all the cell lines of each study groups. This is, one cannot compare the abundancy between different lipid classes, as the intensities vary according to the adducts formed for the mass spectrometry approach, which are very different depending on the lipid species. Hence, for example, we cannot know if there are more phospholipids than sphingolipids in a concrete cell type, but we can determine if there are more phospholipids in one group (melanocytes, e.g.) than in other (primary melanoma, e.g.).

## 2.4. Cell membrane analysis

Employing functional cell membrane microarrays, cell membrane lipids were studied. This is a new biotechnological tool developed by IMG Pharma S.L., which, using specific printing protocols, maintains the lipid environment of the membranes, so that the lipid profile of the samples can be determined. In addition, hundreds of samples can be immobilized on the same pre-treated microscope glass slide, allowing the analysis of all of them at the same time, saving time and expenses. Specifically for the analysis of lipids, a mass spectrometry technique was applied on the membranes immobilized in the microarrays.

### 2.4.1. Cell membrane isolation

Using a Teflon-glass grinder and Ultra-Turrax® disperser, cell membranes of the stored cell pellets were isolated using a 50 mM Tris buffer supplemented with 1 mM EGTA, 3 mM MgCl<sub>2</sub> and 250 mM sucrose. After centrifuging the suspension for 5 minutes at 40 g, the resulting supernatants were centrifuged again at 18,000 g for 15 minutes at 4 °C. Then, the supernatants were discarded and the pellets washed in 20 volumes of 50 mM Tris buffer and centrifuged again at 18,000 g for 15 minutes at 4 °C. Once again, the supernatant was discarded and both pellets mixed. Finally, the protein concentration was determined using the Bradford method. The cell membrane preparations were stored at -80 °C until use.

### 2.4.2. Protein quantification

Protein quantification of the cell membrane preparations was performed by the Bradford protein quantification assay<sup>149</sup>. This is a colorimetric analytical procedure that is based on the color shift of the Coomassie Brilliant Blue dye in an acidic environment, which changes its color from red to blue, after binding to the protein present in the solution. In the absence of protein, the dye remains red and its absorption spectrum is at 465 nm. However, the blue dye bound to the protein has the maximum absorbance at 595 nm, so the experiment was carried out at this wavelength.

First, a BSA standard curve (0-0.1 mg/mL) was prepared. Then, in a 96 well-plate in triplicate, 10 µL of each sample and standard curve condition were mixed with 250 µL of Bradford working solution (0.01% Coomassie Brilliant Blue, 0.05% Ethanol 95°, 0.1% Phosphoric Acid). After 10 minutes of agitation in the dark, the absorbance was analyzed at 595 nm. Using the results obtained in the Bradford method, all the samples were diluted to the same protein concentration, in order to immobilize the same protein quantity in each spot of the array.

Then, after the printing of the samples, the protein concentration of each spot of the array was measured. For this, the slides with the cell membrane preparations printed on them were introduced in the Bradford working solution for 10 minutes and washed in water for 5 minutes. Then, the color intensity for each spot was determined. This is used as a quality control of the printing, as all the spots representing different samples must have similar protein concentration.

### 2.4.3. Microarray development

Three normal skin melanocyte cell lines, nine melanocyte cell lines isolated from nevus, six primary melanomas and nine metastatic melanoma cell lines were placed. Here, replicates of three different passages of each sample were printed.

All cell pellets were diluted to the same concentration and printed on expressly pre-treated glass slides by a non-contact microarrayer (Nano\_plotter NP 2.1). The piezoelectric tip dispenses 4 nL per dot, and in this case, 20 drops per sample were spotted. The microarrays were stored at -20°C until use.

After printing the arrays, three different slides from each batch were randomly chosen and stained using the Bradford method. This enables to calculate the protein concentration in each spot. Nonetheless, in the same microarrays together with the samples, different concentrations of BSA were printed, in order to establish an internal calibration curve that allows the transformation of the intensities of each spot for the Bradford into nanograms of proteins. In this way, the results obtained in the lipidomic assay can be normalized to the protein quantity on each spot.

#### 2.4.4. Lipidomic analysis

The research group of Professor J.A. Fernandez of the UPV/EHU carried out this analysis. It is based on Matrix Assisted Laser Desorption Ionization (MALDI) mass spectrometry using a LTQ-Orbitrap XL analyzer.

##### - MALDI mass spectrometry:

For the preparation of the sample, first, the microarrays were allowed to reach room temperature. Then, using a glass sublimator (Ace Glass 8023) the matrices were placed on the samples, using MBT (2-Mercaptobenzothiazole) for positive ionization or DAN (1,5-Diaminonaphthalene) for negative ionization. In this way, uniform thin layers are formed, allowing the scanning of the molecules in positive or negative ion mode for several hours.

Next, using the MALDI methodology and a N<sub>2</sub> laser as ionization source (100  $\mu$ J maximum power, elliptical spot, 60 Hz repetition rate), the molecules were ionized, irradiating the spots with the laser, inducing absorption by the matrix in the wavelength of the laser and desorption of the sample and the matrix with minimal fragmentation. Then, using a LTQ-Orbitrap XL analyzer, trapped ions were detected and a mass spectrum was generated. This was provided as an image, where each peak was mapped along the sample. Data was acquired both in positive and negative ionization-mode with 150  $\mu$ m spatial resolution and a mass resolution of 60.000 FWHM at  $m/z=400$ , and with a laser energy between 20-30  $\mu$ J/pulse. All the data acquired was in the range between 550-1200 units in the negative ionization mode and 480-1000 units in the positive ionization mode.

In order to ensure the reproducibility of this methodology, and thus, of the data obtained, five different arrays were analyzed in different days for both ionization modes. Besides, the spots corresponding to the melanocytes were printed in four different locations of the array to check if the results were the same in all the locations of the slides.

##### - Lipid assignment:

Before the identification of each mass channel detected, all the spectra were aligned and normalized to the total ion current (TIC). Then, each ion channel was assigned to a concrete lipid molecule using an in-house synthetic database, constructed by the combination of side-chains and polar head groups of lipids, with more than 30,000 entries. Next, the MALDI assignments were compared to the ones achieved in UHPLC-MS/MS, and the peaks that correspond to the matrix, lipid fragments (PA and CerP), matrix adducts and isotopic distributions were removed. Eventually, PCs, ether PCs, PEs, ether PEs, PSs, PGs, ether PGs, PIs, ether PIs and SMs were detected in  $MS^-$ , while PCs, ether PCs, ether PCs, PEs, ether PEs, HexCer, SMs, DGs and TGs are identified in  $MS^+$ .

In addition, as UHPLC-MS/MS gives better description of the side-chains structure of the lipids, if the molecule was detected in both methodologies the nomenclature of UHPLC-MS/MS was used thereafter.

- Statistical analysis:

For the statistical analysis, SPSS Software was used. The first approach was to conduct a t-test comparing the intensity detected for the different lipid molecular species between normal melanocytes (skin + nevus) and melanoma cells (primary + metastatic). Next, a multi-comparison paired t-test between all the groups was carried out ( $p < 0.05$ ), which compared each lipid specie in a paired analysis as follows: skin vs nevus melanocytes; skin melanocytes vs primary melanoma; nevus melanocytes vs primary melanoma; skin melanocytes vs metastatic melanoma; nevus melanocytes vs metastatic melanoma; primary vs metastatic melanoma. For the post-hoc correction, Levene's test was conducted to assess the equality of the variances and choose the correct post-hoc method, either Bonferroni or Games-Howell. If the significance of Levene's test was  $p < 0.05$ , the null hypothesis of equal variances was rejected, and it was concluded that there is a difference between the variances in the population. In this case, Games-Howell must be applied. However, if  $p > 0.05$ , the null hypothesis is assumed and Bonferroni is conducted.

## 2.5. Protein analysis

### 2.5.1. Western blot

This widely used analytical tool allows the separation by the molecular mass of proteins within a complex mixture using gel electrophoresis and the subsequent detection of specific proteins by immunoblotting with specific antibodies. With this procedure, the molecular weight of the protein of interest can be estimated, study if it has post-translational modifications such as phosphorylation and ubiquitination, and a semi-quantitative estimate of the protein levels can be made by comparing all the samples studied.

- Protein extraction:

Protein extraction was performed from stored cell pellets or from newly prepared cultured cell pellets. If stored cell pellets were used, they were first kept on ice for 10 minutes until they were thawed. For protein extraction, 250  $\mu\text{L}$  of RIPA Buffer was added per  $5 \times 10^6$  cells. This buffer is composed of 150 mM sodium chloride, 1% IGEPAL<sup>®</sup>ca-630, 0.5% sodium deoxycholate, 0.1% SDS and 50 mM Tris-HCl at a pH of 8. Additionally, 1X protease inhibitor cocktail-3 and 1X phosphatase inhibitor were added to protect the sample, since as soon as the lysis begins, the proteolytic and dephosphorylating processes start.

After vigorously re-suspending the samples in the lysis buffer, the solution was kept on ice for 15 minutes. In this process, the cellular DNA escapes from the nucleus and a cloud of high-density DNA is formed. Considering that it would interfere with the experiments, this was broken by passing the solution through a 20G needle. Immediately, the solution was centrifuged at 15,000 g for 5 minutes at 4 °C. The supernatant was transferred to a new tube, since the proteins of interest were dissolved there. Cell lysates were stored at -20 °C until use.

- SDS-polyacrylamide gel electrophoresis (SDS-PAGE):

The SDS-PAGE technique separates proteins according to their molecular weight, based on the ability of charged molecules to move in an electric field. Prior to electrophoresis, the samples are denatured by heat in the presence of a denaturing agent such as SDS. This detergent binds to the proteins destroying their secondary and tertiary structure, and covering their intrinsic charge, conferring them a negative charge. One SDS molecule binds to two amino acids, so the mass-charge-ratio would be similar in each protein analyzed. Reductive electrophoresis was run, so that reducing agents such as DTT (dithiothreitol) were added. The denaturation was completed by DTT as it breaks the disulfide bonds of the proteins. In this way, when voltage was applied, all the proteins migrated from the cathode (-) to the anode (+) at different speed depending on their molecular weight.

For the separation, a gel of polyacrylamide was used, which was constructed by crosslinking acrylamide and bis-acrylamide molecules. This polymerization was initiated with ammonium persulfate and catalyzed with temed (N,N,N,N'-tetrametilnediamina). Depending on the concentration of acrylamide and bis-acrylamide used, different pore sizes were formed within the gels. Thus, the higher the concentration of acrylamide, the smaller the pore size and vice versa. In this way, if the protein of interest has a high molecular weight, a low concentration of acrylamide should be used for a higher resolution. However, the higher the acrylamide concentration, the more separated the lower molecular weight proteins will be.

**Table 10. Percentage of acrylamide needed to resolve the proteins according to their molecular weight.**

<b>Acrylamide %</b>	15	12	10	7.5
<b>kDa range</b>	12-45	10-70	15-100	25-200

The gels used for western blot are composed of two different parts. The biggest is the running. Here, the proteins are separated, so that depending on the molecular weight of the proteins of interest, the percentage of acrylamide used can be adapted. The top is the stacking, which is a small portion where all the proteins are concentrated and begin to migrate at the same time through the running gel. It is always prepared at the 4% of acrylamide.

For casting the gels, first, the shorter and taller glass plates were cleaned with 70% ethanol and water. Then, they were introduced into the casting frame, which was placed in the casting support. When the apparatus was assembled, the running gel solution was prepared and added inside both glass plates, leaving 2-3 cm from the top. After that, water was added in order to explode the bubbles that could have formed and achieve a straight surface.



Table 11. Composition of the running and stacking gels relying on the acrylamide percentage.

	RUNNING GEL				STACKING GEL
	7.5%	10%	12%	15%	4%
<b>30% Acry-Bis</b>	4.3 mL	5 mL	6 mL	7.5 mL	2 mL
<b>Tris-HCl 0,5M pH=6,8</b>	-	-	-	-	1.5 mL
<b>Tris-HCl 2M pH=8.8</b>	3.4 mL	3 mL	3 mL	3 mL	-
<b>Agua MilliQ</b>	10.15 mL	7 mL	6 mL	4.5 mL	1.5 mL
<b>20% SDS</b>	85 µL	75 µL	75 µL	75 µL	75 µL
<b>10% APS</b>	85 µL	75 µL	75 µL	75 µL	125 µL
<b>TEMED</b>	5.64 µL	5 µL	5 µL	5 µL	12.5 µL

When the running gel polymerized, the water was removed. At the same time, the stacking gel solution was prepared and the rest of the plate was filled with it. Then, the comb was placed to form the wells. Once the gel polymerized it was ready to use.

Table 12. Reagents used for casting the gels and their functions.

Reagent	Function
<b>Acrylamide</b>	The monomers that polymerize forming the gel matrix
<b>Bisacrylamide</b>	Cross-linking reagent to form polyacrylamide
<b>APS</b>	Polymerization initiator
<b>TEMED</b>	Polymerization catalyst
<b>Tris (C<sub>4</sub>H<sub>11</sub>NO<sub>3</sub>)</b>	Solvent for preparing the gels
<b>SDS</b>	Denatures and negatively charges the proteins

The gels were run under reducing conditions by the addition of DTT to the samples. In fact, it ensures the denaturation of the proteins, since it cleaves the sulfide bonds of the chains and disrupts the tertiary and quaternary structure of the macromolecules. Therefore, under these conditions, the migration speed of the proteins is proportional to their molecular mass, and not due to their charge or 3D structure. Before adding the samples to the gel, 40 µg of each sample was mixed with Laemml 5X loading buffer (60 mM Tris-HCl at pH 6.8, 2% w/v SDS, 10% glycerol, 0.002% bromophenol blue) and also with DTT reducing agent at 1 mM. In addition, RIPA buffer was added up to 25 µL, so that all the samples contained 40 µg of protein in a volume of 25 µL. Then, the samples were heated at 37 °C for 30 minutes, since the proteins of interest were mainly membrane proteins and they tend to aggregate if denatured at 95 °C<sup>150</sup>.

Table 13. Loading buffer composition.

Reagent	Function
<b>Bromophenol blue</b>	Monitor the migration of the samples through the gel
<b>Glycerol</b>	Increases the density of the sample so that it layers in the well and does not get mixed with the running buffer
<b>DTT</b>	Break the disulfide bonds and disrupt the tertiary and quaternary structure of proteins
<b>SDS</b>	Denatures the proteins and gives them overall negative charge

At the same time, the gels were assembled in the electrophoresis tank and the inner chamber between the gels was filled with running buffer (25 mM Tris pH 8.3, 190 mM Glycine, 0.1% SDS). When the samples were denatured, the comb was taken out and 20  $\mu$ L of each sample was loaded inside each well. The first well was left empty for the molecular weight marker to estimate the mass of the proteins of interest that were resolved in the gel. When all the wells were filled, the inner chamber and the bottom of the outer chamber were filled with running buffer. Then, the electrophoresis was run at 120V for the first 10 minutes to concentrate all the proteins in the stacking gel. After this time, the voltage was set at 180 V for 1 hour to separate the proteins.

- Transfer:

After separating the proteins throughout the gel, they were transferred to a solid support membrane of nitrocellulose for immunodetection with specific antibodies. Based on the same principle as electrophoresis, in this case, a horizontal electric field was applied, so that the separated proteins were immobilized in the same migration position as in the gel. For this, the membrane and the gel were assembled inside a paper and sponge sandwich, and when voltage was applied, the proteins migrated from the gel towards the anode, where the membrane was located. The wet transfer method was employed, so all the sandwich elements (paper, sponge, gel, membrane) were completely immersed in transfer buffer before assembly. This method is recommended for larger proteins and higher quality blots are achieved. However, it is a slow approach and the system is heated, so an ice bucket was introduced into the tank, which was placed in a tray surrounded by ice.

After constructing the sandwich, it was introduced into the tank, which was filled with transfer buffer (25 mM Tris pH 8.3, 190 mM Glycine, 0.1% SDS, 5% Methanol) and an ice bucket. The transference was carried out for 3 hours at 300 mA.

Once it finished, the membrane was stained with Red Ponceau solution (0.1% of Red Ponceau, 1% of glacial acetic acid) to confirm the correct transfer of proteins, since this solution stains all the protein bands that have been immobilized in the membrane. Then, the membrane was rinsed with TBS until the staining was removed.

- Immunoblotting:

To avoid non-specific binding of antibodies to the membrane, membrane spaces not occupied by transferred proteins were blocked, using a blocking reagent with higher affinity for the membrane than the antibodies used afterwards. In this case, 5% of non-fat milk diluted in 0.1% TBS-Tween 20 (TBS-T) was used under stirring at room temperature for 1 hour. After this, the membrane and the primary antibody diluted in the blocking reagent at the recommended concentration (**Table 14**) were incubated overnight at 4  $^{\circ}$ C under agitation.

Table 14. Primary antibodies used for western blot.

Primary antibody	Reference	Company	Origin	Dilution
<b>PLD2</b>	#AO2358a	Abgent	Mouse	1/1500
<b>EGFR</b>	Ab52894	Abcam	Rabbit	1/2000
<b>PKC<math>\alpha</math></b>	Sc-8393	Santa Cruz	Mouse	1/1000
<b>PLD1</b>	#3832	Cell Signaling	Rabbit	1/1000
<b>PLA<sub>a</sub></b>	Sc-376563	Santa Cruz	Mouse	1/1000
<b>PLC</b>	Sc-5291	Santa Cruz	Mouse	1/1000
<b><math>\alpha</math>-Tubulin</b>	T9026	Sigma Aldrich	Mouse	1/3000

After this first incubation, the primary antibody was discarded and the membrane was washed three times for 5 minutes with TBS-T. Next, the secondary antibody diluted (**Table 15**) in blocking reagent was incubated with the membrane for 2 hours at room temperature. This is a species-specific antibody directed against the constant region of the primary antibody and is labeled with HRP (horseradish peroxidase).

Table 15. Secondary antibodies used for western blot.

Secondary antibody	Reference	Company	Dilution
<b>Anti-Mouse IgG<math>\kappa</math>-HRP</b>	Sc-516102	Santa Cruz	1/5000
<b>Anti-Mouse IgG-HRP</b>	1032-05	Southern Biotech	1/8000
<b>Anti-Rabbit IgG-HRP</b>	Ab102279	Abcam	1/10,000

- Detection:

The HRP enzyme conjugated to the secondary antibody generates chemiluminescence when incubated with ECL solution (Enhanced ChemiLuminescence). The enzyme catalyzes the oxidation of the luminol present in the ECL, resulting in the emission of light. Using a charge-couple device camera-based imager, digital images of the chemiluminescence of the membrane were captured using the Gene Snap program.

- Image analysis:

The band intensity analysis for each protein detected was performed by determining the densitometry of each lane with Image J program. The intensity of each lane was normalized to the relative amount of the control protein –tubulin- of each sample.

#### 2.5.2. Immunofluorescence

This widely used approach allows the localization and the determination of the expression levels of a given protein. This methodology can be used in both tissue sections and cultured cells. This immunostaining technique is based on tagging antigens by using fluorescent molecules such as Hoechst to stain the DNA or specific antibodies labeled with fluorochromes. These molecules absorb ultraviolet light at a certain wavelength, but emit light at a higher wavelength, which is captured by specific filters of a fluorescence microscope. Here indirect immunofluorescence was used. Thus, an unlabeled antibody specifically detected the antigen of interest. Then, a species-specific fluorescent-labeled secondary antibody was bound to the primary antibody and this sandwich was detected using a fluorescence microscope.

In this study, cultured cells were analyzed. For this, the cells were seeded in round coverslips assembled inside the wells of 24-well plates. In each coverslip, 500  $\mu$ L of cells were incubated

overnight to allow their adhesion to the immunostaining support. Then, the cell medium was removed and the cells were washed with PBS. For the immobilization of the antigens, the cells were fixed with 4% of paraformaldehyde for 15 minutes at room temperature. After washing the cells three times with PBS, they were permeabilized for 5 minutes with 0.1% triton-X100 in PBS to ensure the entry of the antibody to its antigen. At that time, the cells were rinsed abundantly with PBS, and all nonspecific binding sites were blocked using 5% FBS diluted in PBS for 1 hour at room temperature. Then, the blocking solution was discarded and the primary antibody was diluted in blocking solution for an overnight incubation at 4 °C. After washing the cells with PBS to remove the unbound primary antibody, the secondary antibody tagged with the fluorescence dye was added for 2 hours in the dark. Finally, the cells were washed and Hoechst was added for 5 minutes at a concentration of 1 µg/mL to stain the nucleus of the cells. Immediately, coverslips were mounted with Fluoromount-G on a microscope slide. Then, the samples were visualized in a fluorescence microscope.

### 2.6. PLD enzymatic activity assay *in vitro*

This assay was carried out in the laboratory of Dr. Julian Gomez-Cambronero in Wright State University (OH, USA) following their own protocol<sup>151</sup>. Under normal conditions, PLD enzyme cleaves the phospholipids of the biological membranes, releasing phosphatidic acid and the polar group of the phospholipid. However, in the presence of a primary alcohol such as butanol, PLD follows a specific reaction called transphosphatidylation, in which phosphatidylbutanol is generated as an end-product.

Before starting the experiment, cellular sonicates were prepared. The stored cell pellets were re-suspended in a special lysis buffer (5 mM HEPES, pH 7.8, 100 µM Na orthovanadate, 0.4% Triton X-100) plus Aprotinin (2 µg/mL) and Leupeptin (5 µg/mL) protease inhibitors. Keeping the samples on ice, they were sonicated for 10 seconds. Next, BCA assay was carried out for protein quantification and 50 µg were processed for the measurement of PLD activity.

First, liposomes containing PC(8:0/8:0) and PIP<sub>2</sub> (Phosphatidylinositol 4,5-bisphosphate), which is a cofactor of PLD, were prepared. Then, [<sup>3</sup>H]butanol and the liposomes were mixed. The final concentration of all the reagents in the assay mix was: 45 mM HEPES pH 7.8, 150 nM NaCl, 0.16% Triton X-100, 3.5 mM PC(8:0/8:0), 1 µM PIP<sub>2</sub>, 0.9 µCi [<sup>3</sup>H]butanol. This reaction mixture was incubated together with the cell sonicates at 30 °C for 20 minutes in a shaker incubator to allow the enzyme act. At this point, the reaction was stopped using an ice-cold stopping solution (2 MeOH/ 1 Cl<sub>3</sub>CH/ 10 N-HCl), Cl<sub>3</sub>CH and H<sub>2</sub>O. After vortexing all the tubes 3 times, they were centrifuged at 14,000 g for 30 seconds, and a biphasic separation was achieved: in the upper phase there was an aqueous phase containing the unincorporated [<sup>3</sup>H]butanol; separated by a white meniscus was the chloroform phase where all the lipids were dissolved. Forthwith, the aqueous phase was aspirated and the meniscus discarded, while the lipid phase was transferred to new clean tubes, which were tightly capped to avoid evaporation.

At this point, the chromatography solvents and the TLC plate were prepared. For this, in a separatory funnel, 260 mL ethyl acetate, 40 mL iso-octane, 60 mL acetic acid and 200 mL H<sub>2</sub>O were stirred and let to stand to allow phase separation. Once proper separation was achieved, the lower phase was discarded and the upper phase was poured into the TLC chamber. At the same time, the TLC plate was activated by heating it at 115 °C for 15 minutes.

After drying the samples under a N<sub>2</sub> stream, they were reconstituted in 37 µL of Cl<sub>3</sub>CH/MeOH (9:1) and loaded on the TLC plate. On both side-lanes of the plate, phosphoethanol and phosphobutanol standards were spotted respectively, so they run at the same time as the study samples. When the chromatography was stopped, the radiolabeled phosphobutanol from the study samples would have run in the area between both standards. Therefore, in each lane, the area between both standards was scraped and introduced into a scintillation vial together with scintillation cocktail. Eventually, the radioactivity of each sample was determined in a scintillation counter.

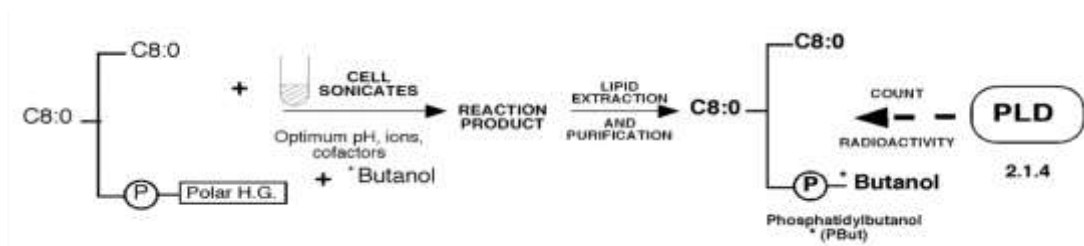


Figure 26. Schematic representation of the PLD enzymatic assay reaction<sup>149</sup>.



# **RESULTS**

El capítulo Results está sujeto a confidencialidad por la autora







# **DISCUSSION**

El capítulo Discussion está sujeto a confidencialidad por la autora







# **CONCLUSIONS**

El capítulo Conclusions está sujeto a confidencialidad por la autora







# **HIPOTESIA ETA HELBURUAK**



## 1. Hipotesia

Melanoma, melanozitoen eraldaketa gaiztoaren ondorioz sortzen den minbizia da. Toki ezberdinenetan sor daitekeen arren, normalean larruazalean agertzen da. Melanomaren intzidentzia etengabe handitu da azken hamarkadetan, eta Europan zazpigarren minbizi diagnostikatuena da. Larruazaleko tumore guztien %4a baino ez bada ere, minbizi horiek eragindako heriotzen %80ren erantzule da (street). Aipatzekoa da, 2019an, Espainian 150000 kasu berri diagnostikatuko direla iragarri dela (who).

Melanoma tumoreetan ikusitako heterogeneotasunak biomarkatzaileak edo benetan eraginkorrak diren tratamenduak identifikatzea zaildu du. Horregatik, heriotza tasak oso altuak dira, melanoma metastatikoarentzat bereziki. Beraz, itxaropenak gisa erabil daitezkeen edo detekzio goiztiarrean, diagnostikoan eta pronostikoan lagun dezaketen biomarkatzaile berriak identifikatzeko premia handia dago; izan ere, errekupeazio-tasak oso handiak dira tumorea goiz detektatzen bada.

Ilido horretan, zelulen metabolismoa minbiziaren ezaugarri gisa ezarri da. Jakina da zelula horiek jasaten dituzten bide metabolikoen aldaketak tumore zelulek hartutako fenotipo gaiztoa babesten dutela. Zehazki, lipidoen metabolismoak prozesu kartzinogenikoan duen inplikazioak interesa sortu du minbiziaren ikerketarako. Metabolismoa eraldatuta dago zelula tumoraletan, eta horrek lipido batzuen konposizioan eta kantitatean aldaketak eragiten ditu. Horregatik, hurrengo hipotesia planteatu da: lipidoen konposizio eta kantitatean eta horien metabolismoan gertatzen diren aldaketek, melanozito ez-patologikoak melanoman bihurtzea eragin dezakete. Beraz, melanozito ez patologikoekin alderatuz, melanoman modu aberrantean adierazten diren espezie lipidiko jakinen identifikazioa, gaixotasun honetarako biomarkatzaile garrantzitsuak aurkitzea izan liteke. Bestalde, espezie horiek melanomaren garapenean eta progresioan duten inplikazioa ezagutzea ahalbidetuko luke. Lipidoen edukian ematen diren aldakuntzak molekula horien metabolismoan parte hartzen duten entzimen adierazpen eta jarduera-alterazioekin batera doaz. Adibidez, fosfolipasa entzimek glizerofosfolipidoen katabolismoan hartzen dute parte, eta entzima familia horren isoforma ezberdinak minbiziarekin lotu izan dira. Izan ere, PLD2-k hainbat minbizi zelulen gaiztotze prozesuan eta barreiadura metastasikoan laguntzen duela frogatu da.

## 2. Helburuak

Doktorego tesi honen helburu nagusia melanomarentzako biomarkatzaile lipidiko berriak identifikatzea izan zen, melanomaren detekzio goiztiarrean, diagnostikoan eta pronostikoan lagunduko zutenak. Horretarako, hainbat ikuspegi lipidomiko aplikatu ziren. Gainera, lan honetan lortutako emaitzek melanomaren garapenean eta progresioan inplikaturako mekanismo molekular eta zelularrak hobeto ulertzen lagunduko zuela espero zen.

Horrela, doktorego tesi honen helburu nagusiak hurrengo helburu espezifikoetan zehaztu diren ziren:

- Melanozito osasuntsuen, nevusetatik eratorritako melanozitoen, melanoma primarioen eta melanoma metastatikoaren lerro zelularren lipidoma aztertu, hainbat lerro zelularretatik erauzitako lipido erauzkinean analisi lipidomikoa eginez.
- Biomarkatzaile lipidomikoak detektatzeko erabili daitezkeen translazio-potentziala duen tresna bioteknologiko eraginkor berri bat ezarri.
- Melanoma diagnostikatzeko eta pronostikoa definitzeko balioa duten espezie lipidiko zehatzak identifikatu.
- PLD2 entzimak melanomaren jarduera kartzinogenikoetan duen inplikazio funtzionalak zehaztu *in vitro*.

**EZTABAIDA**



### 1. Giza melanozito eta melanoma lerro zelular ezberdinen profil lipidiko globala

Larruazaleko melanomaren intzidentzia-tasa etengabe igo da azken hamarkadetan. Izan ere, Europan gehien diagnostikatutako zazpigarren minbizi mota da, eta larruazaleko minbiziek eragindako heriotzen %80ren erantzulea da<sup>1</sup>. Hala ere, heriotza-tasak ez du intzidentziaren joera bera jarraitu, eta egonkor mantendu da azken 20 urteetan. Egonkortze hori kontzientzian, diagnostiko goiztiarrean eta tratamenduetan izandako hobekuntzengatik gertatu da<sup>4</sup>. Aipatu beharra dago 2011z geroztik FDA-k 10 tratamendu-aukera desberdin onartu dituela, urtebeteko biziraupena orokorra %16-30etik %50-70rera handituz. Pazientearen etorkizunak zerikusi zuzena du diagnostikoa ematen denn etaparekin. Bada, errekupeazio-tasa %100 ingurukoa izaten da diagnostiko goiztiarra egiten denean, aldiz, ez dago terapia eraginkorrik melanoma metastatikoak tratatzeko<sup>29</sup>. Diagnostikoa behaketa klinikoan eta geroagoko baieztapen histopatologikoan oinarrituta egiten da. Hala ere, ez dago biomarkatzaile erabat eraginkorrik larruazaleko melanomarentzat. Beraz, diagnostiko eta pronostiko goiztiarrean lagun dezaketen edo itu terapeutikoak izan daitezkeen biomarkatzaile berriak aurkitzea premiazkoa suertatzen da.

Azkenaldian, zelulen eduki lipidikoaren, hau da lipidoma, eta lipido horien metabolismoaren azterketak minbiziarekin duen lotura etorkizun handiko ikerketa eremu bihurtu da. Izan ere, zelula-energiaren kudeaketaren desregulazioa eta egokitzapen metabolikoa minbizi zelulek bereganatutako ezaugarriak dira<sup>42</sup>. Lan askok erakusten dute tumore zelulek beren lipido edukia eta horien metabolismoa egokitzen dituztela zelulen fenotipo gaiztoa bermatzeko. Aldaketa horiek tumorearen mikroingurumenak ezarritako egoera latzetan bizirautea, ugaritzea eta haztea ahalbidetzen dute. Tumore-zeluletan gertatzen den lipido-metabolismoaren egokitzapena, bereziki, lipidoen *de novo* biosintesi eta oxidazio areagotu batek definitzen du. Alterazio horiek seinalezapen-bide aberranteak, energia ekoizpen etenduna, zelula-mintzetan egitura-alterazioak, eta gene eta proteinen bestelako adierazpena sortzen dituzte. Horren ondorioz, zelula-hazkuntza, ugalketa, heriotza desarautua eta farmakoekiko eta kimioterapiarekiko erresistentzia ematen da<sup>49</sup>, besteak beste. Gainera, minbizi zelulen lipido metabolismo aberranteak zelulen barreiadura metastatikoarekin lotura estua duela frogatu da<sup>114</sup>. Hori bularreko, koloneko, biriketako eta prostatatako minbizietan aztertu da bereziki<sup>49,96,159</sup>, baina ezer gutxi dakigu lipidoma eta metabolismo aldaketek melanoma zeluletan eragiten dituzten alterazioei buruz.

Horretarako, melanozitoen eta melanoma zelulen lipidomaren azterketa bereizgarri bat proposatu zen, melanoma eta melanozito zelulen aztarna lipidiko globala aztertzeko. Bestalde, zelula normal eta minbizidunek lipido eduki ezberdinak izatea azaltzen dituzten lipido espezie partikularrak identifikatu, eta aldaketa horien inplikazio biologikoa ere ikasi nahi zen. Horretarako, larruazaleko eta neuseko melanozitoen lipidoma aztertu zen, bai eta melanoma primarioaren eta metastatikoaren lerro zelularrena ere, hainbat metodologia lipidomiko erabiliz. Horiek tumore zelulak eta ehunak identifikatzeko eta sailkatzeko erabiltzen dira, lagin baten lipido edukia eta lipido horiek beste lipido batzuekin, proteinekin, metabolitoekin, eta eduki genetikorekin dituzten elkarrekintzak definitzen dituzte<sup>96</sup>.

Analisi lipidomikoak, nagusiki, masa espektrometria teknikan oinarritzen dira. ESI (elektrosprai bidezko ionizazioa) eta MALDI (laser bidezko desortzioa eta ionizazioa matrize bidez lagunduta) masa espektrometria bidez biomolekulak aztertzeko ionizazio-iturri garrantzitsuenak dira (chen). MALDI-MS biomarkatzaileak identifikatzeko erabiltzen da maiz, eta lipidoak zuzenean identifikatzeko aplikatzen da, ez baitira lipidoak aurretik erauzi behar. MALDI-MS-ak pisu molekular txikiko matrize organiko baten metaketa behar du, laser erradiazioa

xurgatzen duenak eta ioi molekularrak igortzen dituenak. MALDI ionizazioa erabiltzearen abantaila nagusiak hainbat dira, hala nola molekularak markatzeko beharrik ez izatea, sentsibilitate handia izatea, errendimendu altuko teknika erabiltzea eta espezifikotasun molekularra izatea<sup>105</sup>. Hala ere, MALDI ionizazio leuneko teknika bat denez, lipidoaren egitura orokorraren informazio lortzen da soilik, alboko kateak zeintzuk diren zehaztu gabe. Hori gainditzeko, ESI-MS/MS tandem metodologia erabil daiteke. Hori sarritan kromatografia likidoarekin konbinatzen da lipido erazkinetan dauden lipido familiak alde aurretik bereizteko molekulen identifikazio zehatzago bat lortuz. Gainera, tandem bidezko MS/MS estrategia bat erabiltzean, ioi aitzindaria eta horren zatiketaren ondorioz sortzen diren molekularak detektatzen dira, molekula aitzindariaren egitura eratuz. Izan ere, ESI lipidoetarako gehien erabiltzen den ionizazio-metodoa da<sup>105</sup>.

Lan honetan burutu den lehenengo estrategian larruazaleko melanozitoetatik, nevuseko melanozitoetatik, melanoma primarioetatik eta melanoma metastatikoetatik erazutitako ekstraktu lipidikoen edukian dauden ezberdintasunak identifikatu ziren. Horretarako, lipidoen azterketarako oso erabilia den UHPLC-ESI-MS/MS estrategia erabili zen. Lortutako emaitzak analisi estatistiko ez-gainbegiratuaren (PCA) eta gainbegiratuaren (PLS-DA) bidez aztertu ziren. Larruazaleko eta nevuseko melanozitoen, eta bestaldetik, melanoma primario eta metastatikoaren edukia alderatzean, ez ziren ezberdintasun nabarmenak identifikatu ikuspegi analitiko horiek erabilia. Ostera, zelula osasuntsuek (larruazaleko eta nevuseko melanozitoek) eta gaiztoek (melanoma primario eta metastatikoek) lipido profil ezberdina dutela ziurtatu zen. Beraz, erabilitako ikuspegi lipidomikoa egokia da minbizi zelulek erakusten duten lipidoma aberrantea aztertzeke.

Emaitzen ikuspegi sakonago batek agerian utzi zuen lipido-familia bakoitzean lortutako intentsitateak azterketa-taldean arabera aldatzen direla, lipidoen edukia aldatzeko eraldaketa gaiztoari eta minbizi-zelulen biziraupenari lagunduz. Gure emaitzen deskribapen orokor batek, kolonadun lipidoek melanoma metastatiko zeluletan azaleko melanozitoetan baino intentsitate altuagoa erakusten dutela plazaratzen du. Ezaugarri hori hainbat tumoreetan ikusi da, hala nola, bularreko, garuneko, biriketako, obario eta prostatako minbizietan<sup>153,154</sup>. Kolina glizerolipidoek egitura-funtzioa betetzen dute bereziki, mintzaren lipidoen %50 baitira. Honetaz gain, seinaleztapen molekularak ere badira, seinale mitogenikoetan bihurtzen baitira. Familia horretan antzemandako intentsitate altuak minbizi zelulek jasaten dituzten metabolismo aldatetekin lotu izan dira. Lehenik, kolonaren xurgapena handitzea minbizi ezberdinen ezaugarri komuna da, eta, horretarako, kolina-garraiatzaileak behar dira, melanoma zeluletan oso gainadieraziak aurkitu direnak<sup>127</sup>. Biosintesiari dagokionez, Kennedy bidezko lehen entzima, kolina kinasa, modu aberrantean detektatu da biriketako, koloneko, bularreko, prostatako, umetoki-lepoko eta obarioko tumore zeluletan. Kolonaren sintesian ematen diren aldatetak, Ras eta PI3K seinaleztapen bidean ikusi diren alterazioen ondorioz sortzen direla proposatu da<sup>55</sup>. Bide horiek melanomaren bide nagusiak dira eta modu konstitutiboan aktibatzen dira. Modu nabarmenean, kolina-lipidoen intentsitateak kimioterapiaren eraginkortasuna kontrolatzeko erabiltzen dira, seinale gutxituak erantzun terapeutiko on bati lotzen baitira<sup>123</sup>. Aitzitik, gure azterlanean hautemandako mintzetan kokatzen diren bigarren glizerofosfolipo familia ugariak fosfatidiletanolamina duten espezie lipidikoak izan dira. Horien intentsitatea murriztuta identifikatu da melanoma zeluletan eta nevuseko melanozitoetan, larruazaleko melanozitoekin alderatuta. Hala ere, aldakuntza handia detektatu da azterketa talde bereko zelula lerroen mailetan. Izan ere, bibliografian eztabaida handia dago minbizi zeluletan fosfatidiletanolamina lipidoek dituzten adierazpen mailekin, eta emaitzak minbizi motaren arabera dira. Adibidez, gure emaitzen antzera, PE mailak gutxituta agertu



---

ziren giltzurrun kartzinoman, eta, zelula gaizto horiek etanolaminarekin inkubatzean, zelulen hazkuntza murriztu egin zen, zelula normaletan inolako eraginik detektatu ez zen bitartean<sup>155</sup>.

Mintzen homeostasia, bere konposizio lipidikoaren arabera da, eta bere eduki lipidikoan aldaketa txikiek ere mintzaren integritatea aldatzen dute. Fosfolipidoek mintz lipido gehienak hartzen dituzte, eta horien buru-polarrak zein azilo albo-kateek mintzen propietate biofisikoak zehazten dituzte. PC-ak, bigeruzetan gehien agertzen diren lipidoak, forma molekular zilindriko bat dute, euren buru taldearen tamaina dela eta. Horri esker, estuki lotzen dira, mintz egonkor bat osatuz. Gainera, PC-ek normalean cis-asegabea den gantz azido kate bat izaten dute, eta horrek fosfolipidoen paketatzea murrizten du eta mintzaren jariakortasuna handituz. Aldiz, PE-k forma konikoa dute, beren buru-polarreko taldearen tamaina txikia dela eta, eta horrek tentsio negatiboko kurbadura bat ezartzen du mintzean. Horrek lipidoen paketatze-akatsak sortzen ditu eta mintzaren fusioa, fisioa eta gemazioa errazten du<sup>156,157</sup>. Beraz, lipido zilindriko/konikoen proportzioa kritikoa da bigeruzen osotasun eta funtzio egokiari eusteko; izan ere, PCak kanpoko xafla daude nagusiki, eta PE gehienak, berriz, xafla zitoplasmatikoan<sup>156,158</sup>. Gure lanean lortutako PC/PE proportzioek erakusten dute, ratio hori areagotu egiten dela melanomaren garapenarekin; izan ere, azaleko melanozitoetan 1ekoa da, eta 1,5era igotzen da melanoma primarioan eta 1,7ra melanoma metastatikoan. Horrek esan nahi du melanoma zelulen mintzen jariora eta iragazkortasuna handituta dagoela<sup>159,160</sup>. Ezaugarri hori tumore solido askotan ikusten da, fenotipo ugalkor eta inbaditzailea sustatzen baitu. Izan ere, tumore zelulen potentzial metastatikoa nabarmen korrelatzen da mintzaren jariakortasun areagotuarekin<sup>161</sup>. Gainera, tratamendu kimioterapeutiko eraginkorrak mintzaren jariakortasuna murriztearekin eta mintzaren iragazkortasuna handitzearekin lotu dira; aldiz, zelula erresistenteek mintz zurruna, eta, beraz, iragazkortasun txikiagoko mintza erakusten dute, farmakoaren sarrera eragotziz<sup>162</sup>. Minbizi mota askotan ikusitako kolina lipidoen xurgapen eta *de novo* sintesi areagotua ez lirateke nahikoak izango hazkuntza tasa oso altua duten minbizi zelulek behar duten PC guztia hornitzeko. Horretarako, baliteke melanoma zelulek PEMT-ren adierazpena eta jarduera areagotzea, euren kolina beharrak asetzeko. PEMT mintzeko entzima bat da, PE-ak zuzenean PC bihurtzen dituen ondoz ondoko hiru metilazioren ondoren. Beste tumore mota batzuei dagokienez, datuak ez dira sendoak; gibealeko eta bularreko minbizian haien jarduera nabarmen jaisten bada ere, gerora etanolamina-lipidoen presentzia areagotuz<sup>127</sup>, kontrako emaitzak ikusi dira biriketako minbizi zeluletan, gure emaitzekin bat eginez<sup>153</sup>. Oro har, tumore erasokorrak PC/PE erlazioa handitzearekin eta PEMT jarduera handiagorekin lotu dira<sup>153</sup>. Gure emaitzek entzima horrek melanomaren garapenean jarduera handiagoa izan dezakeela iradokitzen dute; izan ere, azilo-kate berberak partekatzen dituzten PC/PE lipido espezie zehatzen arteko proportzioa handitu egiten da melanoma metastatikoan kasu guztietan bat izan ezik: PC(16:0/20:4) - PE(18:1/18:3) edo PE(16:0/20:4).

Taula 4. Azilo albo-kate berdinak dituzten PC eta PE espezieen intentsitatearen PC/PE proportzioa, kontroleko taldeak lortutako emaitzekin erlazionatuta (larruzaleko melanozitoak = 1).

	PC/PE proportzioa larruzaleko melanozitoekin erlazionatuta			
	Larruzaleko melanozitoak	Nevuseko melanozitoak	Melanoma primarioa	Melanoma metastatikoak
PC(16:0/16:1)/ PC(14:0/18:1)	1,00	1,09	1,61	2,26
PE(16:0/16:1)				
PC(16:0/18:2)	1,00	2,39	0,73	1,32
PE(34:2)				
PC(16:0/18:1)	1,00	1,32	1,43	1,65
PE(34:1)				
PC(18:0/18:1)	1,00	2,46	1,26	2,10
PE(18:0/18:1)				
PC(38:3)	1,00	2,12	1,62	2,25
PE(18:1/20:2)/ PE(18:0/20:3)				
PC(18:0/20:2)	1,00	1,28	3,26	4,33
PE(18:1/20:1)/ PE(18:0/20:2)				
PC(40:5)	1,00	1,97	1,05	1,23
PE(18:1/22:4)/ PE(20:2/20:3)				
PC(40:4)	1,00	2,42	2,07	1,76
PE(18:0/22:4)				
PC(16:0/20:4)	1,00	1,50	0,88	0,87
PE(18:1/18:3)/ PE(16:0/20:4)				

Kolina eta etanolamina eter lipidoak mintzetan dauden fosfolipido guztien %15-20 inguru dira, eta egitura-eginkizun garrantzitsua betetzen dute hemen. Gure emaitzen ikuspegi orokor batek melanoma lerro zelularretan kolina eter lipidoen intentsitatea nabarmen handitzen dela erakusten du. Aitzitik, etanolamina eter lipidoak lerro zelular gaiztoetan murrizten dira, eta hori, alde batetik, bularreko minbizi zelula migratzaileak eta epitelio zelulak<sup>163</sup>, eta bestetik, kolon adenokartzinoma zelulak eta ehun normaleko zelulak<sup>164</sup> konparatzen zituzten beste lan batzuetan lortutako emaitzekin korrelazionatzen du. Izan ere, eter lipidoen presentzia handitua fenotipo ugaltzailearekin eta minbizi-zelulen potentzial tumorigenikoarekin erlazionatu da<sup>125</sup>. Eter lipidoen biosintesiaren lehen urratsak peroxisometan egiten dira, AGPS (alkilglizerona fosfato sintasa) bidearen lehen urratsaren arduraduna delarik. Entzima hori melanoma metastatikoan, bularreko eta prostatako minbizietan gainadierazten da. Bere inaktibazioa ostera, eter lipidoen sintesia murriztu, eta melanoma eta bularreko minbizi zelulen mugigarritasuna eta inbasio ahalmena gutxitzen ditu<sup>72</sup>. Gure lanean eter lipidoetan lortutako emaitzek kolina eta etanolamina glizerofosfolipidoen joera bera jarraitzen dute, eta horrek melanoma zeluletan kolina molekula gehiago dagoela eta etanolamina talde nagusiaren presentzia eskasa dagoela iradokitzen du. Minbizi zeluletan hautemandako ezaugarri komun bat PC/kolina eter lipidoen proportzioaren murrizketa da, gure emaitzetan ere agertzen dena; izan ere, melanoma primario eta metastatikoek PC/kolina erlazioan jaitsiera nabarmena erakusten dute (0,3), azaleko melanozitoekin alderatuta (1). Nevus melanozitoek aitzitik, PC/kolina eter

lipidoen proportzioan igoera nabarmena erakusten dute (2,9), larruazaleko melanozitoekin alderatuta (1). Emaitza horien arabera, baliteke peroxisomak nevus eta melanomaren garapenean eta progresioan parte hartzea. Aldiz, etanolamina lipidoetarako ez zen desberdintasun nabarmenik ikusi, ez melanoman, ezta nevus zeluletan ere.

Presentzia erlatibo txikiagoa izan arren, glizerofosfolipido anionikoak, fosfatidilserina, fosfatidilinositola eta fosfatidilglizerola barne, batez ere bigeruzen aurpegi zitoplasmatikoan agertzen dira, eta egitura-funtzio garrantzitsua dute<sup>158</sup>. Izan ere, mintzen gainazaleko karga zehazten laguntzen dute eta, ondorioz, positiboki kargatuta dauden mintzeko proteinek edo proteina periferikoekin elkarrekintzak modulatzeko dituzte<sup>156</sup>. Fosfatidilserinek konkretuki, zelula tumoraletan oso garrantzitsuak diren seinaleztapen-molekulekin elkarrengaitan dute. Adibidez, PS Ras eta Rho familiako GTP-asekin lotzen da, baita Src kinasa tirosinarekin ere, bere mintzerako mobilizazioa modulatzeko eta ondoren aktibatuz<sup>57</sup>. Gainera, PS Akt-ra lotzen da, eta horrek Akt-ren seinaleztapen bidea aktibatzen du, zelulen biziraupena areagotuz<sup>165</sup>. PS-ren biosintesia ugaztun zeluletan, buru polarrak trukatzeko erreakzio baten bidez gauzatzen da, jada existitzen den PC edo PE baten talde nagusia L-serinarekin ordezkatzeko baita. Erreakzio hori PSS1-ek katalizatzen du (fosfatidilserina sintasa 1), baldin eta trukea PC-tik egiten bada, eta PSS2-k etanolaminaren ordezkapenerako jarduten du<sup>57</sup>. Gure emaitzek PSS1 melanoma primario eta metastatiko zeluletan inhibituta egon daitekeela iradokitzen dute; izan ere, badirudi azilo-kate berberak dituzten PC-PS molekulen bihurketa gutxitu egiten dela zelula gaiztoetan (5. taula). Hala ere, ez da aldaketa esanguratsurik ikusi PE-PS bihurketan; hortaz, ez da aldaketarik espero PSS2-ren jardueran. Bestalde, PS-ren funtzio garrantzitsu bat zelula barruan PE sintetizatzea da, PS deskarboxilasa entzima mitokondrialaren bidez (PSD), zebra-arraina melanoma eredian gainadierazia agertzen dena<sup>132</sup>. Izan ere, gure emaitzetan ikusi dezakegu azilo albo-kate berdinak dituzten PE eta PS molekulen kasuan, horien arteko erlazioa handiagoa dena 3 kasuetatik baten. Beste bi kasuetan ostera, igoera txikia da (6. taula). Laburbilduz, gure emaitzek zelula gaiztoetan ematen den PC metaketa azaltzen laguntzen dute, PSS1 bidez ematen den PC-PS bihurketa negatiboki araututa dagoela baitirudi. Gainera, gure zelula tumoraletan PE maila baxuak daudenez, PSS2 bidez PE-PS bihurketa inhibititu egin liteke, eta PE ekoizteko PS-ren deskarboxilazioa melanoman apurtxo bat handituta dago, baina molekula gutxi daude, eta, beraz, ikerketa gehiago behar da ondorio esanguratsu batera iristeko.

Taula 5. Azilo albo-kate berdinak dituzten PC eta PS espezieen intentsitatearen PC/PS proportzioa, kontrolako taldeak lortutako emaitzekin erlazionatuta (larruazaleko melanozitoak = 1).

	PC/PS proportzioa larruazaleko melanozitoekin erlazionatuta			
	Larruazaleko melanozitoak	Nevuseko melanozitoak	Melanoma primarioa	Melanoma metastatikoia
PC(16:0/18:1) PS(16:0/18:1)	1,00	0,98	1,50	1,63
PC(18:1/18:1)/PC(18:0/18:2) PS(18:2/18:0)/PS(18:0/18:2)/PS(18:1/18:1)	1,00	1,54	1,82	2,57
PC(18:0/18:1) PS(18:1/18:0)/PS(18:0/18:1)/PS(16:0/20:1)	1,00	2,04	2,21	3,98
PC(18:0/20:2) PS(18:0/20:2)/PS(18:1/20:1)	1,00	1,04	3,89	4,63
PC(40:2) PS(18:1/22:1)/PS(18:0/22:2)	1,00	0,90	1,61	2,23

Taula 6. Azilo albo-kate berdinak dituzten PE eta PS espezieen intentsitatearen PE/PS proportzioa, kontroleko taldeak lortutako emaitzekin erlazionatuta (larruazaleko melanozitoak = 1).

	PE/PS proportzioa larruazaleko melanozitoekin erlazionatuta			
	Larruazaleko melanozitoak	Nevuseko melanozitoak	Melanoma primarioak	Melanoma metastatikoak
PE(34:1)	1,00	0,74	1,05	0,99
PS(16:0/18:1)				
PE(18:0/18:1)	1,00	0,83	1,76	1,89
PS(18:1/18:0)/PS(18:0/18:1)/PS(16:0/20:1)				
PE(18:1/20:1)/PE(18:0/20:2)	1,00	0,81	1,19	1,07
PS(18:0/20:2)/PS(18:1/20:1)				

Gure azterketan, fosfatidilinositolak, zelula-mintzetan kokatzen den glizerofosfolipido anionikoen beste azpimota bat, melanoma metastatikoetan euren intentsitatea areagotzen dutela ikusi da. Ezaugarri hori bera beste autore batzuk ere antzeman zuten melanoma metastatikoan<sup>166</sup>. PI zikloan, PI3K-k zuzendutako PI-ren fosforilazio itzulgarria dago. Entzima hori minbizi mota askotan mutatuta aurkitu da, melanoman barne. Entzima horren produktua, PIP<sub>3</sub>, bigarren mezulari pro-tumoral indartsu bat da, ahalmen metastatikoarekin estuki lotu dena, eta ugalketa, hazkuntza eta zelulen migrazioa modulatzeko baititu<sup>166</sup>. Hala ere, gure lanean erabili dien analisi lipidomikoekin ezin dira PI fosforilatuak ikasi, eta, beraz, soilik PI mailak gora egin duela baieztatu dezakegu.

Mintzetan aurkitzen den lipido anionikoen azken azpimota fosfatidilglizerolak dira, nahiz eta kopuru oso baxuetan dauden (glizerofosfolipido guztien %1-2)<sup>65</sup>. Gure emaitzek larruazaleko melanozito (1,00) eta melanoma metastatiko (1,02) zelula lerroetan PG mailak ez direla aldatzen erakusten dute. Hala ere, nevuseko melanozitoen (0,65) eta melanoma primarioen (0,54) mailak murriztuak aurkitu dira. PG-ak kardiolipina molekulen aitzindariak dira, mitokondrio-funtzio egokia mantentzeko garrantzitsuak direnak. Hala ere, ez dugu kardiolipinarik detektatu gure lanean, horien masa molekularra 1500 unitate baino gehiagokoa baita, eta erabilitako masa-espektrometria estrategiarekin, 50 eta 1200 unitate arteko masadun espezie molekular lipidikoak bakarrik detektatu ditugulako.

Zelula-mintzetan glizerofosfolipidoekin batera dagoen beste lipido mota garrantzitsu bat, esfingolipidoak dira. GPL-ek ez bezala, esfingolipidoek, nagusiki, albo-kateetan gantz-azido aseak edo trans-asegabeak dituzte, zilindro-formako egitura altuago eta estuago bat osatuz. Horrela mintzaren paketatze-dentsitatea handiagoa da eta bigeruzaren barruko mugikortasuna aldiz, txikiagoa. Zeramiden egitura zurrinak ere bigeruzaren arintasuna gutxitzen parte hartzen du<sup>156,157</sup>. Esfingomielina, ugaztun-mintzetan ugariena den esfingolipidoen azpiklasea da<sup>158</sup>, eta kolina molekula bat du bere egituran. Gure emaitzetan, esfingomielinen eta zeramiden intentsitatean murrizketa nabarmena aurkitu dugu zelula gaiztoetan. Beraz, horrek tumore zelulen bigeruzaren jariakortasuna handitzen laguntzen duela iradokitzen dugu, eta hori bat dator kolina-lipidoen gorakadarekin eta kolina/etanolamina lipidoen erlazioan lortutako emaitzekin. Izan ere, ezaugarri horrek zelula gaiztoen mugikortasuna eta ahalmen metastatikoak sustatzen ditu, deformazio ahalmen handiagoa baitute<sup>145,161,167</sup>. Edmond et al-ek epitelio-mesenkima trantsizioek mintzaren jariakortasuna handitzeko esfingolipidoen mailak aldatzen dituztela eta, horrela, zelulen migrazioa errazten dutela proposatu zuten<sup>168</sup>.

Esfingomielina espezieen maila baxuak partzialki azal daitezke, SM-en sintesi murriztua dela eta. Izan ere, esfingomielina sintasa 1 (SMS1) hainbat minbizi ehunetan modu negatiboan

erregulatuta aurkitu da<sup>166,169</sup>. Zehazki, melanoman, melanoma primarioan zein metastatikoan larruzaleko melanozitoekin eta nevusekin alderatuta SMS1 mailak jaisten direla frogatu da. Gainera, ezaugarri bereizgarri hori melanoma metastatikoaren duten pazienteek emaitza okerragoa izatearekin eta melanomaren zelulen migrazio ahalmen handiagoarekin lotu da. Horrek, SM-en maila baxuek melanomaren progresioan parte hartzen dutela iradokitzen du<sup>166,169</sup>. Sintesia murriztuta egoteaz gain, SM-en metabolismoaren gorakadak ere lagun lezake zelula gaiztoetan aurkitu ditugun SM maila baxuetan. SM-en katabolismoaren ondoren, zeramida bat sortzen da. Azilo-kate berdinak dituzten esfingomielina/zeramida espezieen proportzioak behera egiten du melanoman, hau da, zeramiden intentsitateak gora egiten du dagokion esfingomielinarekin alderatuta. Horrek, bihurketa hori gure melanoma lerro zelularretan handituta dagoela iradokitzen du (7. taula). Aldiz, beste egile batzuk zeramidak sortzen dituzten entzimak, hau da esfingomielinasak, melanoman gutxituta daudela zehaztu dute<sup>170-172</sup>. Horren ondorioz SM-Cer bihurketak behera egingo luke. Beste egile batzuek osteria, giltzurrun kartzinoman bihurketa hori handituta dagoela ikusi zuten, guk lortutako emaitzekin bat etorriz<sup>155</sup>. Gainera, esfingomielinasaren jardueraren ondorioz, fosfokolina bat ere askatzen da, kolina-lipidoen sintesia areagotzeko erabil daitekeena eta, beraz, gure aurreko emaitzekin bat datorrena.

Taula 7. Azilo albo-kate berdina duten SM eta Cer espezieen intentsitatearen SM/Cer proportzioa, kontrolako taldeak lortutako emaitzekin erlazionatuta (larruzaleko melanozitoak = 1).

	SM/Cer proportzioa larruzaleko melanozitoekin erlazionatuta			
	Larruzaleko melanozitoak	Nevuseko melanozitoak	Melanoma primarioak	Melanoma metastatikoak
SM(d18:1/16:0)	1,00	1,44	0,46	0,53
Cer(d18:1/16:0)				
SM(d18:1/18:0)	1,00	0,79	0,48	0,36
Cer(d18:1/18:0)				
SM(d16:1/24:1)/SM(d18:1/22:1)/SM(d18:2/22:0)	1,00	0,93	0,39	0,44
Cer(d18:2/22:0)				
SM(d18:1/22:0)	1,00	1,12	0,35	0,39
Cer(d18:1/22:0)/Cer(d16:1/24:0)				
SM(d18:1/24:1)	1,00	0,95	0,36	0,36
Cer(d18:1/24:1)				
SM(d18:1/24:0)	1,00	1,67	0,51	0,55
Cer(d18:1/24:0)				

Fosfokolinarekin batera, zeramida ere sortzen da esfingomielinaren metabolismoaren ondoren. Zeramidak lipido bioaktibo oso garrantzitsuak dira, eta, gure lanean, melanoma zelulek zeramida maila oso txikiak erakutsi dituzte. Uchidaren taldeak deskribatu zuenez, melanozitoen zelula-kultiboan zeramida exogenoa gehitzeak melanozitoen hazkuntza oztokatzen du Akt-ren inaktibazioaren ondorioz<sup>173</sup>. Zeramidak molekula ez-tumorigenikotzat hartzen dira, zeramida-maila altuak hazkuntza gelditzearekin, seneszentziarekin, apoptosiarekin eta autofagiarekin erlazionatu baitira<sup>174,175</sup>. Gainera, zeramidek tumore-zelulen potentzial metastatikoaren gutxitzen dute, integrinen azaleko adierazpena erregulatzen baitute<sup>175</sup>. Izan ere, tratamendu kimioterapeutiko batzuk, daunorrubizina, kanptotezina eta etoposidoa barne, zeramida mailak igotzen dituzte zelulen barruan, apoptosia eraginez<sup>84,176</sup>. Hala ere, tumore-zelulek zeramiden metabolismoaren areagotzen dute funtzio pro-tumoralak dituzten beste esfingolipido batzuk sortuz. Adibidez, jakina da zeramidasa azidoa (ACDase) melanoman eta beste tumore zelula

batzuetan gainadierazten dela, eta zeramidak esfingosina-1-fosfato bihurtzea errazten duela. Molekula horrek melanoma zeluletan melanozito normaletan baino maila altuagoak erakusten ditu, eta tumore zelulen hazkuntza eta migrazioa sustatzen ditu<sup>174,175</sup>. Gainera, dakarbazinarekin *in vitro* egindako azterketek, terapiari erantzuten dioten lerro zelularretan, ACDase mailen dosi-eta denboraren-menpeko beherakada ematen dela erakutsi da; izan ere, lisosometan ACDase degradatu egin da eta zelula barneko 16-18 karbonodun zeramiden mailak areagotu egin dira<sup>174,175,177</sup>. Bitxia bada ere, ACDase-n inhibizio farmakologikoak zeramida mailak handitzen ditu, eta horrek eragile kimioterapeutikoen eta erradioterapiaren efektu zitotoxikoak sinergikoki hobetzen ditu melanoma kultiboetan. Gainera, ACDase-n espresio altua izateak melanomaren tratamenduarekiko erresistentziarekin erlazionatu da<sup>84,174,176</sup>. Gure emaitzei dagokienez, melanoma primarioek melanoma metastatikoek baino zeramida maila baxuagoak erakutsi dituzte, eta hori bat dator Realini *et al.* eta Leclerc *et al.*-en aurkikuntzekin. Lan horietan, hazkuntza-fasean dauden melanomek zelula inbaditzaileek baino ACDase maila eta aktibitate altuagoak erakusten dituztela frogatu zuten<sup>174,178</sup>.

Melanoma zeluletan aurkitutako zeramida maila baxuak, bere katabolismoa handituta egon ez ezik, zeramida sintasa entzimen (CerS) bidez ematen den *de novo* sintesiaren gutxitzearen ondorio ere izan daiteke. Entzima horien sei isoforma ezberdin identifikatu dira, eta horietako bakoitzak funtzio ezberdinak betetzen dituzte ehunetan, kate luzera ezberdina duten zeramidak ekoizten baitituzte. Adibidez, CerS1-ek 18-karbonodun zeramidak sortzen ditu, apoptosiaren aldeko funtzioak dituztenak. Horren mailak gutxituta ikusi dira buru eta lepoko minbizi zeluletan, zeramida horien mailak murriztuz<sup>84,179</sup>. CerS6-k ostera, 16-karbonodun zeramidak ekoizten ditu, eta melanoman eta beste minbizi-ehun batzuetan negatiboki erregulatuta aurkitu da<sup>84,175,179</sup>. Izan ere, melanoma zeluletan CerS6 isilarazteak zelula horien hazkuntza eta inbasio-ahalmen handiagoa sortzen du, beste aldaketa batzuen artean<sup>180</sup>. Gure emaitzek melanoma zeluletan bai CerS1 bai CerS6 ere modu negatiboan araututa egon litezkeela iradokitzen dute, kate laburreko (16- eta 18-karbonodun) zeramida mailak txikiagoak baitira zelula gaiztoetan, azaleko melanozitoekin alderatuta. Hala ere, kate luzeko zeramidek (24-K) nevus eta melanoma garapenean beren mailak igotzen dituzte. Kate luzeko zeramidak CerS2-k sintetizatzen ditu, gure emaitza lipidomikoen arabera melanoma eta nevuseko zeluletan gainadierazita ager daitekeena. Izan ere, 24-K zeramidak zelulen biziraupenarekin erlazionatu dira<sup>175,181</sup>.

Egitura-funtzioa ez duten lipidoei dagokienez, hala nola, gantz-azido askeak, diglizeridoak eta triglizeridoak, gure analisietan intentsitate baxua erakusten dute zelula gaiztoetan, bereziki triglizerido edukiarri dagokionez melanoma metastatikoetan. Haatik, tumore ehunetan lipido klase horien maila altuak deskribatu dira batik bat, eta, beraz, ikerketa gehiago behar da hiru lipido familia horiek melanoman duten presentzia zehazteko.

## 2. Melanomarako biomarkatzaile lipidiko berrien aurkikuntza

UHPLC-MS/MS-n lortutako emaitza lipidomiko orokorrek lipido edukia melanozitoen eta melanoma zelulen artean aldatzen dela baieztatu zuten. Bestalde, lipido espezie bakoitzak azterketa talde bakoitzean izandako intentsitateen azterketak OPLS-DA analisi gainbegiratu erabiliz, argi utzi zuen 45 lipidoz osatutako panel bat dagoela melanozito eta melanoma zelulak bereiz ditzakeena. Emaitza horiek gure hipotesia baieztatu zuten: lipido espezie zehatzen presentzia larruazaleko melanozito arruntan eta melanomaren etapa desberdinen artean aldatzen da. Beraz, gure ikerketa melanoma-biomarkatzaileen aurkikuntzara bideratu genuen, translazio-potentziala duen tresna bat erabiliz: zelula-mintz funtzionalez osatutako mikroarraiak. Horietan, aztertutako lerro zelularretatik erauzitako mintzak immobilizatu ziren, eta MALDI-MS ikuspegi lipidomikoa aplikatu zen. Tresna hori onuragarria da hainbat arrazoiengatik: lagin bakoitzaren kantitate txiki bat nahikoa da, lipidoak erauzteko metodo konplexurik ez da behar, MALDI-MS biomarkatzaileak identifikatzeko metodo estandarra da, eta UHPLC-ESI-MS/MS-n antzemandako aldaketa garrantzitsu gehienak mintzean kokatzen diren lipido familietan ikusi ziren. Aldiz, MALDI-MS-aren eragozpen nagusietako bat ionizazio leuneko teknika lipidomiko bat dela da, eta, beraz, batzuetan ezin da molekularen azilo albo-kateen deskribapen osoa eman. Hori gainditzeko, bai MALDI-MS eta bai UHPLC-ESI-MS/MS bidez identifikatutako molekuletan, bigarrenarekin lortutako molekularen deskribapena erabiliz izendatu dira.

Lipido biomarkatzaileak aurkitzeko lehen estrategia t-test proba ( $p < 0.05$ ) bat egitea izan zen. Horretan, zelula ez-gaiztoetarako (larruazaleko + nevusetako melanozitoak) eta zelula gaiztoetarako (melanoma primario + metastatikoak) lortutako lipido espezie ezberdinen intentsitateak alderatuziren. 116 lipido espezie nabarmen aldatuta agertu ziren eta, beraz, biomarkatzaile lipidomikoak detektatzeko ikuspegi analitiko hori erabil genezakeela baieztatu genuen. Ondoren, konparazio anitzeko t-test proba bat eta post-hoc zuzenketak ( $p < 0.05$ ) erabili ziren detektatutako lipido espezieen intentsitatea lau azterketa-taldeen artean konparatzeko. Gure analisi estatistikoek lau azterketa-taldeen artean intentsitate mailak esanguratsuki aldatzen dituzten 122 lipido espezie daudela erakutsi zuten (8. taula).

Burututako PCA eta klusterizazio analisek nevuseko melanozitoen lipidoma, azaleko melanozitoen antzekoa dela, eta aldiz, melanoma zelulena baino ezberdinagoa dela erakutsi zuten. Hori dela eta, nevuseko melanozitoak zelula ez gaizto gisa sailkatu ditugu burututako hainbat analisi estatistikotan. Hala ere, nagusiki neoplasia onberak diren arren, tumoreak dira, eta, beraz, euren lipidoma azaleko melanozito arruntetatik ezberdina da. Izan ere, azalaren eta nevuseko melanozitoen artean bereiztu dezaketen 11 lipido espezie aurkitu ditugu (8. taula). Bitxia bada ere, markatzaile horietako 10 azaleko melanozitoen eta melanoma primario edo metastatikoaren zelulen arteko alderaketetan ere agertu dira. Horrek, molekula horien maila aldatuek nevusetik melanomarako trantsizioan lagundu dezaketela iradokitzen du. Bestalde, larruazaleko edo nevuseko melanozitoetan melanoma primarioetan lortutako emaitzak alderatzean, adierazpena nabarmenki aldatzen duten 48 eta 54 lipido espezie daudela ikusi zen. Gainera, nevus *versus* melanoma primarioko zelulen konparazioan esanguratsuak aurkitu ziren 54 lipido espezieetatik 33 ere esanguratsuak izan ziren larruazaleko melanozitoak eta melanoma primarioak konparatzean. Beraz, 21 lipido espezie daude, euren mailak soilik nevuseko melanozitoetatik melanoma primarioetarako trantsizioan aldatzen dituztenak, eta, beraz, nevusetik abiatuta melanomaren garapenean markatzaile bezala erabil daitezkenak.

Larruazaleko edo nevuseko melanozitoen eta melanoma metastatikoaren arteko lipido edukia aldea ere agerikoa da. Izan ere, larruazaleko edo nevuseko melanozitoen eta melanoma

metastatikoaren arteko biomarkatzaile potentzialak diren 82 eta 81 lipido espezie baitaude, hurrenez hurren (8. taula).

Melanomaren ikerketaren erronka nagusietako bat melanoma metastatikoarentzat progresio markatzaileak aurkitzea da, gaixoen biziraupen tasa izugarri jaisten baita tumorea goiz detektatzen ez bada. Era interesgarri batean, hiru lipido espezie daude, melanoma primariotik metastatikora euren adierazpena nabarmen handitzen dituztenak: 10 lipidoa, 11 lipidoa eta 22 lipidoa. Beraz, lipido espezie zehatz horien ikerketa sakonagoa egin behar da, melanoma primariotik metastatikorako progresioan duten zeregina ebaluatzeko.

Lipido erauzkintan lortutako emaitzen joera bera jarraituz, 17 esfingomielinek bere intentsitatea nabarmen murriztu zuten zelula gaiztoetan, eta horrek minbizi zeluletan SM molekulen galera baieztatzen du. Gainera, bi DG molekula eta HexCer molekula bat zeuden melanozitoetan maila handituak zituztenak melanomarekin alderatuz. Bestalde, 13 PI molekulek euren intentsitatea esanguratsuki igotzen dute melanoman, melanoma metastatikoan bereziki. Lehen aipatu bezala, PI molekulak funtzio pro-tumoralak dituzte eta oso erlazionatuta daude minbizi zelulen potentzial metastatikoarekin. Beste lipido azpimoten barruan, lipido espezie guztiek ez dute joera bera jarraitzen. Adibidez, peroxisometan eratzen diren eter lipidoetan aldakortasuna dago, eta minbizian aldatuta daudela frogatu da. Horien artean, 18 PC eter lipido daude, horietatik 16k melanoma zeluletan euren mailak handitzen dituzte, eta bik, berriz, euren intentsitatea murriztu. Bestetik, maila diskriminatzaileak dituzten sei PE eter lipidoetatik 3 molekulek euren mailak igotzen dituzte melanoman, eta aldiz, beste hirurek murriztu. Gainera, PC edo PE eter lipidoak diren baieztatu ezin dugun arren, zazpi PC edo PE eter lipido esanguratsu daude eta horietako sei melanoman maila handitua dituzte. Emaitza horiek eta UHPLC-ESI-MS/MS atalean lortutakoek peroxisomek melanomaren garapenean eta progresioan zeregin garrantzitsua betetzen dutela baieztatzen dute, eta, beraz, organulu horien azterketa zehatzagoa behar dela, horien ekarpena ulertzeko.

Lipido espezie ezberdinen mailetan ikusten den aldakortasunak molekula bakoitzak eginkizun bakarra duela erakusten du. Molekularen buru polarrak eta azilo albo-kateen konposizioa molekula bakoitzaren funtzioa zehazteko oso garrantzitsuak dira. Beraz, lan honetan atzemandako biomarkatzaile potentzial guztien papera banan-banan ikertzea interesgarria izango lirateke. Bestalde, melanoma zelulen eta melanozitoen lipidoma ezberdina dela baieztatu ondoren, analisi lipidomiko ezberdinak eta osagarriak egin behar dira funtsezko lipidoek melanoman duten garrantzia aztertzeko, hala nola, PI fosforilatuak, glukosfingolipidoak eta esterolak.



**Taula 8. Konparazio estatistikoetan euren mailak esanguratsuki aldatuta dituzten lipido espezieen zerrenda.** \*-ren koloreak espezie bakoitza zein azterketa-taldean den ugariago adierazten du. Zelula osasuntsuak (larruazal eta nevus melanozitoak): more; zelula gaiztoak (melanoma primario eta metastatikoak): marroi argia; larruazal melanozitoak: verde; nevus melanozitoak: hori; melanoma primarioak: gorri; melanoma metastatikoak: urdin. Esangarritasuna: \*<0.05; \*\*<0.01; \*\*\*<0.001; \*\*\*\*<0.0001.

Lipido azpimota	Lipido espezie	Osasuntsu vs Gaizto	M vs N	M vs MP	N vs MP	M vs MM	N vs MM	MP vs MM
SM	Lipido 1	***		**	***	**	***	
	Lipido 2				*			
	Lipido 3	***		*	**		*	
	Lipido 4	**	*	***	*	***		
	Lipido 5	**		*	***	*	***	
	Lipido 6	****		*	**	*		
	Lipido 7	***		****	****	***	****	
	Lipido 8	***			**		*	
	Lipido 9				*			
	Lipido 10	****						*
	Lipido 11	***						*
	Lipido 12	**			**		***	
	Lipido 13	***		*	****		****	
	Lipido 14			*	*		*	
	Lipido 15	****			***		**	
	Lipido 16	**			****		***	
	Lipido 17	***			****		****	
HexCer	Lipido 18					*		
DG	Lipido 19	****				**	**	
	Lipido 20	***			*	***	****	
TG	Lipido 21						*	
	Lipido 22							*
PC	Lipido 23	***				*		
	Lipido 24			*		*		
	Lipido 25	***		*	*	*	****	
	Lipido 26	***		****	***	***	***	
	Lipido 27	***				**	*	
	Lipido 28		**	***		****		
	Lipido 29	**					***	
	Lipido 30					**		
	Lipido 31	***		**	**	***	**	
	Lipido 32	**						
	Lipido 33	***			**		**	
	Lipido 34	**					*	
	Lipido 35	**						
	Lipido 36	*		**		**		
	Lipido 37	**			*		**	

	Lipido 38	***			****		****	
	Lipido 39	****				***	**	
	Lipido 40	***				*		
	Lipido 41					*	**	
	Lipido 42	***						
	Lipido 43						*	
	Lipido 44	***		**	**	***	****	
	Lipido 45	****			**		**	
	Lipido 46	****						
	Lipido 47	***		*		**	**	
	Lipido 48	***		*		**		
	Lipido 49						*	
	Lipido 50	****						
	Lipido 51	****		***		**		
	Lipido 52	****						
	Lipido 53		**	**		***		
	Lipido 54		**	**		**		
	Lipido 55		***	***		**		
PC eter	Lipido 56	****						
	Lipido 57		*			*		
	Lipido 58	****		*	*	*	*	
	Lipido 59	****		*	*	**	**	
	Lipido 60	***		**	***	**	****	
	Lipido 61	***				**	**	
	Lipido 62	**		*		***	***	
	Lipido 63	***					**	
	Lipido 64					*		
	Lipido 65	***						
	Lipido 66	***		**	**	***	***	
	Lipido 67	***			*	*	***	
	Lipido 68	***				*	*	
	Lipido 69	***						
Lipido 70	****		*		*			
Lipido 71	***		*		*			
Lipido 72	***	*			*			
Lipido 73					*	*		
Lipido 74	***				*	*		
Lipido 75	***				*	*		
Lipido 76	***				*	*		
PE	Lipido 77					*		
	Lipido 78	***		*		**		
	Lipido 79	***						
	Lipido 80	**		**	**	**	**	
	Lipido 81	***	*	*		****		

	Lipido 82			*		**		
	Lipido 83	***		*	*	**	**	
	Lipido 84	***			*			
	Lipido 85	***		**	*	*	*	
PE eter	Lipido 86	**	*			**	*	
	Lipido 87		*					
	Lipido 88	**			****	*	****	
	Lipido 89	**						
	Lipido 90	***					**	
	Lipido 91	***			**			
	Lipido 92				**			
PC/PE	Lipido 93	****						
	Lipido 94	****					*	
	Lipido 95					***		
	Lipido 96	***		**	*	**	*	
	Lipido 97					*		
	Lipido 98	****				**	*	
	Lipido 99	****				**	***	
	Lipido 100	**		*	*	***	***	
	Lipido 101	****						
	Lipido 102	****						
	Lipido 103	****				***	**	
PC/PE eter	Lipido 104	***					*	
	Lipido 105	***					**	
	Lipido 106	****						
	Lipido 107	***		**	**	**	***	
	Lipido 108	****						
	Lipido 109	****		*	*	*	*	
	Lipido 110	***				**	**	
	Lipido 111			**		**		
	Lipido 112	****						
	Lipido 113	***						
Lipido 114	****				***	**		
PS	Lipido 115					***		
	Lipido 116	***						
	Lipido 117	***		**	**	*	**	
	Lipido 118	****		**		****	*	
	Lipido 119	****				**	*	
PG	Lipido 120	**	*	**	*	***	**	
	Lipido 121	****			**			
	Lipido 122	***						
	Lipido 123	***			*		*	
	Lipido 124	****			*		*	
	Lipido 125					***		

	Lipido 126	***						
	Lipido 127	***				**	*	
PI	Lipido 128	***						
	Lipido 129	**						
	Lipido 130	***		*	*	**	**	
	Lipido 131	***		*	*	**	**	
	Lipido 132	****		*	*	*	*	
	Lipido 133	***		**	**	**	*	
	Lipido 134	***			*		****	
	Lipido 135	**			**		*	
	Lipido 136	****		*	*	****	***	
	Lipido 137	***				**	**	
	Lipido 138	****				*	**	
	Lipido 139	***		**	**	****	**	
	Lipido 140	***				****	****	
	Lipido 141	**				****	****	
Lipido 142	****			*	*	**		
Lipido 143	****							

### 3. D2 fosfolipasak melanomaren ezaugarri protumoral eta prometastatikoak sustatzen ditu

Fosfolipidoek zelula-mintzetan burutzen duten egiturazko paperaz gain, metabolizatu eta bigarren mezulari ere bihur daitezke. Fosfolipasak fosfolipidoen ester edo fosfodiester loturak hidrolizatzen dituzten entzimak dira. Entzima horiek egitura-funtzioan eragiten dute bigeruzen sintesian, organuluen degradazioan eta biogenesisian parte hartuz. Horrez gain, molekula bioaktiboek ekoizpenean ere parte hartzen dute<sup>182</sup>. PC, PE, PI, PG eta PS-en erreakzio katabolikoak A, C eta D fosfolipasak arautzen dituzte. Fosfolipasa bakoitzak, nagusiki, GPL mota bat hidrolizatzen du eta seinaleztapen-bide espezifikoak erregulatzen ditu, baina guztiek zelulen zorian parte hartzen dute, hainbat funtzio arautzen baitituzte, hala nola, hazkuntza, biziraupena, migrazioa, besikula-trafikoa, hantura, gaiztotzea eta metastasia. Izan ere, entzima horien adierazpena eta jarduera handitua aurkitu dira minbizi ugarritan. Beraz, ikertutako melanoma zelula lerroetan GPL azpimota ezberdinen maila aldatuak, fosfolipasak melanoman jarduera eta adierazpena aldatuta izan zezaketenaren hipotesia proposatu zen, GPL horiek fosfolipasen substratuak baitira. Western blot bidez PLA2, PLC, PLD1 eta PLD2 adierazpen-mailen azterketa egin zen gure zelula lerroetan. Emaitzetan PLD entzimek, bereziki PLD2 entzimak, larruazaleko melanozitoetatik melanoma metastatikorako trantsizioan mailak handitzen dituela frogatu zen. Gainera, melanoma zeluletan PLD2-ren gainadierazpena immunofluoreszentzia bidez berretsi zen. Gomez-Cambronero et al-ek minbizi ehunetan PLD entzimen adierazpena ez ezik, jarduera entzimatikoa ere handitzen dela adierazi zuen<sup>138</sup>. Ezaugarri hori gure melanoma zeluletan ere egiaztatu zen, lerro zelular primario eta metastatikoetan PLD jarduera nabarmen handitzen dela frogatu baikenuen.

PLD entzimek, zelula-mintzetan dauden PC molekula hidrolizatu eta seinale mitogeniko eta biziraupeneko seinale bihurtzen dituzte. Konkretuki, PLD-ak tumore zelulen migrazioa eta metastasi handiagoarekin lotu dira; izan ere, minbizi-zelulen progresioan, zitoeskeletoaren dinamikan, mintzaren birmoldaketan eta zelula-ugalketan parte hartzen baitute, besteak beste<sup>137</sup>. PLD bidez PC-a apurtu ondoren, kolina bat eta PA molekula bat askatzen dira. Lehen aipatu bezala, PC-ak nabarmenki gainadierazita aurkitu dira aztertutako melanoma zeluletan, eta PLD bidezko kolina askearen ekoizpena PC molekula gehiago sortzeko erabil liteke, prozesu tumoral hobeto sustatzen duten azilo-kate zehatzekin. Gainera, prozesuan sortutako PA molekula bigarren mezulari lipidikoak dira. Jakina da PA-k proteina ezberdinekin elkarrekintzan diharduela, seinale mitogenikoak sortzen dituzten Akt eta mTOR-rekin kasu<sup>133,183</sup>. Bestal, PA desfosforilatu ere egin daiteke DAG sortuz edo hidrolizatu daiteke Liso-PA sortuz; biak seinaleztapen-lipido indartsuak dira eta gaiztotze prozesua errazten dute<sup>184</sup>. Izan ere, PA maila altuak aurkitu genituen lehen deskribatutako ikuspegi lipidomikoetan. Hala ere, lipidoen azpimota hau ez zen analisi estatistikoan sartu, ezin izan baitzen bere jatorria baieztatu, lipido aitzindari baten zatiketaren ondoren detektatu ahal izan baitzen<sup>185</sup>.

PLD entzimek PIP<sub>2</sub> kofaktorea behar dute beren jarduerarako, eta PI molekulek melanoma zeluletan presentzia handiagoa dutela frogatu dugu, ziurrenik PI-fosforilatuen mailak handitzen lagunduz. Izan ere, Epanand et al-ek PI zirkulazioa PLD jardueraren bidez handitzen duela frogatu zuten<sup>61</sup>. Gure aurreko emaitzen eta PLD jardueraren handitzearen arteko beste lotura bat Diaz et al-ek baieztatu zuena da: esfingomielinasek nabarmen handitzen dute PLD-ren jardueraren<sup>186</sup>. Gure emaitzetan ikusitako SM/Cer erlazioa murrizketa melanoma zeluletan, SMase-ek melanoma zeluletan aktibitate handiagoa izan dezaketela iradokitzen du; beraz, ezaugarri horrek zelula gaiztoetan PLD jardueraren handiagoa izatea ere lagundu lezakeela proposatzen dugu. Gainera, esfingosina-1-fosfatoa (S1P) ere PLD aktibatzaile gisa proposatu da<sup>136</sup>. Gure UHPLC-ESI-MS/MS emaitzek melanoma zeluletan zeramida maila baxuak daudela adierazten dute, neurri batean zeramidak S1P bezalako molekula pro-tumorigenikoetan bihurtzearen ondorioz azal daitekeena.

PLD1 eta PLD2-ren adierazpena eta jardueraren altuak minbizi mota ezberdinetan deskribatu da, melanoma barne<sup>139</sup>. Egile batzuek PLD1-ek mikroinguru tumorelean eragin handiagoa duela iradokitzen dute; PLD2-k, berriz, tumore-zelulei eragiten diela batez ere melanoman, bularreko eta biriketako minbizian, besteak beste<sup>145</sup>. Beraz, Western blot, immunofluoreszentzia eta entzima-jardueraren lortutako emaitzetan oinarrituta, PLD2 entzima melanoma primario eta metastatiko zeluletan gainadierazi eta isilarazi genuen, entzima horrek oinarritzko tumore-prozesuetan (zelulen hazkuntza, migrazioa eta inbasioa) duen eragina aztertzeko. Gure emaitzek, PLD2 jardueraren eta adierazpenaren handitzeak hazkuntza, migrazioa eta inbasioa nabarmen areagotzen dituela erakusten dute, PLD2-ren isilpenak prozesu horiek murrizten dituen bitartean. Emaitza horiek bat datoz beste egile batzuen ekarpenekin. Linfoman<sup>146</sup> eta bularreko minbizi zeluletan<sup>139</sup>, PLD2-k zelulen fenotipo ugalkorra eta inbaditzailea sustatzen dituela frogatu da. Izan ere, PLD2-k prozesu metastatikoak sustatzen du FAK fosforilatu eta mTOR eta Akt aktibatuz<sup>146</sup>. Garrantzitsua da nabarmentzea PLD jardueraren eta analisi funtzionalen artean hautemandako aldakortasunaren arrazoia, lipasa jardueraren PLD2-ren ekintza-mekanismo bakarra ez dela izan litekeela. Izan ere, PLD1 ez bezala, GEF jardueraren PLD2-ren ezaugarri da, eta hori oso garrantzitsua da zelulen mugigarritasunerako, besteak beste<sup>135,137</sup>. PLD2-k minbizian duen eragina horrela laburbil daiteke: biziraupen-seinaleak areagotu, hazkuntza handitu, MAPK, Akt eta mTOR-en seinaleztapen bideak aktibatu, apoptosiaren aurkako erresistentzia, angiogenesisia, tumoreen hazkuntza zailtzen duten faktoreak ekidin, zelulen inbasioa eta metastasia sustatu, eta energia zelular etendua<sup>137</sup>.



**ONDORIOAK**





1. Nevus eta azaleko melanozitoek eduki lipidiko global bereizgarria dute melanoma primarioko eta metastatikoko zelulekin alderatuta, eta horrek melanomaren garapenean zehar metabolismo lipidikoaren egokitzapen berri bat dagoela iradokitzen du.
2. Antzemandako aldaketa lipidiko garrantzitsuenak, melanoma primario eta metastatikoetan esfingomielina, triglizerido eta gantz azido aske espezieen gutxitzearekin lotuta daude. PI espezieen presentzia, ostera, areagotuta dago melanoman, bereziki lerro zelular metastatikoetan.
3. Mikroarriaren teknologia erabiliz, zelula normalen eta tumoralen konparazioan mailak esanguratsuki ezberdinak dituzten 116 lipido espezie detektatu ziren, eta horiek melanoma-biomarkatzaileen hautagai potentzialak dira.
4. Mikroarriak erabilia, hiru lipido espezie identifikatu ditugu, melanoma metastatikoetan horien mailak nabarmen handituta dituztenak melanoma primarioekin alderatuta; horiek pronostikorako biomarkatzaile-hautagai potentzialak dira.
5. Mintz funtzionalez osatutako mikroarriaren teknologia berria azterketa lipidomikoetarako tresna bioteknologiko translazional egokia da, eta bere erabilera beste ehun eta patologia batzuk aztertzeke zabaldu daiteke.
6. PLD2 entzimak adierazpen eta jarduera handiagoa du melanoma zeluletan, bereziki melanoma metastatikoetan. PLD2-k zelula horien hazkuntza, migrazio eta inbasio ahalmena sustatzen ditu, zelula horien gaiztotze prozesua faboretuz.



**REFERENCES**

**/**

**ERREFERENTZIAK**



1. Street W. Cancer Facts & Figures 2018. 2018:76.
2. Hawryluk EB, Fisher DE. Melanoma Epidemiology, Risk Factors, and Clinical Phenotypes. In: April Armstrong, editor. *Advances in Malignant Melanoma - Clinical and Research Perspectives*. InTech; 2011. <http://www.intechopen.com/books/advances-in-malignant-melanoma-clinical-and-research-perspectives/melanoma-epidemiology-risk-factors-and-clinical-phenotypes>. doi:10.5772/23293
3. WHO | Skin cancers. WHO. 2019 [accessed 2019 Jan 16]. <http://www.who.int/uv/faq/skincancer/en/>
4. Horrell EMW, Wilson K, D’Orazio JA. Melanoma — Epidemiology, Risk Factors, and the Role of Adaptive Pigmentation. In: Murph M, editor. *Melanoma - Current Clinical Management and Future Therapeutics*. Intech; 2015. <http://www.intechopen.com/books/melanoma-current-clinical-management-and-future-therapeutics/melanoma-epidemiology-risk-factors-and-the-role-of-adaptive-pigmentation>. doi:10.5772/58994
5. Ward WH, Farma JM, editors. *Cutaneous Melanoma: Etiology and Therapy*. Brisbane (AU): Codon Publications; 2017. <http://www.ncbi.nlm.nih.gov/books/NBK481860/>
6. Erdei E, Torres SM. A new understanding in the epidemiology of melanoma. Expert review of anticancer therapy. 2010;10(11):1811–1823. doi:10.1586/era.10.170
7. D’Orazio JA, Marsch A, Lagrew J, Brooke W. Skin Pigmentation and Melanoma Risk. In: Armstrong A, editor. *Advances in Malignant Melanoma - Clinical and Research Perspectives*. InTech; 2011. <http://www.intechopen.com/books/advances-in-malignant-melanoma-clinical-and-research-perspectives/skin-pigmentation-and-melanoma-risk>. doi:10.5772/18681
8. Rosenkranz AA, Slastnikova TA, Durymanov MO, Sobolev AS. Malignant melanoma and melanocortin 1 receptor. *Biochemistry (Moscow)*. 2013;78(11):1228–1237. doi:10.1134/S0006297913110035
9. Fortes C, Vries ED. Nonsolar occupational risk factors for cutaneous melanoma. *International Journal of Dermatology*. 2008;47(4):319–328. doi:10.1111/j.1365-4632.2008.03653.x
10. Tortora, G. J. Derrickson, B. *Principles of Anatomy and Physiology*.
11. Gogas H, Eggermont AMM, Hauschild A, Hersey P, Mohr P, Schadendorf D, Spatz A, Dummer R. Biomarkers in melanoma. *Annals of Oncology*. 2009;20(Suppl 6):vi8–vi13. doi:10.1093/annonc/mdp251
12. Miller AJ, Mihm MC. Melanoma. *New England Journal of Medicine*. 2006;355(1):51–65. doi:10.1056/NEJMra052166
13. Goldstein AM, Tucker MA. Dysplastic Nevi and Melanoma. *Cancer Epidemiology Biomarkers & Prevention*. 2013;22(4):528–532. doi:10.1158/1055-9965.EPI-12-1346
14. Arozarena I, Wellbrock C. Targeting invasive properties of melanoma cells. *The FEBS Journal*. 2017;284(14):2148–2162. doi:10.1111/febs.14040

15. Lugassy C, Zadrán S, Bentolila LA, Wadehra M, Prakash R, Carmichael ST, Kleinman HK, Péault B, Larue L, Barnhill RL. Angiotropism, Pericytic Mimicry and Extravascular Migratory Metastasis in Melanoma: An Alternative to Intravascular Cancer Dissemination. *Cancer Microenvironment*. 2014;7(3):139–152. doi:10.1007/s12307-014-0156-4
16. Damsky WE, Rosenbaum LE, Bosenberg M. Decoding Melanoma Metastasis. *Cancers*. 2010;3(1):126–163. doi:10.3390/cancers3010126
17. Staging Melanoma - Society for Immunotherapy of Cancer (SITC). 2019 [accessed 2019 Feb 14]. <https://www.sitcancer.org/patient/resources/melanoma-guide/staging>
18. Gallagher C, MD. Clark Level and Breslow Thickness for Melanoma Staging. Verywell Health. 2019 [accessed 2019 Feb 13]. <https://www.verywellhealth.com/clark-level-and-breslow-thickness-for-melanoma-staging-3010751>
19. Hansen LA. Melanoma☆. In: Reference Module in Biomedical Sciences. Elsevier; 2014. <http://www.sciencedirect.com/science/article/pii/B9780128012383051382>. doi:10.1016/B978-0-12-801238-3.05138-2
20. Ballo MT, Burmeister BH. Malignant Melanoma. In: *Clinical Radiation Oncology*. Elsevier; 2016. p. 777-787.e2. <https://linkinghub.elsevier.com/retrieve/pii/B9780323240987000423>. doi:10.1016/B978-0-323-24098-7.00042-3
21. Swetter SM, Kashani-Sabet M, Johannet P, Reddy SA, Phillips TL. 67 - Melanoma. In: Hoppe RT, Phillips TL, Roach M, editors. *Leibel and Phillips Textbook of Radiation Oncology (Third Edition)*. Philadelphia: W.B. Saunders; 2010. p. 1459–1472. <http://www.sciencedirect.com/science/article/pii/B978141605897700069X>. doi:10.1016/B978-1-4160-5897-7.00069-X
22. *Cancer of the Skin - 2nd Edition*. 2011 [accessed 2019 Feb 22]. <https://www.elsevier.com/books/cancer-of-the-skin/rigel/978-1-4377-1788-4>
23. Rigel DS, Carucci JA. Malignant melanoma: prevention, early detection, and treatment in the 21st century. *CA: A Cancer Journal for Clinicians*. 2000;50(4):215–236. doi:10.3322/canjclin.50.4.215
24. Stroján P. Role of radiotherapy in melanoma management. *Radiology and Oncology*. 2010;44(1):1–12. doi:10.2478/v10019-010-0008-x
25. Bello DM. Indications for the surgical resection of stage IV disease: BELLO. *Journal of Surgical Oncology*. 2019;119(2):249–261. doi:10.1002/jso.25326
26. Patel D, Witt SN. Ethanolamine and Phosphatidylethanolamine: Partners in Health and Disease. *Oxidative Medicine and Cellular Longevity*. 2017;2017:1–18. doi:10.1155/2017/4829180
27. Wilson MA, Schuchter LM. Chemotherapy for Melanoma. In: Kaufman HL, Mehnert JM, editors. *Melanoma*. Cham: Springer International Publishing; 2016. p. 209–229. (Cancer Treatment and Research). [https://doi.org/10.1007/978-3-319-22539-5\\_8](https://doi.org/10.1007/978-3-319-22539-5_8). doi:10.1007/978-3-319-22539-5\_8

- 
28. Sanlorenzo M, Vujic I, Posch C, Dajee A, Yen A, Kim S, Ashworth M, Rosenblum MD, Algazi A, Osella-Abate S, et al. Melanoma immunotherapy. *Cancer Biology & Therapy*. 2014;15(6):665–674. doi:10.4161/cbt.28555
29. Luther C, Swami U, Zhang J, Milhem M, Zakharia Y. Advanced stage melanoma therapies: Detailing the present and exploring the future. *Critical Reviews in Oncology/Hematology*. 2019;133:99–111. doi:10.1016/j.critrevonc.2018.11.002
30. Márquez-Rodas I, Cerezuela P, Soria A, Berrocal A, Riso A, Martín-Algarra S. Immune checkpoint inhibitors: therapeutic advances in melanoma. *Annals of Translational Medicine*. 2015;3(18):16.
31. Liu JY, Lowe M. Neoadjuvant Treatments for Advanced Resectable Melanoma: LIU AND LOWE. *Journal of Surgical Oncology*. 2019;119(2):216–221. doi:10.1002/jso.25352
32. Hartman RI, Lin JY. Cutaneous Melanoma—A Review in Detection, Staging, and Management. *Hematology/Oncology Clinics of North America*. 2019;33(1):25–38. doi:10.1016/j.hoc.2018.09.005
33. Muñoz-Couselo E, García JS, Pérez-García JM, Cebrián VO, Castán JC. Recent advances in the treatment of melanoma with BRAF and MEK inhibitors. *Annals of Translational Medicine*. 2015;3(15):15.
34. Guterres AN, Herlyn M, Villanueva J. Melanoma. In: John Wiley & Sons Ltd, editor. eLS. Chichester, UK: John Wiley & Sons, Ltd; 2018. p. 1–10. <http://doi.wiley.com/10.1002/9780470015902.a0001894.pub3>. doi:10.1002/9780470015902.a0001894.pub3
35. Maverakis E, Cornelius L, Bowen G, Phan T, Patel F, Fitzmaurice S, He Y, Burrall B, Duong C, Kloxin A, et al. Metastatic Melanoma – A Review of Current and Future Treatment Options. *Acta Dermato Venereologica*. 2015;95(5):516–524. doi:10.2340/00015555-2035
36. Rosenberg SA, Yang JC, Sherry RM, Kammula US, Hughes MS, Phan GQ, Citrin DE, Restifo NP, Robbins PF, Wunderlich JR, et al. Durable Complete Responses in Heavily Pretreated Patients with Metastatic Melanoma Using T Cell Transfer Immunotherapy. *Clinical cancer research: an official journal of the American Association for Cancer Research*. 2011;17(13):4550–4557. doi:10.1158/1078-0432.CCR-11-0116
37. Henry NL, Hayes DF. Cancer biomarkers. *Molecular Oncology*. 2012;6(2):140–146. (Personalized cancer medicine). doi:10.1016/j.molonc.2012.01.010
38. Weinstein D, Leininger J, Hamby C, Safai B. Diagnostic and Prognostic Biomarkers in Melanoma. 2014;7(6):12.
39. Belter B, Haase-Kohn C, Pietzsch J. Biomarkers in Malignant Melanoma: Recent Trends and Critical Perspective. In: Ward WH, Farma JM, editors. *Cutaneous Melanoma: Etiology and Therapy*. Brisbane (AU): Codon Publications; 2017. <http://www.ncbi.nlm.nih.gov/books/NBK481856/>

- 
40. Goossens N, Nakagawa S, Sun X, Hoshida Y. Cancer biomarker discovery and validation. *Translational cancer research*. 2015;4(3):256–269. doi:10.3978/j.issn.2218-676X.2015.06.04
41. Hanahan D, Weinberg RA. Hallmarks of Cancer: The Next Generation. *Cell*. 2011;144(5):646–674. doi:10.1016/j.cell.2011.02.013
42. Broertjes J. The Ten Hallmarks of Cancer in Cutaneous Malignant Melanoma. 2015:7.
43. Gunstone FD, Harwood JL, Padley FB. *The Lipid Handbook, Second Edition*. CRC Press; 1994.
44. Prostaglandins, eicosanoids, resolvins, fatty acids - saturated, polyunsaturated, hydroxy, cyclic analysis, composition, biochemistry and function. 2019 [accessed 2019 Jun 25]. <http://www.lipidhome.co.uk/lipids/fa-eic.html>
45. Baumann J, Sevinsky C, Conklin DS. Lipid biology of breast cancer. *Biochimica et Biophysica Acta (BBA) - Molecular and Cell Biology of Lipids*. 2013;1831(10):1509–1517. doi:10.1016/j.bbalip.2013.03.011
46. Di Pasquale MG. The Essentials of Essential Fatty Acids. *Journal of Dietary Supplements*. 2009;6(2):143–161. doi:10.1080/19390210902861841
47. Guillou H, Zadavec D, Martin PGP, Jacobsson A. The key roles of elongases and desaturases in mammalian fatty acid metabolism: Insights from transgenic mice. *Progress in Lipid Research*. 2010;49(2):186–199. doi:10.1016/j.plipres.2009.12.002
48. Currie E, Schulze A, Zechner R, Walther TC, Farese RV. Cellular Fatty Acid Metabolism and Cancer. *Cell Metabolism*. 2013;18(2):153–161. doi:10.1016/j.cmet.2013.05.017
49. Pakiet A, Kobiela J, Stepnowski P, Sledzinski T, Mika A. Changes in lipids composition and metabolism in colorectal cancer: a review. *Lipids in Health and Disease*. 2019 [accessed 2019 May 13];18(1). <https://lipidworld.biomedcentral.com/articles/10.1186/s12944-019-0977-8>. doi:10.1186/s12944-019-0977-8
50. Lee C, Hajra AK. [18] - Quantitative Analysis of Molecular Species of Diacylglycerol in Biological Samples. In: Fain JN, editor. *Methods in Neurosciences*. Vol. 18. Academic Press; 1993. p. 190–198. (Lipid Metabolism in Signaling Systems). <http://www.sciencedirect.com/science/article/pii/B9780121852856500245>. doi:10.1016/B978-0-12-185285-6.50024-5
51. Phosphatidic acid, lysophosphatidic acid and the related lipids cyclic phosphatidic acid and pyrophosphatidic acid. 2019 [accessed 2019 May 26]. <http://www.lipidhome.co.uk/lipids/complex/pa/index.htm>
52. Blanco A, Blanco G. Lipids. In: *Medical Biochemistry*. Elsevier; 2017. p. 99–119. <https://linkinghub.elsevier.com/retrieve/pii/B9780128035504000057>. doi:10.1016/B978-0-12-803550-4.00005-7



53. Phosphatidylcholine, lysophosphatidylcholine, structure, occurrence, biochemistry and analysis. 2019 [accessed 2019 May 26]. <http://www.lipidhome.co.uk/lipids/complex/pc/index.htm>
54. Zeisel SH, da Costa K-A. Choline: An Essential Nutrient for Public Health. *Nutrition reviews*. 2009;67(11):615–623. doi:10.1111/j.1753-4887.2009.00246.x
55. Gibellini F, Smith TK. The Kennedy pathway-De novo synthesis of phosphatidylethanolamine and phosphatidylcholine. *IUBMB Life*. 2010:n/a-n/a. doi:10.1002/iub.337
56. Phosphatidylethanolamine and Related Lipids (N-acylphosphatidylethanolamine, N-monomethylphosphatidylethanolamine, N,N-dimethylphosphatidylethanolamine, phosphatidylethanol, lysophosphatidylethanolamine - structure, occurrence, biochemistry). 2019 [accessed 2019 May 26]. <http://www.lipidhome.co.uk/lipids/complex/pe/index.htm>
57. Vance JE, Tasseva G. Formation and function of phosphatidylserine and phosphatidylethanolamine in mammalian cells. *Biochimica et Biophysica Acta (BBA) - Molecular and Cell Biology of Lipids*. 2013;1831(3):543–554. doi:10.1016/j.bbalip.2012.08.016
58. Phosphatidylserine and Related Lipids (lysophosphatidylserine, phosphatidylthreonine) - structure, occurrence, biochemistry and analysis. 2019 [accessed 2019 May 26]. <http://www.lipidhome.co.uk/lipids/complex/ps/index.htm>
59. LIPID MAPS Lipidomics Gateway. 2019 [accessed 2019 May 26]. [https://www.lipidmaps.org/resources/tutorials/lipid\\_tutorial.html#D](https://www.lipidmaps.org/resources/tutorials/lipid_tutorial.html#D)
60. Phosphatidylinositol, phosphatidylinositol phosphates and related phosphoinositides: structure, composition, biochemistry, and analysis. 2019 [accessed 2019 May 26]. <http://www.lipidhome.co.uk/lipids/complex/pi/index.htm>
61. Epand RM. Features of the Phosphatidylinositol Cycle and its Role in Signal Transduction. *The Journal of Membrane Biology*. 2017;250(4):353–366. doi:10.1007/s00232-016-9909-y
62. Phan TK, Williams SA, Bindra GK, Lay FT, Poon IKH, Hulett MD. Phosphoinositides: multipurpose cellular lipids with emerging roles in cell death. *Cell Death & Differentiation*. 2019;26(5):781–793. doi:10.1038/s41418-018-0269-2
63. Fernandis AZ, Wenk MR. Lipid-based biomarkers for cancer. *Journal of Chromatography B*. 2009;877(26):2830–2835. doi:10.1016/j.jchromb.2009.06.015
64. Phosphatidylglycerol and Related Lipids. 2019 [accessed 2019 Jun 27]. <http://www.lipidhome.co.uk/lipids/complex/pg/index.htm>
65. Stillwell W. Chapter 5 - Membrane Polar Lipids. In: Stillwell W, editor. *An Introduction to Biological Membranes (Second Edition)*. Elsevier; 2016. p. 63–87. <http://www.sciencedirect.com/science/article/pii/B9780444637727000051>. doi:10.1016/B978-0-444-63772-7.00005-1

66. Schlame M, Brody S, Hostetler KY. Mitochondrial cardiolipin in diverse eukaryotes. *European Journal of Biochemistry*. 1993;212(3):727–733. doi:10.1111/j.1432-1033.1993.tb17711.x
67. Haines TH, Dencher NA. Cardiolipin: a proton trap for oxidative phosphorylation. *FEBS Letters*. 2002;528(1–3):35–39. doi:10.1016/S0014-5793(02)03292-1
68. Belikova NA, Vladimirov YA, Osipov AN, Kapralov AA, Tyurin VA, Potapovich MV, Basova LV, Peterson J, Kurnikov IV, Kagan VE. Peroxidase Activity and Structural Transitions of Cytochrome c Bound to Cardiolipin-Containing Membranes. *Biochemistry*. 2006;45(15):4998–5009. doi:10.1021/bi0525573
69. Ortiz A, Killian JA, Verkleij AJ, Wilschut J. Membrane fusion and the lamellar-to-inverted-hexagonal phase transition in cardiolipin vesicle systems induced by divalent cations. *Biophysical Journal*. 1999;77(4):2003–2014.
70. Dean JM, Lodhi IJ. Structural and functional roles of ether lipids. *Protein & Cell*. 2018;9(2):196–206. doi:10.1007/s13238-017-0423-5
71. Ether lipids - glyceryl ethers, plasmalogens, aldehydes, structure, biochemistry, composition and analysis. 2019 [accessed 2019 May 27]. <http://www.lipidhome.co.uk/lipids/complex/ethers/index.htm>
72. Braverman NE, Moser AB. Functions of plasmalogen lipids in health and disease. *Biochimica et Biophysica Acta (BBA) - Molecular Basis of Disease*. 2012;1822(9):1442–1452. doi:10.1016/j.bbadis.2012.05.008
73. Drechsler R, Chen S-W, Dancy BCR, Mehrabkhani L, Olsen CP. HPLC-Based Mass Spectrometry Characterizes the Phospholipid Alterations in Ether-Linked Lipid Deficiency Models Following Oxidative Stress Gill MS, editor. *PLOS ONE*. 2016;11(11):e0167229. doi:10.1371/journal.pone.0167229
74. Lodhi IJ, Semenkovich CF. Peroxisomes: A Nexus for Lipid Metabolism and Cellular Signaling. *Cell Metabolism*. 2014;19(3):380–392. doi:10.1016/j.cmet.2014.01.002
75. Wanders RJA. Peroxisomes, lipid metabolism, and peroxisomal disorders. *Molecular Genetics and Metabolism*. 2004;83(1–2):16–27. doi:10.1016/j.ymgme.2004.08.016
76. Shindou H, Shimizu T. Acyl-CoA:Lysophospholipid Acyltransferases. *Journal of Biological Chemistry*. 2009;284(1):1–5. doi:10.1074/jbc.R800046200
77. Wang B, Tontonoz P. Phospholipid Remodeling in Physiology and Disease. *Annual Review of Physiology*. 2019;81(1):165–188. doi:10.1146/annurev-physiol-020518-114444
78. Wang L, Shen W, Kazachkov M, Chen G, Chen Q, Carlsson AS, Stymne S, Weselake RJ, Zou J. Metabolic Interactions between the Lands Cycle and the Kennedy Pathway of Glycerolipid Synthesis in Arabidopsis Developing Seeds. *The Plant Cell*. 2012;24(11):4652–4669. doi:10.1105/tpc.112.104604

79. Yang Y, Lee M, Fairn GD. Phospholipid subcellular localization and dynamics. *Journal of Biological Chemistry*. 2018;293(17):6230–6240. doi:10.1074/jbc.R117.000582
80. Sphingolipids, analysis, composition, biochemistry and function. 2019 [accessed 2019 Jun 25]. <http://www.lipidhome.co.uk/lipids/sphingo.html>
81. Taniguchi M, Okazaki T. The role of sphingomyelin and sphingomyelin synthases in cell death, proliferation and migration—from cell and animal models to human disorders. *Biochimica et Biophysica Acta (BBA) - Molecular and Cell Biology of Lipids*. 2014;1841(5):692–703. doi:10.1016/j.bbalip.2013.12.003
82. Ceramides, sphingolipids, skin, structure, occurrence, biosynthesis, function and analysis. 2019 [accessed 2019 May 28]. <http://www.lipidhome.co.uk/lipids/sphingo/ceramide/index.htm>
83. Fahy E, Subramaniam S, Brown HA, Glass CK, Merrill AH, Murphy RC, Raetz CRH, Russell DW, Seyama Y, Shaw W, et al. A comprehensive classification system for lipids. *Journal of Lipid Research*. 2005;46(5):839–862. doi:10.1194/jlr.E400004-JLR200
84. Ogretmen B. Sphingolipid metabolism in cancer signalling and therapy. *Nature Reviews Cancer*. 2018;18(1):33–50. doi:10.1038/nrc.2017.96
85. Grösch S, Schiffmann S, Geisslinger G. Chain length-specific properties of ceramides. *Progress in Lipid Research*. 2012;51(1):50–62. doi:10.1016/j.plipres.2011.11.001
86. Kitatani K, Idkowiak-Baldys J, Hannun YA. The sphingolipid salvage pathway in ceramide metabolism and signaling. *Cellular signalling*. 2008;20(6):1010–1018. doi:10.1016/j.cellsig.2007.12.006
87. Sphingomyelin and related sphingophospholipids (lysosphingomyelin, ceramide phosphoethanolamine, ceramide phosphoglycerol). 2019 [accessed 2019 May 28]. <http://www.lipidhome.co.uk/lipids/sphingo/sph/index.htm>
88. Galactosylceramide, glucosylceramide, cerebrosides, psychosine, phosphoglycoceramides - structure, occurrence, biochemistry and function. 2019 [accessed 2019 May 28]. <http://www.lipidhome.co.uk/lipids/sphingo/cmh/index.htm>
89. Hidari KI-PJ, Ichikawa S, Fujita T, Sakiyama H, Hirabayashi Y. Complete Removal of Sphingolipids from the Plasma Membrane Disrupts Cell to Substratum Adhesion of Mouse Melanoma Cells. *Journal of Biological Chemistry*. 1996;271(24):14636–14641. doi:10.1074/jbc.271.24.14636
90. Gangliosides, sialic acids - structure, occurrence, biochemistry and function. 2019 [accessed 2019 May 28]. <http://www.lipidhome.co.uk/lipids/sphingo/gang/index.htm>
91. Cholesterol and Cholesterol Esters - structure, occurrence, biochemistry and function. 2019 [accessed 2019 May 28]. <http://www.lipidhome.co.uk/lipids/simple/cholest/index.htm>

92. Synthesis of cholesterol and ketone bodies. 2019 [accessed 2019 Oct 26]. <https://greek.doctor/biochemistry-1/lectures/9-synthesis-of-cholesterol-and-ketone-bodies/>
93. Buhaescu I, Izzedine H. Mevalonate pathway: A review of clinical and therapeutical implications. *Clinical Biochemistry*. 2007;40(9):575–584. doi:10.1016/j.clinbiochem.2007.03.016
94. Peck B, Schulze A. Lipid desaturation - the next step in targeting lipogenesis in cancer? *The FEBS Journal*. 2016;283(15):2767–2778. doi:10.1111/febs.13681
95. Liebisch G, Vizcaíno JA, Köfeler H, Trötz Müller M, Griffiths WJ, Schmitz G, Spener F, Wakelam MJO. Shorthand notation for lipid structures derived from mass spectrometry. *Journal of Lipid Research*. 2013;54(6):1523–1530. doi:10.1194/jlr.M033506
96. Perrotti F, Rosa C, Cicalini I, Sacchetta P, Del Boccio P, Genovesi D, Pieragostino D. Advances in Lipidomics for Cancer Biomarkers Discovery. *International Journal of Molecular Sciences*. 2016;17(12):1992. doi:10.3390/ijms17121992
97. Yang K, Han X. Lipidomics: Techniques, Applications, and Outcomes Related to Biomedical Sciences. *Trends in Biochemical Sciences*. 2016;41(11):954–969. doi:10.1016/j.tibs.2016.08.010
98. Zhao Y-Y, Cheng X-L, Lin R-C, Wei F. Lipidomics applications for disease biomarker discovery in mammal models. *Biomarkers in Medicine*. 2015;9(2):153–168. doi:10.2217/bmm.14.81
99. Zhao Y-Y, Miao H, Cheng X-L, Wei F. Lipidomics: Novel insight into the biochemical mechanism of lipid metabolism and dysregulation-associated disease. *Chemico-Biological Interactions*. 2015;240:220–238. doi:10.1016/j.cbi.2015.09.005
100. Work TS, Work E, editors. Chapter 3 Lipid extraction procedures. In: *Laboratory Techniques in Biochemistry and Molecular Biology*. Vol. 3. Elsevier; 1972. p. 347–353. <http://www.sciencedirect.com/science/article/pii/S0075753508705497>. doi:10.1016/S0075-7535(08)70549-7
101. Bligh EG, Dyer WJ. A rapid method of total lipid extraction and purification. *Canadian Journal of Biochemistry and Physiology*. 1959;37(8):911–917. doi:10.1139/o59-099
102. Cajka T, Fiehn O. Comprehensive analysis of lipids in biological systems by liquid chromatography-mass spectrometry. *TrAC Trends in Analytical Chemistry*. 2014;61:192–206. doi:10.1016/j.trac.2014.04.017
103. Mass Spectrometry :: Introduction, Principle of Mass Spectrometry, Components of Mass Spectrometer, Applications. 2019 [accessed 2019 Oct 25]. [http://premierbiosoft.com/tech\\_notes/mass-spectrometry.html](http://premierbiosoft.com/tech_notes/mass-spectrometry.html)
104. Tandem mass spectrometry. In: *Wikipedia*. 2019. [https://en.wikipedia.org/w/index.php?title=Tandem\\_mass\\_spectrometry&oldid=908597167](https://en.wikipedia.org/w/index.php?title=Tandem_mass_spectrometry&oldid=908597167)

105. Zhang Y, Wang J, Liu J, Han J, Xiong S, Yong W, Zhao Z. Combination of ESI and MALDI mass spectrometry for qualitative, semi-quantitative and *in situ* analysis of gangliosides in brain. *Scientific Reports*. 2016;6:25289. doi:10.1038/srep25289
106. Astigarraga E, Barreda-Gómez G, Lombardero L, Fresnedo O, Castaño F, Giralt MT, Ochoa B, Rodríguez-Puertas R, Fernández JA. Profiling and Imaging of Lipids on Brain and Liver Tissue by Matrix-Assisted Laser Desorption/Ionization Mass Spectrometry Using 2-Mercaptobenzothiazole as a Matrix. *Analytical Chemistry*. 2008;80(23):9105–9114. doi:10.1021/ac801662n
107. Barcelo-Coblijn G, Fernandez JA. Mass spectrometry coupled to imaging techniques: the better the view the greater the challenge. *Frontiers in Physiology*. 2015 [accessed 2019 Jun 17];6. <http://journal.frontiersin.org/article/10.3389/fphys.2015.00003/abstract>. doi:10.3389/fphys.2015.00003
108. DeBerardinis RJ, Chandel NS. Fundamentals of cancer metabolism. *Science Advances*. 2016;2(5):e1600200. doi:10.1126/sciadv.1600200
109. Omabe M, Ezeani M, Omabe KN. Lipid metabolism and cancer progression: The missing target in metastatic cancer treatment. *Journal of Applied Biomedicine*. 2015;13(1):47–59. doi:10.1016/j.jab.2014.09.004
110. Filipp FV, Ratnikov B, De Ingeniis J, Smith JW, Osterman AL, Scott DA. Glutamine-fueled mitochondrial metabolism is decoupled from glycolysis in melanoma: **Exploring the metabolic landscape of melanoma**. *Pigment Cell & Melanoma Research*. 2012;25(6):732–739. doi:10.1111/pcmr.12000
111. Smith LK, Rao AD, McArthur GA. Targeting metabolic reprogramming as a potential therapeutic strategy in melanoma. *Pharmacological Research*. 2016;107:42–47. doi:10.1016/j.phrs.2016.02.009
112. Vazquez A, Kamphorst JJ, Markert EK, Schug ZT, Tardito S, Gottlieb E. Cancer metabolism at a glance. *Journal of Cell Science*. 2016;129(18):3367–3373. doi:10.1242/jcs.181016
113. Ratnikov BI, Scott DA, Osterman AL, Smith JW, Ronai ZA. Metabolic rewiring in melanoma. *Oncogene*. 2017;36(2):147–157. doi:10.1038/onc.2016.198
114. Beloribi-Djefaflija S, Vasseur S, Guillaumond F. Lipid metabolic reprogramming in cancer cells. *Oncogenesis*. 2016;5(1):e189–e189. doi:10.1038/oncsis.2015.49
115. Carracedo A, Cantley LC, Pandolfi PP. Cancer metabolism: fatty acid oxidation in the limelight. *Nature Reviews Cancer*. 2013;13(4):227–232. doi:10.1038/nrc3483
116. Costa ASH, Frezza C. Metabolic Reprogramming and Oncogenesis. In: *International Review of Cell and Molecular Biology*. Vol. 332. Elsevier; 2017. p. 213–231. <https://linkinghub.elsevier.com/retrieve/pii/S1937644817300011>. doi:10.1016/bs.ircmb.2017.01.001
117. Zhang F. Dysregulated lipid metabolism in cancer. *World Journal of Biological Chemistry*. 2012;3(8):167. doi:10.4331/wjbc.v3.i8.167

118. Corbet C, Feron O. Emerging roles of lipid metabolism in cancer progression: Current Opinion in Clinical Nutrition and Metabolic Care. 2017;20(4):254–260. doi:10.1097/MCO.0000000000000381
119. Cha J-Y, Lee H-J. Targeting Lipid Metabolic Reprogramming as Anticancer Therapeutics. Journal of Cancer Prevention. 2016;21(4):209–215. doi:10.15430/JCP.2016.21.4.209
120. Pascual G, Avgustinova A, Mejetta S, Martín M, Castellanos A, Attolini CS-O, Berenguer A, Prats N, Toll A, Hueto JA, et al. Targeting metastasis-initiating cells through the fatty acid receptor CD36. Nature. 2017;541(7635):41–45. doi:10.1038/nature20791
121. Watt MJ, Clark AK, Selth LA, Haynes VR, Lister N, Rebello R, Porter LH, Niranjana B, Whitby ST, Lo J, et al. Suppressing fatty acid uptake has therapeutic effects in preclinical models of prostate cancer. Science Translational Medicine. 2019;11(478):eaau5758. doi:10.1126/scitranslmed.aau5758
122. Luo X, Cheng C, Tan Z, Li N, Tang M, Yang L, Cao Y. Emerging roles of lipid metabolism in cancer metastasis. Molecular Cancer. 2017 [accessed 2019 May 13];16(1). <http://molecular-cancer.biomedcentral.com/articles/10.1186/s12943-017-0646-3>. doi:10.1186/s12943-017-0646-3
123. Santos CR, Schulze A. Lipid metabolism in cancer: Lipid metabolism in cancer. FEBS Journal. 2012;279(15):2610–2623. doi:10.1111/j.1742-4658.2012.08644.x
124. Iorio E, Caramujo MJ, Cecchetti S, Spadaro F, Carpinelli G, Canese R, Podo F. Key Players in Choline Metabolic Reprogramming in Triple-Negative Breast Cancer. Frontiers in Oncology. 2016 [accessed 2019 Jun 19];6. <http://journal.frontiersin.org/Article/10.3389/fonc.2016.00205/abstract>. doi:10.3389/fonc.2016.00205
125. Benjamin DI, Cozzo A, Ji X, Roberts LS, Louie SM, Mulvihill MM, Luo K, Nomura DK. Ether lipid generating enzyme AGPS alters the balance of structural and signaling lipids to fuel cancer pathogenicity. Proceedings of the National Academy of Sciences. 2013;110(37):14912–14917. doi:10.1073/pnas.1310894110
126. Sonkar K, Ayyappan V, Tressler CM, Adelaja O, Cai R, Cheng M, Glunde K. Focus on the glycerophosphocholine pathway in choline phospholipid metabolism of cancer. NMR in Biomedicine. 2019 Jun 11:e4112. doi:10.1002/nbm.4112
127. Cheng M, Bhujwalla ZM, Glunde K. Targeting Phospholipid Metabolism in Cancer. Frontiers in Oncology. 2016 [accessed 2019 Jun 27];6. <http://journal.frontiersin.org/article/10.3389/fonc.2016.00266/full>. doi:10.3389/fonc.2016.00266
128. Bagnoli M, Granata A, Nicoletti R, Krishnamachary B, Bhujwalla ZM, Canese R, Podo F, Canevari S, Iorio E, Mezzanzanica D. Choline Metabolism Alteration: A Focus on Ovarian Cancer. Frontiers in Oncology. 2016 [accessed 2019 Jun 19];6. <http://journal.frontiersin.org/Article/10.3389/fonc.2016.00153/abstract>. doi:10.3389/fonc.2016.00153

129. Liesenfeld DB, Grapov D, Fahrmann JF, Salou M, Scherer D, Toth R, Habermann N, Böhm J, Schrotz-King P, Gigic B, et al. Metabolomics and transcriptomics identify pathway differences between visceral and subcutaneous adipose tissue in colorectal cancer patients: the ColoCare study<sup>12</sup>. *The American Journal of Clinical Nutrition*. 2015;102(2):433–443. doi:10.3945/ajcn.114.103804
130. Merchant TE, Minsky BD, Lauwers GY, Diamantis PM, Haida T, Glonek T. Esophageal cancer phospholipids correlated with histopathologic findings: a 31P NMR study. *NMR in biomedicine*. 1999;12(4):184–188.
131. Merchant TE, Kasimos JN, de Graaf PW, Minsky BD, Gierke LW, Glonek T. Phospholipid profiles of human colon cancer using 31P magnetic resonance spectroscopy. *International Journal of Colorectal Disease*. 1991;6(2):121–126.
132. Henderson F, Johnston HR, Badrock AP, Jones EA, Forster D, Nagaraju RT, Evangelou C, Kamarashev J, Green M, Fairclough M, et al. Enhanced Fatty Acid Scavenging and Glycerophospholipid Metabolism Accompany Melanocyte Neoplasia Progression in Zebrafish. *Cancer Research*. 2019;79(9):2136–2151. doi:10.1158/0008-5472.CAN-18-2409
133. Aloulou A, Rahier R, Arhab Y, Noiriel A, Abousalham A. Phospholipases: An Overview. In: Sandoval G, editor. *Lipases and Phospholipases*. Vol. 1835. New York, NY: Springer New York; 2018. p. 69–105. [http://link.springer.com/10.1007/978-1-4939-8672-9\\_3](http://link.springer.com/10.1007/978-1-4939-8672-9_3). doi:10.1007/978-1-4939-8672-9\_3
134. Bruntz RC, Lindsley CW, Brown HA. Phospholipase D Signaling Pathways and Phosphatidic Acid as Therapeutic Targets in Cancer. *Pharmacological Reviews*. 2014;66(4):1033–1079. doi:10.1124/pr.114.009217
135. Gomez-Cambronero J. Phospholipase D in Cell Signaling: From a Myriad of Cell Functions to Cancer Growth and Metastasis. *Journal of Biological Chemistry*. 2014;289(33):22557–22566. doi:10.1074/jbc.R114.574152
136. Cho JH, Han J-S. Phospholipase D and Its Essential Role in Cancer. *Molecules and Cells*. 2017;40(11):805–813. doi:10.14348/MOLCELLS.2017.0241
137. Gomez-Cambronero J. Phosphatidic acid, phospholipase D and tumorigenesis☆. *Advances in biological regulation*. 2014;0:197–206. doi:10.1016/j.jbior.2013.08.006
138. Gomez-Cambronero J, Fite K, Miller TE. How miRs and mRNA deadenylases could post-transcriptionally regulate expression of tumor-promoting protein PLD. *Advances in Biological Regulation*. 2018;68:107–119. doi:10.1016/j.jbior.2017.08.002
139. Henkels KM, Boivin GP, Dudley ES, Berberich SJ, Gomez-Cambronero J. Phospholipase D (PLD) drives cell invasion, tumor growth and metastasis in a human breast cancer xenograph model. *Oncogene*. 2013;32(49):5551–5562. doi:10.1038/onc.2013.207
140. Kandori S, Kojima T, Matsuoka T, Yoshino T, Sugiyama A, Nakamura E, Shimazui T, Funakoshi Y, Kanaho Y, Nishiyama H. Phospholipase D2 promotes disease progression of renal cell carcinoma through the induction of angiogenin. *Cancer Science*. 2018;109(6):1865–1875. doi:10.1111/cas.13609

141. Park JB, Lee CS, Jang J-H, Ghim J, Kim Y-J, You S, Hwang D, Suh P-G, Ryu SH. Phospholipase signalling networks in cancer. *Nature Reviews Cancer*. 2012;12(11):782–792. doi:10.1038/nrc3379
142. Roth E, Frohman MA. Proliferative and metastatic roles for Phospholipase D in mouse models of cancer. *Advances in biological regulation*. 2018;67:134–140. doi:10.1016/j.jbior.2017.11.004
143. Chen Y, Zheng Y, Foster DA. Phospholipase D confers rapamycin resistance in human breast cancer cells. *Oncogene*. 2003;22(25):3937. doi:10.1038/sj.onc.1206565
144. Shi M, Zheng Y, Garcia A, Xu L, Foster DA. Phospholipase D provides a survival signal in human cancer cells with activated H-Ras or K-Ras. *Cancer letters*. 2007;258(2):268–275. doi:10.1016/j.canlet.2007.09.003
145. Chen Q, Sato T, Hongu T, Zhang Y, Ali W, Cavallo J-A, van der Velden A, Tian H, Di Paolo G, Nieswandt B, et al. Key Roles for the Lipid Signaling Enzyme Phospholipase D1 in the Tumor Microenvironment During Tumor Angiogenesis and Metastasis. *Science signaling*. 2012;5(249):ra79. doi:10.1126/scisignal.2003257
146. Knoepp SM, Chahal MS, Xie Y, Zhang Z, Brauner DJ, Hallman MA, Robinson SA, Han S, Imai M, Tomlinson S, et al. Effects of active and inactive phospholipase D2 on signal transduction, adhesion, migration, invasion, and metastasis in EL4 lymphoma cells. *Molecular Pharmacology*. 2008;74(3):574–584. doi:10.1124/mol.107.040105
147. Wang Z, Zhang F, He J, Wu P, Tay LWR, Cai M, Nian W, Weng Y, Qin L, Chang JT, et al. Binding of PLD2-generated phosphatidic acid to KIF5B promotes MT1-MMP surface trafficking and lung metastasis of mouse breast cancer cells. *Developmental cell*. 2017;43(2):186–197.e7. doi:10.1016/j.devcel.2017.09.012
148. Smith PK, Krohn RI, Hermanson GT, Mallia AK, Gartner FH, Provenzano MD, Fujimoto EK, Goeke NM, Olson BJ, Klenk DC. Measurement of protein using bicinchoninic acid. *Analytical Biochemistry*. 1985;150(1):76–85. doi:10.1016/0003-2697(85)90442-7
149. Bradford MM. A Rapid and Sensitive Method for the Quantitation of Microgram Quantities of Protein Utilizing the Principle of Protein-Dye Binding. 1976:7.
150. Riebeling C, Müller C, Geilen C. Expression and regulation of phospholipase D isoenzymes in human melanoma cells and primary melanocytes. *Melanoma Research*. 2003;13(6):555–562.
151. Gomez-Cambronero J, Horwitz J, Sha'afi RI. Measurements of Phospholipases A<sub>2</sub>, C, and D (PLA<sub>2</sub>, PLC, and PLD): In Vitro Microassays, Analysis of Enzyme Isoforms, and Intact-Cell Assays. In: *Cancer Cell Signaling*. Vol. 218. New Jersey: Humana Press; 2002. p. 155–176. <http://link.springer.com/10.1385/1-59259-356-9:155>. doi:10.1385/1-59259-356-9:155
152. Li J, Ren S, Piao H, Wang F, Yin P, Xu C, Lu X, Ye G, Shao Y, Yan M, et al. Integration of lipidomics and transcriptomics unravels aberrant lipid metabolism and defines cholesteryl oleate as potential biomarker of prostate cancer. *Scientific Reports*.



- 2016 [accessed 2019 Nov 2];6(1). <http://www.nature.com/articles/srep20984>. doi:10.1038/srep20984
153. Zinrajh D, Hörl G, Jürgens G, Marc J, Sok M, Cerne D. Increased phosphatidylethanolamine N-methyltransferase gene expression in non-small-cell lung cancer tissue predicts shorter patient survival. *Oncology Letters*. 2014;7(6):2175–2179. doi:10.3892/ol.2014.2035
154. Glunde K, Bhujwala ZM, Ronen SM. Choline metabolism in malignant transformation. *Nature Reviews Cancer*. 2011;11(12):835–848. doi:10.1038/nrc3162
155. Saito K, Arai E, Maekawa K, Ishikawa M, Fujimoto H, Taguchi R, Matsumoto K, Kanai Y, Saito Y. Lipidomic Signatures and Associated Transcriptomic Profiles of Clear Cell Renal Cell Carcinoma. *Scientific Reports*. 2016 [accessed 2019 Nov 18];6(1). <http://www.nature.com/articles/srep28932>. doi:10.1038/srep28932
156. Holthuis JCM, Menon AK. Lipid landscapes and pipelines in membrane homeostasis. *Nature*. 2014;510(7503):48–57. doi:10.1038/nature13474
157. van Meer G, Voelker DR, Feigenson GW. Membrane lipids: where they are and how they behave. *Nature Reviews Molecular Cell Biology*. 2008;9(2):112–124. doi:10.1038/nrm2330
158. Epand RM. Introduction to Membrane Lipids. In: Owen DM, editor. *Methods in Membrane Lipids*. Vol. 1232. New York, NY: Springer New York; 2015. p. 1–6. [http://link.springer.com/10.1007/978-1-4939-1752-5\\_1](http://link.springer.com/10.1007/978-1-4939-1752-5_1). doi:10.1007/978-1-4939-1752-5\_1
159. Li Z, Agellon LB, Allen TM, Umeda M, Jewell L, Mason A, Vance DE. The ratio of phosphatidylcholine to phosphatidylethanolamine influences membrane integrity and steatohepatitis. *Cell Metabolism*. 2006;3(5):321–331. doi:10.1016/j.cmet.2006.03.007
160. Dawaliby R, Trubbia C, Delporte C, Noyon C, Ruyschaert J-M, Van Antwerpen P, Govaerts C. Phosphatidylethanolamine Is a Key Regulator of Membrane Fluidity in Eukaryotic Cells. *Journal of Biological Chemistry*. 2016;291(7):3658–3667. doi:10.1074/jbc.M115.706523
161. Sok M, Rott T. Cell Membrane Fluidity and Prognosis of Lung Cancer. *Ann Thorac Surg*.;5.
162. Peetla C, Vijayaraghavalu S, Labhasetwar V. Biophysics of cell membrane lipids in cancer drug resistance: Implications for drug transport and drug delivery with nanoparticles. *Advanced Drug Delivery Reviews*. 2013;65(13–14):1686–1698. doi:10.1016/j.addr.2013.09.004
163. Dória ML, Cotrim CZ, Simões C, Macedo B, Domingues P, Domingues MR, Helguero LA. Lipidomic analysis of phospholipids from human mammary epithelial and breast cancer cell lines. *Journal of Cellular Physiology*. 2013;228(2):457–468. doi:10.1002/jcp.24152

164. Fhaner CJ, Liu S, Ji H, Simpson RJ, Reid GE. Comprehensive Lipidome Profiling of Isogenic Primary and Metastatic Colon Adenocarcinoma Cell Lines. *Analytical Chemistry*. 2012;84(21):8917–8926. doi:10.1021/ac302154g
165. Huang BX, Akbar M, Kevala K, Kim H-Y. Phosphatidylserine is a critical modulator for Akt activation. *The Journal of Cell Biology*. 2011;192(6):979–992. doi:10.1083/jcb.201005100
166. Kim H-Y, Lee H, Kim S-H, Jin H, Bae J, Choi H-K. Discovery of potential biomarkers in human melanoma cells with different metastatic potential by metabolic and lipidomic profiling. *Scientific Reports*. 2017 [accessed 2019 Nov 24];7(1). <http://www.nature.com/articles/s41598-017-08433-9>. doi:10.1038/s41598-017-08433-9
167. Taraboletti G, Perin L, Bottazzi B, Mantovani A, Giavazzi R, Salmona M. Membrane fluidity affects tumor-cell motility, invasion and lung-colonizing potential. *International Journal of Cancer*. 1989;44(4):707–713. doi:10.1002/ijc.2910440426
168. Edmond V, Dufour F, Poiroux G, Shoji K, Malleter M, Fouqué A, Tauzin S, Rimokh R, Sergent O, Penna A, et al. Downregulation of ceramide synthase-6 during epithelial-to-mesenchymal transition reduces plasma membrane fluidity and cancer cell motility. *Oncogene*. 2015;34(8):996–1005. doi:10.1038/onc.2014.55
169. Bilal F, Montfort A, Gilhodes J, Garcia V, Riond J, Carpentier S, Filleron T, Colacios C, Levade T, Daher A, et al. Sphingomyelin Synthase 1 (SMS1) Downregulation Is Associated With Sphingolipid Reprogramming and a Worse Prognosis in Melanoma. *Frontiers in Pharmacology*. 2019 [accessed 2019 Jul 2];10. <https://www.frontiersin.org/article/10.3389/fphar.2019.00443/full>. doi:10.3389/fphar.2019.00443
170. Assi E, Cervia D, Bizzozero L, Capobianco A, Pambianco S, Morisi F, De Palma C, Moscheni C, Pellegrino P, Clementi E, et al. Modulation of Acid Sphingomyelinase in Melanoma Reprogrammes the Tumour Immune Microenvironment. *Mediators of Inflammation*. 2015;2015:1–13. doi:10.1155/2015/370482
171. Bizzozero L, Cazzato D, Cervia D, Assi E, Simbari F, Pagni F, De Palma C, Monno A, Verdelli C, Querini PR, et al. Acid sphingomyelinase determines melanoma progression and metastatic behaviour via the microphthalmia-associated transcription factor signalling pathway. *Cell Death & Differentiation*. 2014;21(4):507–520. doi:10.1038/cdd.2013.173
172. Cervia D, Assi E, De Palma C, Giovarelli M, Bizzozero L, Pambianco S, Di Renzo I, Zecchini S, Moscheni C, Vantaggiato C, et al. Essential role for acid sphingomyelinase-inhibited autophagy in melanoma response to cisplatin. *Oncotarget*. 2016 [accessed 2019 Nov 28];7(18). <http://www.oncotarget.com/fulltext/8735>. doi:10.18632/oncotarget.8735
173. Uchida Y. Ceramide signaling in mammalian epidermis. *Biochimica et Biophysica Acta (BBA) - Molecular and Cell Biology of Lipids*. 2014;1841(3):453–462. doi:10.1016/j.bbalip.2013.09.003
174. Realini N, Palese F, Pizzirani D, Pontis S, Basit A, Bach A, Ganesan A, Piomelli D. Acid Ceramidase in Melanoma: EXPRESSION, LOCALIZATION, AND EFFECTS OF

- PHARMACOLOGICAL INHIBITION. *Journal of Biological Chemistry*. 2016;291(5):2422–2434. doi:10.1074/jbc.M115.666909
175. Dany M. Sphingosine metabolism as a therapeutic target in cutaneous melanoma. *Translational Research*. 2017;185:1–12. doi:10.1016/j.trsl.2017.04.005
176. Lai M, La Rocca V, Amato R, Freer G, Pistello M. Sphingolipid/Ceramide Pathways and Autophagy in the Onset and Progression of Melanoma: Novel Therapeutic Targets and Opportunities. *International Journal of Molecular Sciences*. 2019;20(14):3436. doi:10.3390/ijms20143436
177. Bedia C, Casas J, Andrieu-Abadie N, Fabriàs G, Levade T. Acid Ceramidase Expression Modulates the Sensitivity of A375 Melanoma Cells to Dacarbazine. *Journal of Biological Chemistry*. 2011;286(32):28200–28209. doi:10.1074/jbc.M110.216382
178. Leclerc J, Garandeau D, Pandiani C, Gaudel C, Bille K, Nottet N, Garcia V, Colosetti P, Pagnotta S, Bahadoran P, et al. Lysosomal acid ceramidase *ASAH1* controls the transition between invasive and proliferative phenotype in melanoma cells. *Oncogene*. 2019;38(8):1282–1295. doi:10.1038/s41388-018-0500-0
179. Hannun YA, Obeid LM. Many Ceramides. *Journal of Biological Chemistry*. 2011;286(32):27855–27862. doi:10.1074/jbc.R111.254359
180. Tang Y, Cao K, Wang Q, Chen J, Liu R, Wang S, Zhou J, Xie H. Silencing of *CerS6* increases the invasion and glycolysis of melanoma WM35, WM451 and SK28 cell lines via increased GLUT1-induced downregulation of *WNT5A*. *Oncology Reports*. 2016;35(5):2907–2915. doi:10.3892/or.2016.4646
181. Sassa T, Suto S, Okayasu Y, Kihara A. A shift in sphingolipid composition from C24 to C16 increases susceptibility to apoptosis in HeLa cells. *Biochimica et Biophysica Acta (BBA) - Molecular and Cell Biology of Lipids*. 2012;1821(7):1031–1037. doi:10.1016/j.bbalip.2012.04.008
182. Morris AJ, Frohman MA, Engebrecht J. Measurement of Phospholipase D Activity. :9.
183. Gomez-Cambronero J. New Concepts in Phospholipase D Signaling in Inflammation and Cancer. *The Scientific World JOURNAL*. 2010;10:1356–1369. doi:10.1100/tsw.2010.116
184. Frohman MA. The phospholipase D superfamily as therapeutic targets. *Trends in pharmacological sciences*. 2015;36(3):137–144. doi:10.1016/j.tips.2015.01.001
185. Influence of Lipid Fragmentation in the Data Analysis of Imaging Mass Spectrometry Experiments. [accessed 2020 Feb 12]. <https://pubs.acs.org/doi/pdf/10.1021/jasms.9b00090>. doi:10.1021/jasms.9b00090
186. Diaz O, Mébarek-Azzam S, Benzaria A, Dubois M, Lagarde M, Némoz G, Prigent A-F. Disruption of Lipid Rafts Stimulates Phospholipase D Activity in Human Lymphocytes: Implication in the Regulation of Immune Function. *The Journal of Immunology*. 2005;175(12):8077–8086. doi:10.4049/jimmunol.175.12.8077